Forward osmosis for the concentration of black tea extract: insights into the development of draw solute and extraction of essential tea components

Thesis submitted in partial fulfilment

of the requirements for the degree

of

DOCTOR OF PHILOSOPHY

Submitted by

ANANYA BARDHAN

(Reg. No. 176107102)

DEPARTMENT OF CHEMICAL ENGINEERING

INDIAN INSTITUTE OF TECHNOLOGY, GUWAHATI

GUWAHATI-781039, ASSAM, INDIA

November 2022

This thesis is dedicated to

"Maa-Baba"

Indian Institute of Technology Guwahati
Guwahati-781039, Assam, India
Department of Chemical Engineering

DECLARATION

I hereby certify that the work presented in this thesis entitled **Forward osmosis for the concentration of black tea extract: insights into development of draw solute and extraction of essential tea components"** is the outcome of my original research work carried out at the at Department of Chemical Engineering, Indian Institute of Technology Guwahati, under supervision of **Prof. Kaustubha Mohanty** and **Prof. Senthilmurugan Subbiah.** The result documented in this thesis are not submitted to any other university or institute for the award of any degree or diploma. Due acknowledgment has been made wherever the work described is based on the findings of investigations of others with supporting references.

Date:

Place:

Ananya Bardhan
Roll No. 176107102
Department of Chemical Engineering
Indian Institute of Technology,
Guwahati

Indian Institute of Technology Guwahati
Guwahati-781039, Assam, India
Department of Chemical Engineering

CERTIFICATE

This is to certify that the work contained in this thesis entitled **"Forward osmosis for the concentration of black tea extract: insights into the development of draw solute and extraction of essential tea components"** is being submitted by **Ananya Bardhan (Roll No. 176107102),** for the award of Ph.D. degree, is a record of bonafide original research carried out by her at Department of Chemical Engineering, Indian Institute of Technology Guwahati, under our guidance and supervision. This work embodied in this thesis has not been submitted to any other University or Institute for the award of any other degree or diploma.

Date:

Place:

Prof. Kaustubha Mohanty
Professor
Department of Chemical Engineering
Indian Institute of Technology Guwahati

Prof. Senthilmurugan Subbiah
Professor
Department of Chemical Engineering
Indian Institute of Technology Guwahati

ACKNOWLEDGMENT

With immense gratitude, I would like to acknowledge my thesis supervisors **Prof. Kaustubha Mohanty** and **Prof. Senthilmurugan Subbiah,** for their invaluable guidance, inspiration, and patience throughout my Ph.D. I would like to thank them for providing me with a well-equipped laboratory, vast resources, and a dedicated work culture that has made my working in their laboratory pleasant experience. I am grateful to my supervisors for their constant words of encouragement and motivation to keep me constantly focused on achieving my research objectives.

I would like to thank my doctoral committee members, **Prof. G. Pugazhenthi**, **Prof. Chandan Das**, and **Dr. Pankaj Kalita,** for their kind words, constant encouragement, and constructive inputs during my seminars which helped shape my thesis to its present form.

I am grateful Prof. Kaustubha Mohanty, Head Department of Chemical Engineering, and Prof. Anugrah Singh, Head (Former) Department of Chemical Engineering, for their administrative assistance. I am thankful to the Department of Chemical Engineering, Centre for Environment, Central Instrument Facility (CIF), for providing their state-of-the-art analytical facilities. I am also grateful to all the technical staff from the departments as mentioned above.

With two thesis supervisors, I got the opportunity to be part of two research groups. I would like to take these opportunities to thank all my seniors and lab mates from each research group. Firstly, from Prof. Senthilmurugan's research group (Water-and-Energy Nexus Lab), I would like to thank Dr. Vishal K. Verma, Dr. Vigneshwaran K., Dr. Habtom Teklu, Dr. Arunkumar Chandrasekaran, Dr. Aanisha Akhtar, Dr. Viswanth R., Dr. Nivedhitha S., Dr. Muniraja Tippa, Dr. Senthil S., Mr. Surendhar G., Mr. Munubarthi Kranthi K., Mr. Dinesh K. Gautam, Mr. Balakumara V., Mr. Priyamjeet, Ms. Neelam Dutta, Ms. Seema, Mr. Shanmugam, Mr. Bijoyendra, and Mr. Venkatesh for their constant support, laughter, and motivations. I would also like to thank Dr. Sanjeev Mishra, Dr. Saran Sarangapany, Dr. Madonna Roy, Dr. Sounak Bera, Dr. Bikashbindu Das, Mr. Pranab J. Sharma, Mrs. Barasa Malakar, Ms. Munmi Bhattacharya, Mr. Naveen K. Yaranal, Mr. Ankit Agarwala, Ms. Janaki K., Ms. Anindita Das, and Ms. Pooja Singh from Prof. K. Mohanty's research group. I would also like to thank our lab assistants, Mr. Banajit Saloi, Mr. Rupam, and Mr. Bishnu Sharma, for their timely assistance.

I am grateful to my friends, Kona, Dipshri, Harshita, Nababita, Nabendu, Nayan, Shilpi, Karan, Sikha, Sudeshna, Anweshan, Ankit, Gaffer, Sneha, Prabhat, Pulak, Langtuk, and Dharitri for their constant love, support, and motivations.

No words would suffice to express my most profound sense of gratitude to Maa-Baba (Basabi Bardhan-Bikash Bardhan), and Maa-Baba (Sutapa Khasnabis-Biplab Kumar Khasnabis) for supporting me in all circumstances. I would also like to thank Dada-Boudi (Bikramjeet Bardhan-Tribeni Deka Bardhan), Dadabhai-Didibhai (Ayan Khasnabis-Anwesha Khasnabis), and my dear husband (Sayan Khasnabis) for trusting me. I would also like to thank my three pillars of happiness Diya (Samriddhi Bardhan), Oly (Aishee Khasnabis), and Kush (Aikyo Khasnabis) for cheering me. I would like to extend my sincere gratitude to all my dear friends and well-wishers for their constant support and encouragement.

(Ananya Bardhan)

Department of Chemical Engineering,

Indian Institute of Technology Guwahati

ABSTRACT

In liquid food and beverage processing industries, vast amount of liquid foods are concentrated to reduce packaging storage, and transportation cost, and to improve the stability and handling of the product. Conventionally, the liquid foods concentration techniques (such as multi-stage evaporation) are energy-intensive and have a negative impact on products nutritional quality. Since the recent outbreak of Covid-19, the notable shift in consumer behaviour toward nutritional foods has attracted researchers an alternative concentration technique which are capable of concentrating liquid foods while maintaining its nutritional and sensory quality. Forward osmosis (FO) process is a membrane process that utilises the osmotic pressure gradient for the transportation of solvent from low-concentration feed solution (FS) to high concentration draw solution (DS), across a highly-selective FO membrane. In recent times, the feasibility of the FO process has been widely investigated on a lab-scale and was demonstrated as a potential method for the concentration of liquid foods (such as fruit juice). Compared to thermal processes and pressure-driven membrane separation processes, the FO allows the concentrating liquid food with higher concentration while maintaining the product quality. However, despite these advantages, the commercial viability of FO process for liquid food concentration are yet to be confirmed. The thesis has addressed certain identified research gaps in the fundamental aspects for liquid food concentration using the FO process.

This thesis focuses on determining the feasibility of the forward osmosis (FO) process for the concentration of freshly brewed black tea extract. Apart from its refreshing taste, the thermo-sensitive polyphenolic compounds (such as catechins) also offer several health benefits. The feasibility of the concentration of tea extract using FO process was investigated in this thesis. The increasing concentration trend of essential tea components (such as tea catechins and L-theanine) exhibits the prospects of concentration of tea extract using the FO process.

Once the feasibility of the FO process for black tea concentration was established. The thesis focuses on identifying an appropriate food-grade draw solute for the concentration of black tea extract using FO process. Initially, using the aqueous solution of food-grade inorganic salts such as sodium chloride (NaCl), magnesium chloride ($MgCl_2$), potassium chloride (KCl), and sodium sulphate (Na_2SO_4) were used as draw solution (DS) for concentration of tea extract using a commercially available hollow fiber forward osmosis (HFFO) module. The efficiency of the FO process was determined in terms of water flux, specific reverse solute flux (SRSF), and the concentration of essential tea components in the

final product. Reportedly, compared to monovalent inorganic salt (such as NaCl), the divalent or multi-valent inorganic salts (such as $MgCl_2$ and Na_2SO_4) exhibits lower water flux and lower RSF. The SRSF for divalent or multi-valent inorganic salts ranged from 12.5% to 18.5% lower than monovalent inorganic salt. The increasing concentration of tea components suggests that the FO process can dewater tea extract without compromising its product quality.

Further, in an attempt to enhance the FO performance, the above-mentioned inorganic salts were mixed in different compositions. Since FO is a concentration-driven membrane separation process, and the water flux is a function of the osmotic pressure gradient between the draw and feed solution. Thus, while maintaining similar osmotic pressure (60.56±1.21 bar), the multi-component DS was capable of providing enhanced water flux (16.91 L m^{-2} h^{-1}) with comparatively lower RSF (0.86 L m^{-2} h^{-1}). Irrespective of the multi-component DS composition used, the trend of tea component concentrations were almost the same in all cases. Thereby revealing that role of the FO membrane also needs to be investigated. To understand the role of the membrane in an efficient FO process, the FO performance of two commercially available HFFO membranes for the concentration of tea extract using the FO process and their role in concentration polarisation were investigated. Compared to Toyobo HFFO membranes, the Aquaporin inside HFFO membranes exhibited lower SRSF with about 7.70 to 9.80 times higher water flux. Further, compared to the Toyobo membrane, the negative zeta potential of the Aquaporin HFFO membrane was found to be more effective in rejecting the negatively charged essential tea components.

Once the role of the DS composition and HFFO membrane was established. Using the best-performing multi-component DS composition and HFFO membrane module, an innovative approach for preparing instant tea using the integrating forward osmosis (FO)-crystallisation technique was proposed. Using the given integrated setup, the freshly brewed tea extract was concentrated to 93.67%. At supersaturation concentration when concentrated, tea extract was subjected to low temperature. The solubility reduces, and as a result of the excess solute, the tea components separates from the solution in form of crystals. The quality of the tea crystals was analysed in terms of essential tea component concentration, theaflavin, total polyphenol content (TPC), and water solubility. The obtained result concludes that the final product (crystals) can be either directly used as an RTD beverage or can be further purified to isolate essential tea components for other related industries.

To evaluate the effectiveness of the FO process, freshly brewed tea extract was concentrated up to 8-fold using an integrated FO-crystallisation process and rotary

evaporation technique. The low operating temperature and time in the FO process support the retention of heat-sensitive essential tea components, suggesting the FO process's feasibility for the concentration of black tea extract.

A one-dimensional mathematical model of the given FO process was developed for the concentration of tea extract using the FO process. The developed HFFO model was validated using experimental data to predict the experimental performance of aquaporin FO membrane within allowable error limits. Using the developed model, a series of process flow-sheet simulation studies were performed to investigate the effect of different operating conditions on overall FO performance. Based on the simulation results, a multi-criteria optimisation was developed to attain the maximum permeate and minimum specific reverse solute flux. The feasibility of seawater and high-concentration reject brine as DS was also investigated. Due to high concentration, the reject brine (from the seawater desalination plant) can result in rapid dewatering with minimal SRSF (0.185 g L^{-1} to 0.207 g L^{-1}) along with simultaneous seawater dilution.

After analysing the performance of inorganic salt as draw solute, the feasibility of hydrogels as a draw solute was also investigated. This thesis provides a detailed overview of the synthesis, characterisation, and FO performance analysis of hydrogel as a draw solute. Due to high regenerative capability and minimal RSF, the recent research trend has shifted toward investigating the role of the hydrogel as draw solute for the FO process. The performed study confirmed the synthesis of an ideal DS, fulfilling all three primary criteria for an appropriate food-grade DS with high osmotic pressure, low RSF, and easy/cost-effective recovery. The regeneration of the hydrogel was investigated against thermal influence, solar radiation, and high-concentration reject brine. The prospect of regeneration of swollen hydrogel using high-concentration brine solution was explored in this study using a three-tier membrane module. Compared to thermal regeneration, average FO flux was observed to be improved from 4.37 L m^{-2} h^{-1} to 15.01 L m^{-2} h^{-1} when high concentration RO reject brine was used as regenerating fluid against deionised water as feed solution. Further, the feasibility of hydrogel as a draw solute for the concentration of tea extract using the FO process was also investigated in this thesis.

Overall, the results discussed in the given thesis provides a better insight into the forward osmosis in liquid food industries.

***Keywords**: Forward osmosis; Liquid food concentration; Black tea; Draw solution; Hydrogel*

NOMENCLATURE

L_p	Pure water permeability (L m^{-2} h^{-1} bar^{-1})
B	Solute permeability coefficient (L m^{-2} h^{-1})
S	Structural parameter (m)
J_w	Water flux (L m^{-2} h^{-1})
J_s	Reverse solute flux (g m^{-2} h^{-1})
Q	Flow rate (L h^{-1})
k	Mass transfer coefficient (m s^{-1})
K	Solute resistivity (m^{-1})
A_m	Membrane area (m^2)
t_s	Support layer thickness (m)
M	Mass (kg)
M_w	Molecular weight
R	Gas constant (J K^{-1} mol^{-1})
V_{DS}	Volume of draw solution tank (L)
V_{FS}	Volume of feed solution tank (L)
C_{FS}	Concentration of draw solute in feed solution tank (g L^{-1})
C_{DS}	Concentration of draw solute in draw solution tank (g L^{-1})
C_{db}	Draw solution concentration on bulk phase (g L^{-1})
C_{dm}	Draw solution concentration on membrane surface (g L^{-1})
C_{fb}	Feed solution concentration on bulk phase (g L^{-1})
C_{fm}	Feed solution concentration on membrane surface (g L^{-1})

t	Time
T	Temperature
P	Pressure
a_w	Water activity
α, β, γ	Mass transfer coefficient correlations constant (dimensionless)
ε	Porosity
ρ	Density
π	Osmotic pressure (bar)
μ	Dynamic viscosity (Pa s)
τ	Tortuosity of support layer
ϕ	Osmotic coefficient

ABBREVIATIONS

FO	Forward osmosis
PRO	Pressure retarded osmosis
SWRO	Seawater reverse osmosis
AL	Active layer
SL	Support layer
DS	Draw solution
FS	Feed solution
HFFO	Hollow fiber forward osmosis
ALFS	Active layer facing feed solution
ALDS	Active layer facing draw solution
SRSF	Specific reverse solute flux
RSF	Reverse solute flux
ICP	Internal concentration polarisation
ECP	External concentration polarisation
DECP	Dilutive external concentration polarisation
CECP	Concentrative external concentration polarisation
DICP	Dilutive internal concentration polarisation
CICP	Concentrative internal concentration polarisation
CTA	Cellulose triacetate
TFC	Thin-film composite
PVA	Polyvinyl alcohol
PolyDADMAC	Poly (diallyl dimethylammonium chloride)
MBA	N, N′-Methylene bisacrylamide solution
APS	Ammonium persulphate

NIPAM	N-Isopropyl acrylamide
Re	Reynold number
Sh	Sherwood number
Sc	Schmidt number
HPLC	High-performance liquid chromatography
IC	Ion chromatography
UV	Ultraviolet
TPC	Total polyphenol content
TF	Theaflavin
EGCG	Epigallocatechin gallate
ECG	Epicatechin gallate
EC	Epicatechin
EGC	Epigallocatechin

Table of Contents

List of Tables

List of Figures

Chapter 01

Introduction

Abstract: *This chapter provides a general overview of membrane processes in the food and beverage processing industries. The discussion is followed by a detailed discussion on the fundamentals of the forward osmosis process to understand the current status of the given process in liquid food industries, followed by motivation associated with studies conducted in this thesis.*

1.1. Introduction to the Membrane Process

The membrane separation process involves the selective removal of solute, solvent, and suspended solids from the solution using a semi-permeable membrane [1]. In the given process, the feed stream is separated into two fractions: permeate and retentate stream. The fraction of the feed stream (mixture of components A and B) that passes through membranes is called permeate stream (A), whereas the fraction of feed stream that does not pass through the membrane is called retentate (or reject) stream (B) (Figure 1.1).

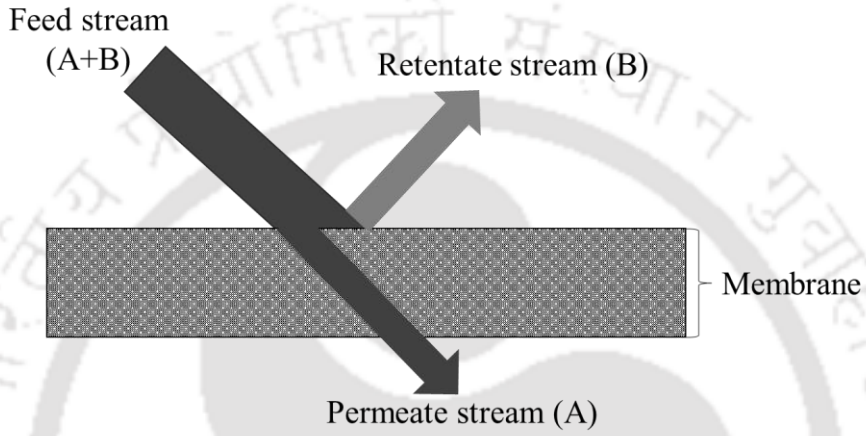

Figure 1.1 Overview of the membrane separation process

1.2. Overview of Membrane Processes in Food and Beverage Processing Industries

In food and beverage processing industries, membrane processes have been extensively used to clarify, concentrate, and recover the value-added components from waste effluents. Liquid foods are concentrated to improve shelf-life and reduce packaging, storage, and transportation cost. In the food industry, liquid foods are concentrated using a traditional thermal-based multi-stage vacuum evaporation process. Due to the thermo-sensitive nature of the essential nutrients and bioactive components, the elevated operating temperature may negatively impact the sensory parameters (such as colour, flavour, and aroma), nutritional components (such as anthocyanins, carotenoids, bioactive proteins, and vitamins), and technological properties. Referring to the recent pandemic, the change in food behaviour resulted in an increased demand for healthy or functional food [2]. The recent developments in the food industry have focussed on developing alternative low-temperature liquid food concentration processes to meet the current market demands. In food processing industries, the membrane separation process has become one of the critical processes for the

concentration, fractionation, and purification of liquid foods and has reportedly proven to be a decent alternative to traditional techniques used for liquid food concentration [3–10].

Compared to other membrane processes, the reverse osmosis (RO) process is currently used on an industrial scale for the concentration of tomato juice [11]. In the comparison of the thermal evaporation process (such as a multi-stage evaporator), the RO process is less energy-intensive, requires less investment costs, and avoids the thermal degradation of compounds (cooking taste) in the food processing industries [12–14]. Despite these advantages, the performance of the RO process was observed to be inferior to thermal concentration processes. For example, although high pressure has been applied, a single-step RO concentration can attain only 25-30 ^{o}Brix due to the high osmotic pressure of the concentrated liquid food [15].

Compared to the RO process, the forward osmosis (FO) process is considered less energy intensive [16] and has been identified as a feasible technique for the concentration of liquid food extract. Reportedly, the given process allows concentrating juice with higher dissolved and suspended solids concentrations without significant membrane fouling.

1.3. Fundamentals of the Forward Osmosis Process

FO is a concentration-driven membrane separation process and has received increased attention in the past decade among both academic and industrial scales [17]. In the FO process, two solutions of different osmotic pressure are separated by a semi-permeable membrane. Due to the osmotic pressure difference, the solvent from the low-osmotic pressure feed solution (FS) moves toward the high-osmotic pressure draw solution (DS). Thus, resulting in simultaneous concentration and dilution of FS and DS, respectively. The appropriate selection of draw solute and FO membrane plays a significant role in the advancement of the FO process. Figure 1.2 provides a basic overview of the FO process, highlighting the crucial criteria to consider when selecting appropriate DS and FO membranes.

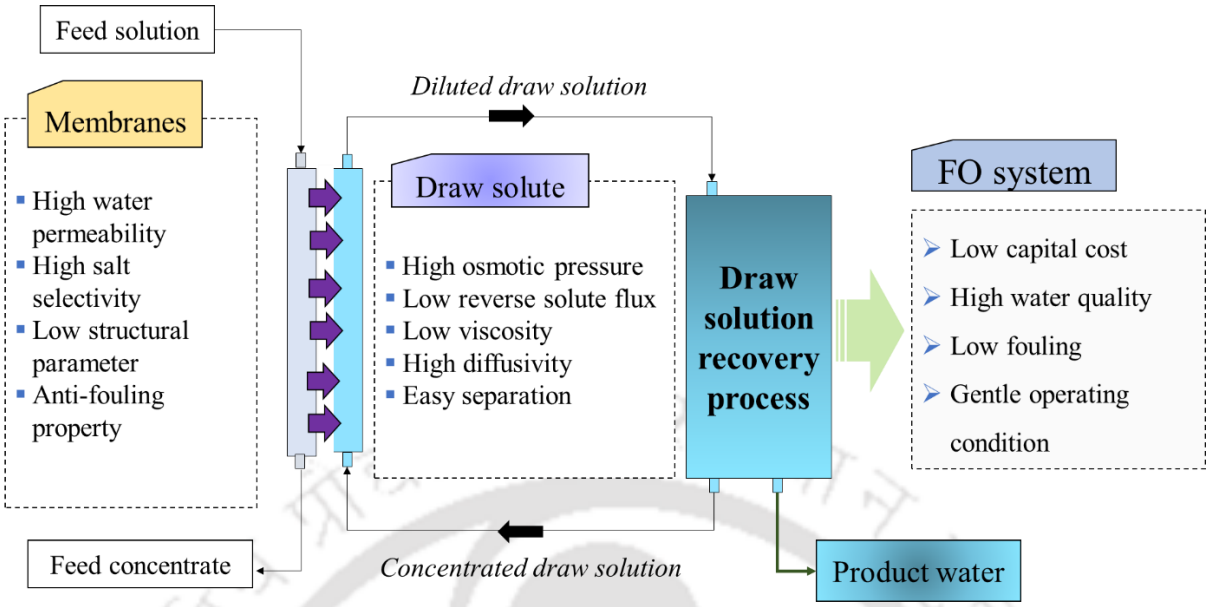

Figure 1.2 Overview of a forward osmosis process

1.3.1. Draw solute

The draw solute plays a significant role in determining the viability of the FO process. The appropriate selection of draw solute is critical in determining the overall FO performance (water flux and reverse solute flux) through the membrane and its regeneration cost. Thus, the selection of an appropriate draw solute is essential for the practical operation of the FO process [18]. Based on the literature, the following are the criteria for an ideal draw solute:

- it must be able to generate a high enough osmotic pressure to allow an effective driving force for the FO water flux;
- it should have a low viscosity to allow easy pumping around the system and improved water fluxes;
- it should have low reverse solute flux, and it will reduce the water flux by reducing the overall DS osmotic pressure across the separation layer and also leads to DS contamination in FS with altered organoleptic properties;
- it should offer a high diffusion coefficient in water, and that will reduce ICP-effect;
- it should be available low cost;
- it should be compatible with the membrane;
- it must be easy to re-concentrate (or regenerate) at a competitive cost, and most importantly, the selected should be non-toxic.

However, while real-time application, there may be certain contradictions or exceptions to some of these draw solute criteria. For example, monovalent inorganic salt (such as NaCl) tends to have high diffusion coefficients, reducing ICP, but their size also leads to relatively high reverse solute fluxes. Additionally, the viscous hydrogel has been examined as a feasible draw solute for FO, which does not necessarily need to be pumped and can be regenerated in-situ, thereby making the criteria for DS irrelevant [19–21].

Reportedly, the draw solute and its regeneration are the critical problems limiting the commercial application of the FO process. The regeneration of draw solute is a critical factor influencing the overall FO energy consumption. Thus, implementing FO technology requires a significant energy cost to develop an efficient DS recovery. In recent times, smart materials such as stimuli-responsive hydrogels have been investigated as a potential draw solute for the FO process. Thereby suggesting that solar energy or waste heat can significantly reduce the cost of draw solute regeneration.

1.3.2. Forward osmosis membranes

The FO membrane is the core of FO applications, and developing an ideal membrane is an active area of research [22]. Ideally, a FO membrane should have high water permeability, high solute rejection, and high mechanical strength. The FO membranes are usually of asymmetric composite and are made of two separate layers: a dense active layer 'AL' (0.1–1 µm) and a porous support layer 'SL' (100-200 µm) [23,24]. An ideal FO membrane should consist of a thin and dense AL to achieve high-salt retention. The thin AL with a dense structure acts as the selective barrier for mass transport, while the loosely bound support layer provides the membrane strength and the thickness of the SL is significantly higher than AL. Thus, the physical properties of both the active and support layer plays a vital role in determining the performance of the FO membranes.

The AL of the FO membrane comprises a dense polyamide thin film layer (TFC) or cellulose triacetate (CTA) material. The CTA membranes were the first commercially available membranes and offered the advantages of good mechanical properties, hydrophilicity, and low fouling. However, low pH (3-8), permeability, and poor rejection rate (85-90%) are identified drawbacks of the CTA membrane. TFC membranes were developed to overcome these drawbacks, offering high pH (2-12) and rejection rates (90–95%). Despite these advantages, TFC membranes still suffer from internal concentration polarisation (ICP) in FO, which severely diminishes the flux. TFC membranes generally treat highly concentrated

wastewater [25], whereas CTA membranes are preferred to treat less concentrated water [25].

Similar to RO membrane modules, FO modules are available in flat sheet, plate-and-frame, spiral wound (SW), tubular, and hollow-fiber (HF) designs. The modules with high specific surface area, and recoveries, such as HF [26,27] and SW [28,29] configurations, are well accepted in wastewater treatment and desalination, whereas the flat-sheet membranes are widely demonstrated for the concentration of liquid food [30,31]. The HF membranes are more suitable for the FO process than flat sheet membranes because of their denser packing density, self-supported mechanical properties, and higher effective membrane surface area [32]. Despite these advantages, most studies reported for the concentration of liquid foods have demonstrated the application of a flat-sheet TFC-FO membrane [33]. The large-scale applications of hollow fiber forward osmosis (HFFO) membranes were limited due to low water flux and poor salt rejection. Reportedly, in commercially available HFFO membranes, the AL is on the inner surface of the hollow fibers. Due to geometrical constriction, the ALFS membrane orientation results in membrane fouling and blockage problems. Therefore, an HFFO membrane with AL on the outer surface of HF would be ideal for improving the packing density, FO performance, and fouling mitigation of different feed solutions (such as liquid food) [22].

1.3.3. Challenges of FO operations

Despite all the advantages offered by the FO process, the application of the FO process is still limited compared to other established technology (such as the RO process). The reduction in water flux in the FO process can be significantly affected by fouling, concentration polarisation, and reverse salt flux (RSF). This section briefly describes the challenges associated with the FO process and their effect on FO performance.

1.3.3.1. Concentration polarisation

Concentration polarisation (CP) refers to the accumulation of solutes near the membrane surface. In an asymmetric FO membrane, the CP is described as external concentration polarisation (ECP) and internal concentration polarisation (ICP). ECP depends on the flow hydrodynamics and the physicochemical properties of the fluid (e.g., viscosity, density, solute diffusivity). Since ICP depends on the structure of SL, usually described by the term structural parameter, thus, unlike the ECP, ICP cannot be mitigated by changing the flow hydrodynamics; hence, this represents the most challenging phenomenon in the FO process.

Based on membrane orientation, a FO process can be performed in either an active layer-facing feed solution (ALFS) or an active layer-facing draw solution (ALDS). Due to the asymmetric nature of the FO membrane, the membrane orientation significantly influences the FO process.

In ALFS (FO)-mode, the ECP occurs when the solutes in the FS accumulate on the membrane's active side, and this phenomenon is known as concentrative ECP (CECP). The simultaneous movement of solvent from FS to DS dilutes the draw solution in the membrane support layer, known as dilutive internal concentration polarisation (DICP).

Therefore, this suggests that CP cannot be avoided in the FO process regardless of the membrane orientation used. In an asymmetric membrane, the ICP plays a significant role in reducing the osmotic pressure. Unlike ECP, the ICP residing in the membrane structure cannot be easily controlled by stirring or spacer design. Therefore, a membrane with low ICP needs to be developed to intensify the FO performance [34].

The tendency of the membrane ICP is determined by the term structural parameter (S), which is primarily influenced by three intrinsic properties of SL, namely thickness (t), porosity (ε), and tortuosity (τ) of the SL:

$$S = \frac{t \times \varepsilon}{\tau} \tag{1.1}$$

As described in equation (1.1), a thinner, more porous, and less tortuous support layer has a lower S-value and can consequently achieve higher osmotic pressure of the DS at the interphase between the AL and SL, resulting in higher water flux.

1.3.3.2. Reverse solute flux

Apart from the CP, another critical challenge that should be taken into consideration is reverse solute flux (RSF). This phenomenon occurs due to imperfect membrane selectivity at high DS concentrations. The RSF may worsen the ICP effect by diminishing the actual osmotic pressure gradient (between the FS and DS). As the DS diffuses and gets accumulated or entrapped inside the porous SL. The RSF also causes DS loss and may negatively impact FS chemistry.

Thus, for food and beverage applications, a FO membrane with both high-water permeability and high salt rejection should be preferred. In the FO process, the ratio of RSF and water flux is majorly influenced by the intrinsic separation properties of the membrane and operating

temperature. In contrast to other factors such as membrane orientation, the DS/FS concentration, and hydrodynamic condition may not affect this ratio significantly [35].

1.3.3.3. Fouling phenomenon

The FO process exhibits a lower fouling tendency than other pressure-driven membrane processes (such as UF, NF, and RO). However, in any membrane process, fouling is inevitable, which becomes a significant obstacle during liquid food concentration. Reportedly, the presence of suspended solids (size> 0.45 µm) and certain foulants (such as protein) are primarily responsible for fouling. Since the driving force is the concentration gradient, the FO-flux is more sensitive to the deposition of foulants than RO. Thus, a suitable pre-treatment is preferable because fouling is reversible in FO since it does not require hydraulic pressure.

Besides FS chemistry, the DS composition also aggravates fouling. The high DS concentration leads to a higher rate of water flux, thereby causing rapid fouling deposition on the membrane surface. Alteration of DS concentration is expected to manage the desirable hydrodynamic conditions. Furthermore, the higher operating temperature is usually preferred due to its contribution to reducing viscosity (water permeability increase) and better solute diffusivity (reduced ICP), which results in a higher osmotic pressure gradient across the membrane.

In ALFS mode, the external fouling occurs due to the deposition of foulants on the AL. The surface properties, such as surface roughness, have a more significant effect on this type of fouling than other properties (e.g., surface hydrophilicity), enabling easier removal and cleaning. Whereas, in ALDS, the constriction of pores due to the deposited foulants on the active layer trapped within the membrane leads to internal fouling, which is very hard to clean up. Additionally, the entrapment of foulants in the support layer would reduce porosity and enhance the effects of ICP in a membrane.

Since membrane fouling can cause a severe decrease in water flux, membrane cleaning is required to recover the water flux. The membrane cleaning includes physical, chemical, and a combination of physical-chemical cleaning. In the FO process, the foulants have a looser structure that can be easily removed by physical and chemical cleaning. Reportedly, a water flux recovery of about 98% was observed using a simple surface washing with a chemical cleaning agent (such as EDTA, NaOH, and NaOCl) [23]. However, the surface cleaning method has better cleaning efficiency. This method consumes significant water during flushing, eventually reducing the overall water recovery, and is ineffective in cleaning internal fouling that occurred in ALDS mode. In such cases, osmotic backwashing can effectively remove most

of the foulants formed in the SL [36]. During osmotic backwashing, the FS and DS are replaced with higher and lower salinity solutions. As a result, the RSF breaks the compact fouling layer and removes the foulants in porous SL.

In ALDS membrane orientation, the membrane fouling is dominated by the deposition of foulant in the membrane support layer. The foulant enters the porous substrate layer and results in high internal foulant concentration to induce the concentrative ICP effect. In the given mode, the degree of the ICP effect is directly proportional to the substrate structural parameter. For instance, a FO membrane with a large *S*-value usually suffers from more severe fouling [22]. However, compared to RO, the degree of fouling in the FO process is less compacted and can be easily removed using physical cleaning such as hydraulic backwashing. Reportedly, hydraulic backwashing of the water flux was restored up to 100% and 75% for HF and flat-sheet membrane modules [37].

In some cases, the foulants have strong adhesion to the FO membrane. The physical cleaning methods are unable to recover water flux effectively [38]. The chemical cleaning agents (such as NaOH, HNO_3, EDTA) can weaken the adhesion between fouling-membrane surfaces by chemical reaction and are often used in the case of organic and bio-fouling [39,40]. However, chemical cleaning alone cannot clean the foulants in the membrane pores. Thus, a suitable combination of chemical and physical cleaning methods should be established for an effective flux recovery.

1.4. Motivation

1.4.1. Importance of developing a mathematical model for hollow fiber forward osmosis process

The membrane configuration plays a significant role in implementing the FO process. The FO membrane modules are available in the plate-and-frame, tubular, SW, and hollow fiber (HF) modules. On a commercial scale, the membrane modules such as SW and HF are widely accepted due to their high specific surface area and recovery efficiency [41–44]. However, in recent times due to the following advantages, the research trend shifted from SW to HF module [45]:

- Higher packing density
- Self-supported membranes eliminate the requirement for spacers and thus improve FO performance while lowering the manufacturing cost
- Easy to scale up since fibers can be easily potted inside the holding vessel

- Enhanced hydrodynamics improve the shear forces on the membrane surface

Most notably, the pressure drop across FS and DS sides is significantly lower in the HF module than in the SW configuration. Thereby suggesting that an optimised membrane FO process module should have: (i) minimum pressure drop DS/FS channel, (ii) superior FO performance (i.e., high-water flux and low RSF); (iii) low manufacturing cost; (iv) chemically inert; and (v) controllable flow hydraulics [26,46].

Apart from appropriate DS and FO membrane selection, a precise model describing the phenomenon occurring during the FO process and its impact on liquid food concentrate is required to exploit the FO technology in liquid food processing industries. The developed model should be capable of integrating the effect of membrane transport and concentration polarisation effect. Unlike the HF reverse osmosis (HFRO) mathematical module, the HFFO membrane module performances have not been extensively studied [26]. Furthermore, considering the HFFO model related to liquid food concentration with experimental and model validation is still limited [47,48] and has not yet been extensively studied.

1.4.2. Importance of non-thermal membrane process in concentration of black tea extract

Tea is one of the most consumed beverages worldwide, and black tea is considered the most commonly consumed tea. Depending upon the production methods, the black tea leaves can be described as a variety when the tea (*Camellia sinensis*) leaves are allowed to be fully oxidised before being processed and dried. Due to the oxidation level, the leaves turn from green to dark brownish colour, and the flavour profile also changes to bold, brisk with a characteristic astringent flavour. Although black tea contains caffeine, it also provides a good dose of flavonoids that helps support the immune system and fight inflammation. Many health benefits are associated with the consumption of black tea, and the benefits are primarily associated with essential tea components (such as essential tea catechins, L-theanine, and theaflavin). The high operating temperature negatively impacts the stability of these essential tea components, thus suggesting that the concentration of tea extracts using non-thermal technologies are more advantageous than conventional evaporation processes [49].

The recent trends suggest that beverage consumption has increased, and black tea consumption is expected to grow by 2% over the next decade [50]. Thus, growing consumer knowledge and awareness about tea consumption's health benefits can propel the global demand for ready-to-drink (RTD) tea. Among the commercially available RTD tea varieties, instant tea powder can be defined as a fully soluble tea solid and has emerged as a fast-growing product globally.

Instant tea is manufactured by brewing tea leaves, and then the extract is concentrated under a vacuum and at low temperatures to minimise the loss of flavour and aroma. Further, the concentrate is dried to powder using spray-drying, freeze-drying, or vacuum drying [51].

Among these processes, spray-drying or multi-stage evaporation techniques are widely used to prepare concentrated green tea extract. Reportedly, due to elevated operating temperature, the taste and consumer acceptability of the final product is low. To mask the altered product quality and improve consumer acceptability, RTD beverages are usually adulterated with artificial colour and flavoring agents [52]. Thus, preserving the sensitive flavour and nutritional profile while concentrating tea extract is a critical challenge that needs to be addressed.

The sensory attributes of tea are diverse in nature, and their flavour characteristic are strongly influenced by the brewing process, which includes: (i) tea/water ratio, (ii) brewing time-temperature, and (iii) source of brewing water [53,54]. Reportedly, the higher pH, and mineral content of the brewing water reduces the flavour attributes, catechin extraction yield, and antioxidant capacity of the black tea [55]. The brewing time and temperature significantly affect the extraction of bioactive compounds and antioxidant capacity [56]. Generally, temperatures below the boiling temperature of the water (100 ^{o}C) are usually recommended for all *Camellia sinensis* teas. However, green or white tea is best brewed at low temperatures. The tea leaves that are heavily roasted (such as black tea), need higher brewing temperatures to 'wake up' the leaves from their shelf-stable dried state.

The essential tea catechins are polar compounds and solubilises in polar organic solvents such as methanol, ethanol, water, and acetone. The studies suggest that at best temperature-time combination for black tea extraction is (80-100) ^{o}C for 30 min [57]. After extraction, the water-soluble tea extract is conventionally concentrated via thermal evaporation. The concentration of epigallocatechin gallate (EGCG) increases when the temperature increases from (80-100) ^{o}C; however, beyond 100 ^{o}C, the concentration of EGCG decreases. Therefore, a non-thermal concentration technique should be employed to prevent the thermal degradation of temperature-sensitive essential tea components.

FO can be considered an efficient concentration process and has been proven effective in preserving thermolabile and bioactive components in liquid food [1,48]. Contrary to the RO process, a higher degree of concentration up to the super-saturated condition can be achieved using the FO process. Despite these advantages, the application is still limited to academic or

research purposes. The literature suggests that the absence of an ideal DS and efficient FO membranes are the main hindrances to commercialising the FO process.

1.4.3. Importance of suitable food-grade draw solute for liquid food concentrate using forward osmosis process

Despite the wide range of available DS, it is still believed that selecting a suitable DS is paramount for an efficient FO process. Along with superior FO performance, economic availability also plays a significant role in determining the commercial viability of the selected DS. Monovalent inorganic salts such as sodium chloride (NaCl) have been widely used as DS for the FO process. Though it provides superior FO performance, the occurrence of RSF is much higher due to its smaller molecular size. On the other hand, divalent ions such as magnesium and calcium reduce RSF, but it promotes organic fouling, resulting in lower FO performance. The application of synthetic DS, such as magnetic nanoparticles, polyelectrolytes, zwitterions, and hydro-acid complexes, has good osmotic potential and low RSF. Unfortunately, these DS are expensive and have a complicated synthesis process, complicating their commercial applications. The food additives such as potassium sorbate and sodium lactate are also investigated recently for the concentration of liquid food extract. Therefore, a suitable food-grade DS must be developed with superior FO performance, reduced RSF, and easy low-cost regeneration, to enhance the commercial feasibility of the given FO process.

1.4.4. Importance of development of hydrogel as a draw solute for the concentration of liquid food concentrate

For an effective FO process, an ideal DS should possess high osmotic pressure and must be easily recovered for continuous process. The feasibility of hydrogel as draw solute, has gathered much attention due to their low RSF and easy regeneration ability. A hydrogel can be defined as a three-dimensional hydrophilic polymeric network that can absorb a considerable amount of water and may potentially undergo an abrupt reversible change in volume due to its ability to respond to external stimuli (such as temperature, pH, and solvent). The potential of the hydrogel as a draw solute was first investigated by Li et al. in 2011 [58]. Hydrogel offers a more convenient way of regeneration and lower energy expenses than conventional inorganic draw agents. Since they only require mild heating for a short period or some other form of external stimuli (such as pH [59], solar radiation [60], and magnetic stimuli [61]). These responsive properties make the hydrogel an excellent osmotic agent for cost-effective

dewatering and regeneration in the FO process. Thermoresponsive polymer hydrogels can reversibly swell and de-swell in response to external temperature change. The thermoresponsive hydrogels were investigated as DS to overcome RSF and water-recovery rates' problems [62–65]. Reportedly, by employing hydrogel as DS, the ICP can be further reduced as hydrogel tend to form a layer on the membrane surface instead of penetrating into a porous layer.

Compared to conventional salt, the challenge of RSF can be avoided by using hydrogel as DS due to its bigger particle size than the ionic radius of inorganic salts. The stimuli-responsive hydrogel provides a promising alternative as a DS due to its control-release of water based on mild stimuli conditions (such as heat and light). The application of thermo-responsive hydrogels, as DS reported in the literature, has been investigated majorly for desalination purposes and has not been investigated for liquid food and beverage processing. Thus, a hydrogel with a comprehensive balance between low-energy regeneration and easy fabrication must be investigated.

1.5. Summary and Scope of Research

Based on the overall discussion, it can be concluded that amongst the alternative processes, FO offers several attractive features that outweigh the drawback of conventional concentration techniques (such as thermal evaporation and RO process). However, despite those advantages, the application of the FO process is still limited to academic or research fields. The present thesis aims to provide further insight into developing suitable draw solute and FO processes to advance its future use in the food and beverage industry.

1.6.Objectives

Based on the above discussion, the lack of suitable FO membrane and efficient recovery (regeneration) of draw solute were identified as the significant limitations in transforming forward osmosis into a full-scale process in the food industry. The objectives for the given doctoral thesis are formulated as follows:

(i) Modelling and experimental validation of the FO process for concentration of tea extract

(ii) Optimisation of multi-component inorganic salt composition as draw solute for preparation of concentrated tea extract using forward osmosis process

(iii) Development of a polymeric network (hydrogel) as draw solute for the forward osmosis process

(iv) Development of a low-cost approach toward the preparation of cold-water-soluble instant tea using integrated forward osmosis and crystallisation technique.

1.7. Organisation of the Thesis

Chapter 01 Introduction: This chapter provides a general overview of membrane processes in food and beverage processing industries, followed by a detailed discussion on the fundamentals of the FO process to understand the current status of the given process in liquid food industries, followed by motivation associated with studies conducted in this thesis, followed by the objectives of the present research work at the end of this chapter.

Chapter 02 Literature review: This chapter is aimed to provide a detailed literature review on the fundamentals of the FO process, the role of draw solution, and the FO membrane. To understand the challenges and perspectives of using forward osmosis in liquid food and related industries. From the outcome of the literature survey, the prominent research gaps were identified.

Chapter 03 Theory: In this chapter, the theory related to developing a one-dimensional mathematical model for the concentration of tea extract has been briefly described.

Chapter 04 Materials and methods: This chapter details all the analytical procedures and protocols employed in characterising the samples. This section also details the methodologies and experimental procedures used for selecting suitable draw solutions and membranes for the concentration of tea extract using the FO process.

Chapter 05 Results and Discussions: This chapter reports the detailed interpretation and discussion of the results obtained from the experiment conducted for the concentration of tea extract using the forward osmosis process.

Chapter 06 Conclusion and Scope of future work

Chapter 02

Literature review and objectives

Abstract: *This chapter is aimed to provide a detailed literature review on the fundamentals of the FO process, the role of draw solution, and the FO membrane. The challenges and perspectives of using forward osmosis in liquid food and related industries are reported in this chapter. From the outcome of the literature survey, the prominent research gaps were identified to frame the objectives of the present research work at the end of this chapter.*

Forward osmosis (FO) is an osmotic-driven membrane separation technique that uses a semi-permeable membrane to separate the high-concentration DS and low-concentration FS [66]. Unlike pressure-driven membrane processes, the osmotic pressure difference between the FS and DS is the main driving force in the FO process. Due to the concentration difference between the two solutions, the solvent from the low-concentration FS moves toward the high-concentration DS across a semi-permeable FO membrane.

Due to its mild operating condition, the FO process has been identified as a potential candidate for a broad range of concentration applications in the food and beverage processing industries. Compared to evaporation and conventional membrane concentration (such as RO and NF) processes, the FO process offers several advantages, such as (i) no or low hydraulic pressure, (ii) high water recovery, (iii) low processing temperature, (iii) lower fouling tendency, and (iv) higher energy efficiency. Despite these advantages, several challenges associated with the FO process (such as CP, fouling, and RSF) must be addressed to make the FO process commercially viable for concentrating liquid foods and beverages.

The appropriate selection of draw solute and FO membrane significantly impacts the overall FO performance and the quality of the final concentrate. So far, no suitable DS that can meet all the criteria mentioned above has been identified. The lack of appropriate DS is one of the significant obstacles to commercial applications of FO technology in food processing.

The first section of this chapter explains the fundamentals of the FO process, followed by the significance of appropriate draw solute and FO membrane. The status of the FO process in liquid food and beverage processing industries were summarised in the next section. The gaps and challenges from respective sections are outlined to define the objective of the present research, followed by the organisation of the thesis.

2.1. Fundamentals of Forward Osmosis Process

2.1.1. Forward osmosis membranes

FO membranes are asymmetric in nature that consists of a dense active layer (AL) and a porous support layer (SL). The dense AL (~100 nm) is responsible for salt rejection, whereas the SL (~200 µm) provides the required mechanical strength to the membrane. Ideally, the FO system requires a semi-porous membrane capable of separating disintegrated solute species from the FS, high solute rejection, high water permeability, and superior chemical and mechanical stability [22].

In the FO process, membranes can be used either with the active layer (AL) facing FS (ALFS or FO-mode) or with the active layer facing DS (ALDS or PRO-mode) [36]. Zhao et al. (2011) [67] investigated the effect of membrane orientation on the FO performance of various applications. Reportedly, the selection of membrane orientation is influenced by the FS composition and the degree of concentration (or water recovery). Depending on the application, the AL-FS membrane orientation is preferred for the treatment of high-saline water, whereas the AL-DS membrane orientation is preferred for treating saline waters (such as brackish water) [68]. In both the membrane orientation, the net driving force is significantly less than the theoretical driving force. The reduction in net driving is apparently due to concentration polarisation.

CP refers to the accumulation of solutes near the membrane surface, which develops due to concentration differences at the membrane-solution interface [69]. Depending upon the nature of solute accumulation, the CP can be categorised as external concentration polarisation (ECP) and internal concentration polarisation (ICP) [70]. ICP occurs on the internal surface of the membrane (i.e., SL), whereas ECP occurs on the external surface of the membrane (i.e., AL). The membrane orientation affects the relative solute accumulation in the SL or AL of the membrane, which gives rise to either dilutive or concentrative ICP or ECP [71]. In ALFS mode, the concentration of DS is higher near the external surface (AL), while the FS becomes less concentrated near the internal surface (SL), contributing to the concentrative ECP (CECP) and dilutive ICP (DICP), respectively. Similarly, for ALDS membrane orientation, concentrative ICP (CICP) and dilutive ECP (DECP) occurs [72].

Reportedly, the membrane orientation in the FO process poses a critical impact on ICP, which dominates the water flux decline. Thus, the impact of both ICP and ECP needs to be reduced to achieve a greater water flux. The section summarises the research advances aimed at

overcoming the problem of concentration polarisation in the FO process. As ECP occurs on the external surface (AL) of the membrane, thus this phenomenon can be controlled by increasing the flow rate of the FS and DS streams. Gruber et al. (2011) [73] claimed that increasing the flow rate equalizes the concentration across the membrane surface, thus reducing the ECP effect.

Unlike ECP, the ICP takes place within the porous SL of the FO membrane. It is considered one of the most troublesome phenomena in FO processes because it cannot be easily eliminated. Therefore, the decline in water flux in FO is primarily caused by ICP, and the percentage of flux reduction can be as high as 80% [74]. In an asymmetric membrane, the ICP plays a significant role in reducing the osmotic pressure. The severity of ICP is influenced mainly by the structure of the SL [75]. The term structural parameter (S) is an intrinsic membrane parameter and describes the structure of SL of the FO membrane. Reportedly, high structural parameter decreases water flux due to increased mass resistance and ICP-effect (refer to equation 1.1).

In an ideal FO membrane, the SL should be thin, highly porous, and minimally tortuous. Shaffer et al. (2015) [17] highlighted two prominent goals for membrane design: (i) minimising the structural parameter of the support layer (to mitigate mass transfer limitations and increase water flux) and (ii) maximising the reverse solute flux selectivity of the active layer (to limit the loss of draw solute). Thus, it suggests that to tackle ICP-effect, the SL should be more porous, but at the same time, to minimize RSF, the selectivity of the AL should be enhanced. However, increasing membrane selectivity reduces water flux, which simultaneously induces RSF and fouling afterward.

Based on the materials used, the membranes used for FO application can be categorized as, Cellulose acetate ‘CA’ (or cellulose triacetate ‘CTA’), thin-film composite (TFC), and biomimetic membranes. TFC membranes comprise a dense AL with high salt rejection and a loosely bound support layer with high-mechanical strengths. Compared to other types of FO membranes, TFC membranes are more popular due to their high permeability, stability, chemical stability (pH 2-6), and design options [70]. However, most TFC membrane suffers from the ICP phenomenon, RSF, and to a certain extent, they are more prone to fouling due to their polyamide surfaces, which is part of their AL) [40].

Reportedly, till 2018 nearly all lab-scale FO experiments were conducted using flat-sheet FO membranes, of which 20% were self-manufactured and 76% were commercial membranes.

Among these, almost 57% of the FO membranes were supplied by Hydration Technology Innovations (HTI, Albany, USA) [33]. Table 2.1 briefly overview some commercially available FO membranes.

Table 2.1 Overview of commercial forward osmosis membrane suppliers

Supplier/ Manufacturer	Membrane type	Configuration	Structural parameter (μm)	Ref.
Aquaporin A/S (Copenhagen, Denmark)	TFC	Hollow fiber	210	[76,77]
		Flat sheet	630	[78]
OASYS Water Inc. (Boston, MA, USA)	TFC	Hollow fiber	550	[79]
Porifera Inc. (Hayward, CA, USA	TFC	Spiral wound	344	[80]
Toyobo Co. Ltd. (Osaka, Japan)	CTA	Hollow fiber	1024	[26]
Hydration Technology Innovations, HTI (USA)	CTA	Flat sheet	663	[16,81]
	TFC	Flat sheet	1227	
Fluid Technology solutions, FTS (USA)	CTA	Spiral wound	707	[80]

TFC: thin-film composite; CTA: Cellulose triacetate

The earliest commercial development of FO technology was reported by Hydration Technology Innovations (HTI) in 1975 for emergency potable water supply for the US military. In 2008, HTI patented commercial asymmetric CA/CTA FO membranes composed of a thin skin layer for salt separation (10–20 μm) and a thicker porous scaffold layer (about 100 μm thick) with a woven or non-woven mesh embedded within it [22]. In 2010, OASYS (Osmotic Applications and Systems) launched the world's first thin-film composite polyamide-based spiral wound (SW) FO membrane element. In 2014, Toyobo's hollow fiber CTA FO membrane demonstrated 10 times the area compared to the flat sheet membrane for seawater desalination and wastewater treatment. This membrane saves energy for seawater desalination as the need for a high-pressure pump and piping can be eliminated. The Aquaporin Inside flat sheet membrane launched the first commercially available thin-film composite FO membrane to incorporate aquaporin protein into its polyamide-based selective layer. Recently, Aquaporin

Inside introduced its hollow fiber forward osmosis (HFFO) membrane module made of polyamide TFC. The manufacturer claims the membrane can reject difficult contaminants while preserving valuable components and offers a high-packing density.

Summary of FO membranes

Significant efforts have been made to improve the performance of FO membranes to achieve high water permeability (hydrophilicity) and high solute rejection ability, diminish the CP-effect (by reducing structural parameters and related membrane morphology), and, most notably, elevate the membrane stability (both chemical and mechanical stability) Figure 2.1 summarizes the critical factors that need to be considered while selecting FO membrane [16]. *Although, most of the membranes mentioned above are developed for desalination and related applications. The detailed investigation of complex, viscous systems, such as liquid food extract, needs to be investigated. Thereby suggesting that there still exists scope for investigating a suitable FO membrane for concentrating liquid food extract.*

Forward osmosis membrane	
Categories	• Cellulosic membranes (CA/ CTA) • Thin-film composite (TFC) membranes • Biomimetic membranes • Chemically prepared membranes
Critical factors	• Membrane material • Membrane morphology (roughness, porosity, hydrophilicity, and structural parameter)
Selection factors	• Internal concentration polarisation • Water permeability • Membrane selectivity • Mechanical strength • Chemical stability • Energy consumption

Figure 2.1 Critical factor for selecting the ideal membranes for forward osmosis process

2.1.2. Draw solute

In the FO process, selecting a suitable draw solute is crucial for advancing the FO technology, as it provides the driving force for the process [82]. Ge et al. (2013) [83] state that selecting an ideal draw solute not only promotes the efficiency of the process but also reduces the

subsequent cost associated with the draw solute recovery and regeneration. Reportedly, in addition to low-cost and minimal toxicity, an ideal draw solute needs to fulfill the following requirements (Figure 2.2) [84]:

(i) An ideal draw solute should be able to generate high osmotic pressure. The osmotic pressure gradient between FS and DS across the membrane is the main driving force for the FO process. A draw solute with osmotic pressure higher than FS ensures a positive permeate flux.

According to the Morse equation, derived from the van't Hoff equation, the osmotic pressure of the solution can be expressed as:

$$\pi = iMRT = i\left(\frac{n}{V}\right)RT \qquad (2.1)$$

where, the term '*i*' refers to van't Hoff factor, and M refers to the molarity of the solute, which is equal to the ratio of the number of solutes (*n*) to the volume of the solution (*V*). The terms '*R*' and '*T*' refer to the gas constant and absolute temperature, respectively.

Equation (2.1) suggests that an ionic compound that can fully dissociate to produce more ionic species is preferred because it may result in a high '*i*' value. Thus, multivalent ionic solute compounds with a high-water solubility and a high degree of dissociation are potential candidates as draw solutes.

(ii) An ideal draw solute should have low reverse solute flux (RSF). Since most FO membranes are not ideally semi-permeable, the RSF occurs due large concentration gradient between FS and DS. The occurrence of RSF adversely affects the FO and subsequent processes. It not only reduces the driving force and contaminates FS but also increases the replenishment cost of the DS. Thus, it suggests that the RSF of the DS must be carefully considered because it may jeopardize the overall performance of the given process [85]. The studies conducted by Lay et al. (2012) [86] demonstrated the correlation between the RSF of the draw solute to membrane fouling.

(iii) An ideal DS must be easily regenerated after the FO process.

(iv) Apart from the traits mentioned above, the draw solutes are preferred to have a small molecular weight and low viscosity in their aqueous solution, as concentration polarisation is inevitable in the FO process. Reportedly, since ICP is partially caused by the low diffusion coefficient of the draw solute, the diffusion coefficient of a draw solute is inversely proportional to its molecular weight and solution viscosity. Thus, a draw solute with a small molecular weight and low viscosity is favorable.

(v)The other critical properties of DS include easy handling and compatibility with FO membranes.

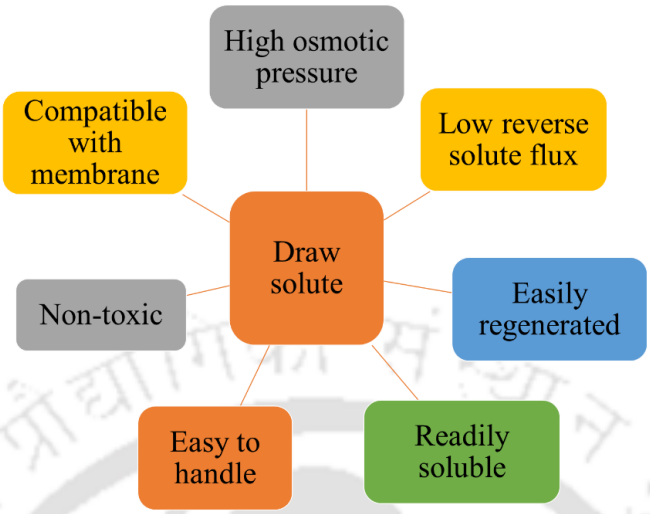

Figure 2.2 Essential properties of an ideal draw solute for the forward osmosis process

2.1.2.1. Inorganic compounds

Inorganic draw solutions are usually monovalent or multivalent ions with high water solubility, capable of generating high osmotic pressure, and can be easily regenerated using the RO process. However, the chances of RSF are prominent due to their small sizes. She et al. (2013) [87] studied the effect of RSF of inorganic draw solutes on organic fouling during PRO operations. The authors claimed that divalent cations promoted significant amounts of fouling by the anionic polysaccharide alginate, a common constituent of bacterial cell walls. Furthermore, increased draw solute concentration dramatically increased fouling due to synergistic effects due to increased water flux and increased reverse solute diffusion occurring at higher concentrations.

Furthermore, multivalent salts, such as $MgCl_2$ and $CaCl_2$, have several advantages over monovalent salts. Their larger hydration radii lead to reduced reverse salt fluxes compared with NaCl, and it is possible to achieve higher osmotic pressures with the same molar concentrations due to the greater number of ionic species formed on dissociation [88]. Achilli et al. (2010) [89] studied a wide variety of mono- and divalent-ions as draw solutes at various concentrations designed to give the same osmotic pressure (~28 bar). Reportedly, the authors observed that even after maintaining the same osmotic pressure, the range of water flux varied from 10.9 L m^{-2} h^{-1} (for KCl) to 5.5 L m^{-2} h^{-1} (for $MgSO_4$). Thereby, it was stated that the differences in

water flux were attributed solely to ICP, as draw solution osmotic pressures had all been set at the same level.

Alnaizy et al. (2013) [90] investigated using $CuSO_4$ as a draw solute for brackish water desalination. Though the osmotic pressure generated by $CuSO_4$ was insufficient for the desalination process, it was considered an attractive approach for brackish or lower salinity water purification due to simple reconcentration by precipitation by reaction with $BaSO_4$.

Ansari at al. (2016) [91] demonstrated the application of seawater for the recovery of phosphorus from digested sludge concentrate. Sea water is an ideal draw solution for dewatering applications, as diluted seawater can be discharged into the sea without the need for further treatment. However, the effect of RSF and contamination were entirely ignored.

Phuntsho et al. (2011) [92] investigated nine fertilizers (Ammonium nitrate, Ammonium sulphate, Ammonium chloride, Calcium nitrate, Sodium nitrate, Potassium chloride, Mono-ammonium phosphate, Di-ammonium hydrogen phosphate, and Potassium nitrate) as to draw solute for desalination. The significant advantage of using concentrated fertilizers as draw solutes is that the diluted DS can be directly used for fertigation after the FO process. However, due to RSF and CP-phenomenon, the application of fertilizers as DS was not suggested for liquid food concentration.

2.1.2.2. Organic draw solutions

- Sugar compounds: Due to their non-toxic nature and easy availability, simple organic compounds (such as sugar compounds) have been investigated as a potential draw solute for the FO process. Kravath and Davis (1975) [93] investigated the potential of simple monosaccharides such as glucose and fructose as a draw solute for desalination using CA membranes. Petrotos et al. (1998) [13] demonstrated the feasibility of disaccharide sucrose as a draw solute for the concentration of tomato juice.
- Ionic liquids (ILs) are salts with low melting points, making them liquid at low temperatures, typically less than 100 °C at atmospheric pressure. The high ionic conductivity, high solubility, negligible vapor pressure, and chemical and thermal stability are favourable properties of ILs, making them an ideal candidate for numerous industrial applications. Cai et al. (2015) [94] investigated several amphiphilic organic ionic liquids (such as tetra butyl phosphonium 2,4 dimethyl benexene sulfonate (P4444 DMBS); tetra butyl phosphonium mesitylene sulfonate (P4444 TMBS); and tributyloctyl-phosphonium bromide (P4448 Br)) as draw solute for desalination. The energy requirement for the FO process plus regeneration

was reported to be significantly lower than for a similar separation performed using RO. Zhong et al. (2016) [95] demonstrated the use of 3.2 M solutions of protonated betainebis (trifluoromethylsulfonyl)imide [Hbet][Tf_2N], which was an upper critical solution temperature (UCST) type ionic liquid to extract water from a feed up to 3.0 M NaCl solution (at 56 ^oC). After the FO process, the diluted draw solution was allowed to cool below the UCST, causing phase separation and forming an ionic liquid-rich and water-rich phase spontaneously.

Organic ionic salts (such as ethylene diaminetetraacetic acid 'EDTA') have been examined as potential draw agents for the FO process. Hu et al. (2014) used EDTA-sodium salt as a draw solute to dewater high-nutrient sludge. Nguyen et al. (2017) [96] investigated the feasibility of EDTA-salt as a recovery draw solute using direct contact membrane distillation. Recently, Wu et al. (2021) [97] demonstrated the recovery of EDTA using a combination of pH-adjustment and microfiltration approach.

The feasibility of another group of organic compounds, such as zwitterions, were investigated as a draw solute for the FO process [98,99]. Pejman et al. (2020b) [100] synthesised a novel DS (zwitterion group of poly-sulphobetaine) through free-radical polymerisation. The zwitterionic substances were able to overcome the drawbacks related to RSF and water flux. However, their short storage time and their susceptibility to biodegradation make them economically unsuitable for large-scale FO applications.

2.1.2.3. Nanoparticles as draw solution

Na et al. (2014) [101] demonstrated the feasibility of functionalized nanoparticles as DS. Ling et al. (2014) investigated the feasibility of using magnetic nanoparticles (MnP) as a draw solute. The author claimed that using MnP can be regenerated using external magnetic fields and requires no chemical reaction. However, the MnP tends to aggregate in aqueous solutions. The aggregation results in a significant reduction in the osmotic pressure, thereby limiting their utility as draw solutes. Further, the application of carbon nanoparticles in the FO process and their role in enhancing water flux due to their high osmotic pressure was demonstrated by Tavakol et al. (2020) [102].

Reportedly, though, the standard organic DS and functionalized nanoparticles-based DS are easy to regenerate and exhibit superior FO performance. However, in some instances, their toxic nature hinders their more comprehensive application, prompting researchers to investigate the potential of hydrogels as a draw solute for the FO process [103].

2.1.2.4. Hydrogel as draw solution

Recently, hydrogels have been proposed as a new class of draw agent for the FO process. Hydrogels are three-dimensional polymeric networks, and depending on the synthesising process and types of monomer used, the hydrogels can be tailored to specific purposes. Compared to organic DS (such as poly-tetra butyl phosphonium styrene sulfonate and diethyl ether), hydrogels yield better water flux and lower RSF with reduced concentration polarisation [104]. Due to the presence of hydrophilic functional groups like hydroxyl (-OH), carboxyl (-COOH), and amide (-$CONH_2$), the hydrogels can hold a significant amount of water while maintaining their structure [105,106]. Depending on the type of monomer used, the hydrogels can be classified as homopolymeric and copolymeric. Similarly, depending on the structure of polymeric chains, the hydrogels can be either an interpenetrating network (IPN) or a semi-interpenetrating network (semi-IPN). Unlike inorganic salts, the osmotic pressure gradient between the FS and DS across the membrane is the true driving force. The actual driving force for producing water flux for hydrogels is still unclear [107,108]. Höhne et al. (2014) [109] suggested that hydrogel swelling pressure (Δp_{swell}) is similar to osmotic pressure contributes to the equilibration of chemical potential between the outside and inside of the swollen gel, respectively.

$$\Delta p_{sewll} = \frac{1}{v_{m,s}}\left(\mu_{lo} - \mu_{ls}\right) \tag{2.2}$$

where, $v_{m,s}$ represents the molar volume of the swelling agent in the gel. The term $\mu_{l,o}$ and $\mu_{l,s}$ are chemical potential of the swelling agent outside and inside the swollen gel.

Wang et al. (2014) [110] suggested that swelling pressure was the true driving force for hydrogel draw solute that originates from polymer-water mixing, elastic reaction force for the network, and osmotic pressure of ionisable groups:

$$\pi_{tot} = \pi_{mix} + \pi_{el} + \pi_{ion} \tag{2.3}$$

where the term π_{tot} represents the swelling pressure of gel and is described as the summation of mixing (π_{mix}), elastic (π_{el}), and ionic (π_{ion}) contributions.

Stimuli-responsive hydrogels can be described as a hydrogel that can undergo a structural or mechanical change under the influence of some external stimulus, such as temperature, pH, solvent composition, magnetic field, or applied electrical charge. Several recent studies exploit this behavior to use responsive hydrogels as draw agents in FO processes [111]. As a draw

agent, hydrogel offers a more convenient way of regeneration at lower energy expense than conventional inorganic draw agents since they only require mild heating for a brief period or some other form of external stimuli. Figure 2.3 provides a schematic representation of draw solute (hydrogel) through various stimulus exposures.

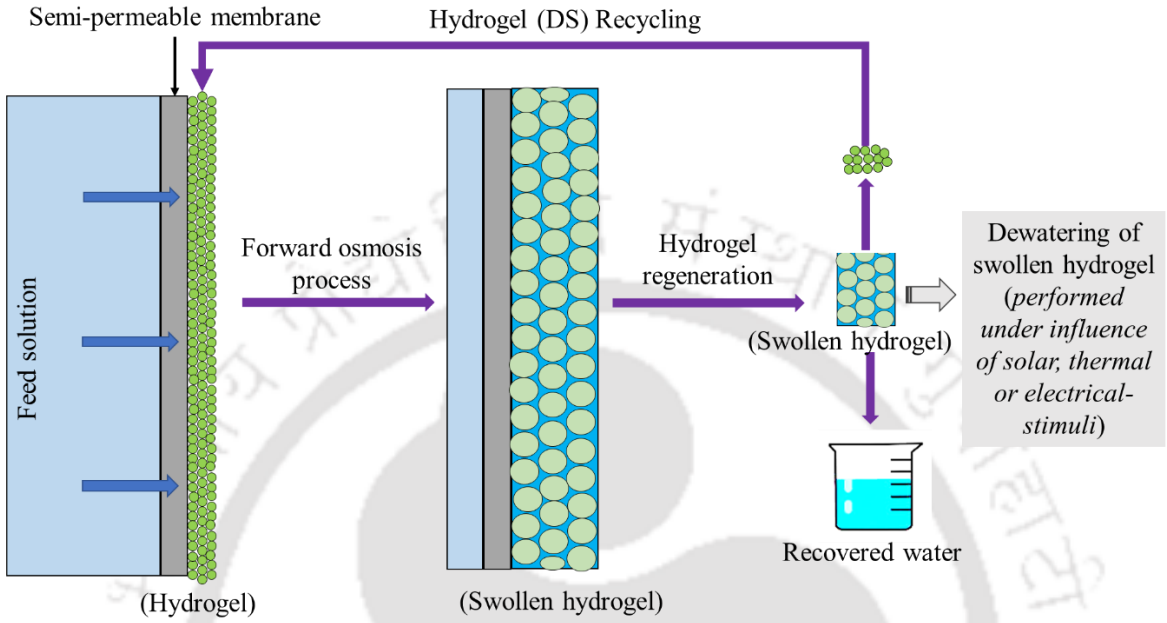

Figure 2.3 Schematic representation for regeneration of hydrogel as draw solute

The potential of hydrogel as draw solutes for the FO process was first investigated by Li et al. (2011) [21]. In the given study, the author demonstrated the applicability of hydrogel as a draw agent for the FO process. The study suggested that the hydrogels can generate high osmotic pressure and the feasibility of hydrogel (draw solute) regeneration was demonstrated using a thermal process.

A thermoresponsive hydrogel typically undergoes swell-shrink transitions either at lower critical solution temperature (LCST) or upper critical solution temperature (UCST). Poly-N-isopropyl acrylamide (PNIPAM) based hydrogels have been extensively investigated as draw agents for FO desalination. Although, PNIPAM hydrogel can swiftly release entrapped water at a temperature above LCST in the regeneration process due to its thermo-sensitivity. However, due to its non-electrolytic nature, the FO performance of PNIPAM-hydrogel is below LCST. Table 2.2 summarises the recent literature review on temperature-responsive hydrogel as a draw solution for the FO process. The efficiency of the synthesised thermosensitive hydrogel as DS was evaluated in terms of water flux and amount from the swollen hydrogel after FO desalination.

Table 2.2 Literature review on temperature-responsive hydrogel as draw solution against NaCl as feed solution

DS (Hydrogel) composition	FS (NaCl) concentration (mg L^{-1})	Membranes used/ membrane area (cm^2)	Membranes orientation	Water flux (L m^{-2} h^{-1})	Result	Ref.
PNIPAM PNIPAM-PSA	2000	CTA	-	0.30 0.55	Ionic hydrogel induced two-times higher flux compared to neutral PNIPAM hydrogel	[112]
PSA-PNIPAM	2000	CTA / (4.5-11.9)	ALFS	0.07 - 0.21	Semi-IPN hydrogels achieved a high swelling ratio and recovery rate compared PNIPAM and co-polymerized SA-NIPAM	[113]
PSA-PNIPAM	2000	CTA/ 1.77	ALDS	0.25	Heat generated by solar energy allows the discharge of water from bilayer thermoresponsive hydrogels	[108]
PSA-PNIPAM-C	2000	-	ALFS	1.32	Incorporation of carbon as solar absorbent successfully heat thermal-sensitive hydrogel for a superior water recovery rate.	[114]

DS (Hydrogel) composition	FS (NaCl) concentration (mg L^{-1})	Membranes used/ membrane area (cm^2)	Membranes orientation	Water flux (L m^{-2} h^{-1})	Result	Ref.
PSSS-PNIPAM	2000	CTA/ 0.06	ALFS	1.4 - 1.9	Copolymerized SA-NIPAM, further interpenetrated by PSSS, allows more substantial osmotic pressure and a more flexible structure, which helped improve water flux.	[115]
PNIPAM-DEAEMA	2000	-/ 3.16	ALDS	5.5	Higher water flux induced by stronger osmotic pressure due to the presence of more tertiary amines in cationic monomer	[62]
AMPS-AM	2000	-/ 22.05	ALDS	0.5-3.25	Increasing concentrations of AMPS induce more substantial osmotic pressure, and more negatively charged groups allow higher water retention due to better expansion.	[116]

CTA: Cellulose triacetate; PSA: poly (sodium acrylate); PNIPAM: poly(N-isopropylacrylamide); PSA-NIPAM: poly (sodium acrylate)-N-isopropylacrylamide; PNIPAM-C: poly(N-isopropylacrylamide)-carbon; PSA-NIPAM-C: poly (sodium acrylate)-N-isopropylacrylamide-carbon; PNIPAM-DEAEMA: Poly(N-isopropylacrylamide-co-Diethylaminoethylmeth-acrylate)

Apart from thermal-responsive hydrogel, the feasibility of other responsive hydrogels, such as electrically responsive polymer hydrogels [117,118], pH-responsive [119], and gas-responsive hydrogels [120] was also investigated for the FO process.

In summary, many novel hydrogels have been developed to replace the conventional DS and to reduce CP, thus improving water recovery efficiency. However, several issues still need to be addressed, including the low water flux, high ECP difficulties in regeneration, and in continuous operation.

Summary of draw solute in forward osmosis process

The selection of an appropriate draw solution is key to the efficient and cost-effective operation of FO. An effective draw solute must be abundant, capable of generating a high osmotic potential, have low reverse solute flux, be non-toxic and non-corrosive, be inexpensive, and be easy and cheap to regenerate. Table 2.3 provides a brief overview of the draw solute used in the FO process. Small ionic species can produce high osmotic pressures, have high diffusion coefficients which limit concentration polarisation, and can be easy to re-concentrate with RO, but on the other hand, have a relatively high reverse solute diffusion. Many innovative draw solutes have been used, including polyelectrolytes, hydrogels, stimuli-responsive polymers, and nanoparticles coated with hydrophilic groups. At the same time, these larger molecules and nanoparticles have low reverse salt diffusion and innovative recovery pathways. They often struggle to match the osmotic pressures exhibited by small molecules.

Table 2.3 An overview of draw solute used in the forward osmosis process

Draw solute		Advantages	Disadvantages
Inorganic compounds	(i) Mono-, di-, multivalent salt	• High solubility • Low-cost • High osmotic pressure • High flux	• High RSF • High fouling and scaling propensity
	(ii) Fertilizers	• Direct fertigation is possible • DS regeneration is not required	• Limited osmotic potential • Dilution of nutrients
Organic compounds	(i) Sugar	• Low RSF	• Less flux • Prone to fouling
	(ii) Ionic liquids	• Low RSF • High DS recovery	• Less flux

Draw solute		Advantages	Disadvantages
	(iii) Zwitterionic compound	• High flux • Low RSF	• Limited storage time • Prone to biodegradation
	(iv) EDTA	• High flux • Low RSF • Regeneration possible using NF	• Expensive • pH dependency • Hazardous to nature
Nanoparticles		• High osmotic pressure at low-concentration • No significant draw solute leakage • Regeneration is possible using the MD process	• Agglomeration during magnetic separation • Ultrasonication weakens magnetic properties • Viscosity of the solution reduces the effective driving force and the flux
Stimuli-responsive hydrogel		• No significant DS leakage • Efficient DS regeneration	• Low permeate flux • Complicated synthesis process • Low durability

DS: draw solution; RSF: reverse solute flux; EDTA: Ethylenediaminetetraacetic Acid

2.2. "Forward osmosis," an Emerging Technique for the Concentration of Liquid Foods

In the food and beverage processing industries, a vast amount of liquid foods are concentrated to improve the shelf-life and reduce the overall cost (in terms of packaging, storage, and transportation cost) [121]. On a commercial scale, thermal processing (such as a multi-stage evaporator) is one of the most widely employed methods for liquid food concentration. However, since all bioactive components are thermo-sensitive. Therefore, the thermal treatment (such as the evaporator) has a negative impact on nutritive components (such as anthocyanin, carotenoids, vitamins, and bioactive proteins), sensory parameters (such as flavor, color, and aromatic profile), and technological parameters.

In recent decades, the increasing demand for high-quality, minimally processed food was observed due to the increasing concern about human health and nutrition. To meet this current market demand, recent developments in food processing industries have shifted their focus toward non-thermal technologies. In such a situation, the FO process can provide the advantage of maintaining the physical properties of the liquid food without deteriorating its overall quality

[12,122,123] Table 2.4 summarises the advantages and disadvantages of the FO process in liquid food and beverage processing industries.

Table 2.4 Advantages and disadvantages of the forward osmosis process for liquid food concentration

Advantages	• Non-thermal technology • High-feed solute rejection • High concentration factor • Preservation of heat-sensitive compounds (such as aroma, color, flavor, and nutritive components)
Challenges	• Reverse solute flux • Draw solution regeneration • Relatively low-flux • Low fouling propensity

A decent number of available literatures briefly discussed the opportunities, challenges, prospects, and limitations of the FO process in the food and beverage processing industries [124,125]. The first application of FO for liquid food concentration was reported by Popper et al. (1966), who successfully concentrated grape juice to 60^{o} Brix using a reverse osmosis membrane and a concentrated brine as the draw agent [126]. Reportedly, high RSF from the draw to feed side discouraged further development in this field. In the 1990s, the development of membranes with higher selectivity and low internal concentration potential encouraged researchers to explore the potential of the FO process in concentrating liquid food and beverages [30,31]. Blandin et al. (2020) [125] summarise the opportunities and challenges of FO as a concentration process in liquid food. The article focuses on lab-sale FO experiments used for the concentration of juice, plant-based colourant, orange peel press liquor, and artificial sugar solutions. In most studies, the inorganic salts (NaCl) were used as DS, and the membranes used were of flat-sheet configuration. Table 2.5 summarises several reported studies on liquid food concentration using the FO process.

Table 2.5 Performance of FO in liquid food concentration

Draw solution	Osmotic pressure (bar)	Feed solution	Membrane type		Membrane module			Membrane orientation		FO performance	Ref.
			CTA	TFC	Flat-sheet	SW	HF	ALFS	ALDS		
Sodium chloride	276.65	Pomegranate juice	✓		✓			✓		Flux: 8.81 to 0.55 L m^{-2} h^{-1} RSF: 1.03 g m^{-2} h^{-1}	[127]
		Beetroot juice	✓		✓			✓		Flux: 12.22 - 1.29 L m^{-2} h^{-1} RSF: 7.2 g m^{-2} h^{-1}	[128]
		Grape juice	✓		✓			✓		Flux: 19.1 - 3.78 L m^{-2} h^{-1} RSF: 3.19 g m^{-2} h^{-1}	[129]
	184.73	Egg white	✓		✓			✓		Flux: 15.1 L m^{-2} h^{-1}	[130]
		Sucrose	✓		✓			✓		Flux: 5.8 L m^{-2} h^{-1}	[131]
		Apple juice		✓	✓			✓		Flux: 20.7 to 7.95 L m^{-2} h^{-1}	[132]
	138.33	Grapefruit juice		✓	✓			✓		Flux: 18.4 L m^{-2} h^{-1} RSF: 1.14 g m^{-2} h^{-1}	[133]
	78.82	Sugarcane juice		✓			✓		✓	SRSF: 1.57 g L^{-1}	[47]
	73.77	Cheese whey	✓			✓			✓	Flux: 7.6 L m^{-2} h^{-1}	[134]

Draw solution	Osmotic pressure (bar)	Feed solution	Membrane type		Membrane module			Membrane orientation		FO performance	Ref.
			CTA	TFC	Flat-sheet	SW	HF	ALFS	ALDS		
	39.41	Black tea extract		✓			✓	✓		Flux: 10.33 L m^{-2} h^{-1} RSF: 0.01 g m^{-2} h^{-1}	[48]
Sodium lactate	652	Orange juice	✓		✓			✓		Flux: 40 L m^{-2} h^{-1} SRSF: 0.3 g L^{-1}	[135]
Sodium diacetate	380	Grape juice		✓	✓			✓		Flux: 27.78 L m^{-2} h^{-1} SRSF: 0.005 g L^{-1}	[136]
Potassium sorbate	46	Grape juice		✓	✓			✓		Flux: 5 L m^{-2} h^{-1} RSF: 2.25 g m^{-2} h^{-1}	[137]

CTA: Cellulose triacetate; TFC: thin-film composite; SW: spiral wound; HF: Hollow fiber; ALFS: active layer facing feed solution; ALDS: active layer facing draw solution, RSF: reverse solute flux, SRSF: specific reverse solute flux

Summary of forward osmosis in liquid food and beverage processing industries

The feasibility of the FO process for the concentration of liquid food and beverages has been investigated by researchers. Compared to thermal processes and pressure-driven membrane separation processes, FO allows the concentrating liquid food with higher concentration while maintaining the product quality (in terms of both nutritional and sensory quality). Despite these advantages, the large-scale application of the FO process for liquid food concentration are yet to be confirmed. The following limitation needs to be addressed to make FO a commercially feasible process in liquid food concentration.

- ✓ *For developing FO for food applications, a suitable food-grade draw solute capable of generating superior FO performance and can be regenerated with energy consumption needs to be investigated. An efficient strategy for DS recovery plays a role in making the FO process economically feasible for liquid food concentration.*
- ✓ *The feasibility of hydrogel as a draw solute for the FO process has been successfully demonstrated for desalination and brackish water treatment. However, the application of hydrogel (as a draw solute) for liquid food concentration needs to be investigated.*
- ✓ *Additionally, a detailed investigation of functional design such as FS/DS flow rate, FS/DS composition, module type (flat, sheet, hollow fiber, or spiral would), module arrangements, flow orientation (co- or counter-current operations), and their effect on FO performance needs to be investigated.*
- ✓ *In the existing literature, the liquid foods are concentrated to a lower degree of concentration factor (~5 fold) and not up to their supersaturated condition.*

2.3. Modeling and Design Optimisation of Forward Osmosis Process

In recent time, HFFO membrane module has drawn significant research attention due to their high packing density and have been widely used in industries due to their economic efficiency. Due to their tubular structure, the HF membranes are mechanically more robust than flat-sheet membranes. The robustness of the HF module gives rise to the possibility of decreasing the thickness of the membrane support layer. As a result, the ICP effect reduces, and separation performance across the FO membrane enhances significantly. Numerous studies have been reported for wastewater reclamation, pesticide rejection, and similar application. However, several theoretical studies were performed to understand the fundamentals of the FO process. However, those reported studies were performed using small membranes in a laboratory-scale setup. Thus, the same study results cannot be applied to the real-scale application of FO process

using a large membrane area. Over large membrane areas, the spatial variation of DS and FS concentration across membrane areas are more profound.

Additionally, a higher pressure drop and concentration effect are found in full-scale FO systems [138]. Therefore, to exploit the FO technology to its full extent, a precise model describing all phenomena occurring during the FO process is required. The developed model should be capable of integrating membrane transport phenomena and CP throughout the module. The modeling of the membrane transport and module characteristics is considered a crucial factor for the design and performance analysis of the FO process.

Unlike HF-RO, the literature available for the HFFO membrane module is limited and has not been exhaustively investigated with experimental model validation [26,47,48,139–143]. In most studies, the ECP effect on the FS side for ALDS orientation was neglected due to low recovery from the process. However, in high recovery, it is essential to incorporate the ECP effect on the FS of the HFFO module. Thus, integrating both ECPs in the membrane transport model equation improves the estimated parameters' accuracy.

Xiao et al. (2012) [27] and Shibuya et al. (2016) [144] investigated the effect of applied hydraulic pressure, DS concentration, flow configurations, and structural parameter of HF on FO performance, and the results were theoretically validated. Using the established solution-diffusion (SD) membrane transport model, Phuntsho et al. (2014) [145] investigated the influence of various operational parameters (such as membrane area, flow configurations, and feed/ draw solution properties) on the overall process performance using a plate-and-frame FO membrane module. In the given study, the effect of both ECP and ICP was considered on FO performance. However, the studies were limited to the impact of the HFFO module length, and detailed discussions on optimisation studies were missing. Thus, a systematic study dedicated to processing optimisation using commercially available HFFO membranes must be performed [146].

Reportedly, two types of HFFO module configurations are available on an industrial scale: radial and axial flow. Considering less pressure drop in the shell side of the membrane module, the axial flow module is usually more suitable for FO applications. Unlike radial flow due to the uniform packing density of fibers. In axial flow, due to the uniform packing density of fibers, the pressure and permeate flux can be considered a function of the effective module length [147]. Tanaka et al. (2018) [148] recommend that wide and short HF module dimensions should be preferred instead of long HF membranes for superior FO performance.

Reportedly, the short membrane offers lower pressure drop than the long membrane but has a limited chemical potential exchange across the membrane. The impact of other operating conditions, such as membrane orientation, the concentration of DS, and flow rate, on overall HFFO performance, was demonstrated by Altee et al. (2019). Teklu et al. (2020) [26]developed a mathematical model for the HFFO module. The developed model was validated with experimental results to estimate the membrane parameters. The simulation results indicate that the DS flowrate was found to be the major contributor to the FO water flux at optimal module length. Reportedly, it is believed that by increasing the flow rate of the DS, the effect of CP reduces. However, this also results in improved outlet DS concentration, eventually improving the cost associated with DS regeneration. Therefore, instead of considering only the net-permeate flow rate, the optimisation of the FO should consider both the final DS concentration and net-permeate flow rate.

Summary for FO process modelling and simulation

An appropriate mathematical model for the axial flow of the HFFO membrane for a concentration of tea extract needs to be developed and validated with the experimental data. The validated model can be used for simulation study with respect to design and operating parameters to formulate an optimisation problem. The optimisation problem must be formulated to achieve maximum permeate flux and minimum SRSF.

2.4. Black Tea

Tea can be described as an infusion made from *Camellia sinensis* leaves and is considered one of the most consumed non-alcoholic beverages. According to the International Tea Committee report, the total tea consumption in the world reached above 5.8 million tons in 2019 [149]. Along with being an aromatic beverage with a refreshing taste, the consumption of tea is also associated with various health benefits characterised by its high phenolic, flavonoids, and associated anti-oxidant properties.

In India, the tea industry originated with the discovery of tea in Assam in 1823 by Robert Bush. Reportedly, in 1839 the first consignment of tea from India was shipped to London. From that day, India exports 193 million kg of tea, contributing 11% of the net share of world tea [150].

Based on the oxidation level, tea can be further classified into black, green, oolong, and white tea. Black tea is one of the popular beverages. Besides its refreshing taste, its consumption also offers everyday life anti-oxidants [151,152]. Taking account of high polyphenolic and nutraceutical properties, black tea concentrate can be potentially used for food and beverage

industries, pharmaceuticals, and edible packaging. The thermo-sensitive polyphenolic compounds are essential in terms of nutritional and flavour profile.

2.4.1. Black tea catechins

Catechins are the polyphenolic compounds in the flavonoid class in various plant-based fruits/ vegetables and beverages (such as tea and red wine) [153,154]. Catechins are usually colourless crystalline substances (with an astringent and bitter taste). They are usually soluble in polar solvents such as methanol and water. The catechin contains two aromatic rings and several hydroxyl groups, based on which they are primarily categorised as free and esterified catechins. The esterified catechins are epigallocatechin gallate (EGCg), epicatechin gallate (ECG), gallocatechin gallate, and catechin gallate, whereas the non-esterified (or free) catechins are catechin, gallocatechin, epicatechin, and epigallocatechin (EGC) [155–157]. The catechins in tea infusion are epimerised during brewing, sterilisation, or long-term heating. The catechin present in tea is sensitive to oxidation by heat, enzymes, and acid. The addition of acid (pH < 4) to the solution increases the stability of catechin. However, the stability progressively decreases with pH > 6 and thermal processing. According to the literature, catechin can potentially epimerise faster in tap water than in purified water.

Catechins are colourless and soluble in water and polar organic solvents. However, the solubility of the individual catechin varies and depends on the extraction temperature, duration, and type of solvents used (Table 2.6). The tea catechins are sensitive to acid, enzymes, and heat oxidation. The catechins are very stable in an acidic solution with (pH of less than 4). Their stability decreases as pH increases from 4 to 8 and becomes high-unstable in alkaline solutions (pH >8). The catechins tend epimerise faster in tap water than in purified water. The interaction of catechin with protein and caffeine results in formation of sediments that makes the solution look hazy when cooled down to temperatures below 10 ^{o}C.

The gallated catechin, such as EGCg and ECG has a stronger affinity to caffeine-creaming ability than ungallated catechins such as EC and EGC. The process of cream formation in tea strongly depends on pH, brewing temperature, and the presence of certain minerals such as magnesium, calcium, and aluminium. Due to its health benefits, tea consumption is highly recommended by the world health organisation (WHO). The potential health benefits associated with tea consumption are partially attributed to the anti-oxidative properties of tea polyphenols. Reportedly, tea consumption is associated with a lower risk of gastric and breast cancer metastasis and reoccurrence [158–164].

Table 2.6 Physical characteristics of major tea catechins

	EC ($C_{15}H_{14}O_6$)	EGC ($C_{15}H_{14}O_7$)	ECG ($C_{22}H_{18}O_{10}$)	EGCg ($C_{22}H_{18}O_{11}$)
Chemical structure	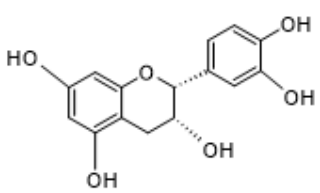	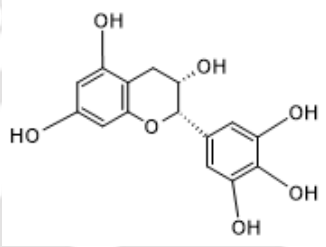	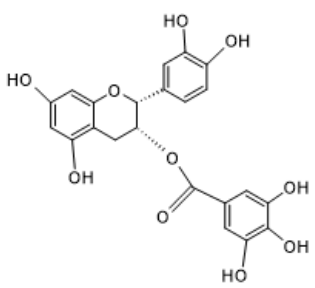	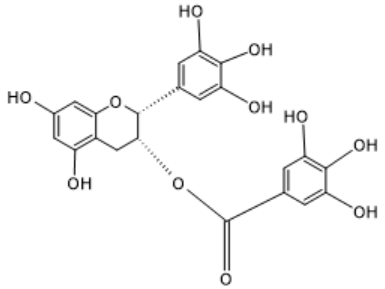
Molecular weight	290	306	442	458
Melting point (^oC)	242	218	257	224
Maximum absorbance (nm)	280	269	280	273
Solubilisation in water/methanol/ ethanol	Soluble	Soluble	Soluble	Soluble
Solubilisation in chloroform	Insoluble	Insoluble	Insoluble	Insoluble
Taste	Bitter with sweet after taste	Bitter with sweet after taste	Astringent and bitter	Astringent and bitter

EC: Epicatechin; EGC: Epigallocatechin; ECG: Epicatechin gallate; EGCg: Epigallocatechin gallate

2.4.2. Method of extraction, isolation, and concentration of tea catechins

For extraction of tea catechin, water is one the inexpensive and safest solvent, which does not leave any residues behind. However, compared to polar organic solvents (such as acetone, methanol, ethanol, or acetonitrile), water alone has the lowest catechin extraction efficiency. The extraction efficiency of tea constituents also depends on the extraction temperature. Higher extraction temperature improves the extraction efficiencies since the heat renders the cell wall resulting in improved permeability of the solvents. However, the excessive extraction temperature can also result in the degradation of catechin (by promoting the change in epi-structured catechin to non-epi-structured catechin). The solvent-to-tea ratio also plays a significant role in determining the overall caffeine and catechin extraction efficiency. Reportedly, with higher solvent-to-tea, the force driving the mass transfer of constituents from solid (say, 'tea') is greater when the solid is placed in a higher volume of solvent. Vigorous agitation during extraction increases the interaction between tea and solvent, resulting in increased extraction efficiency. Water, organic-solvent, and microwave-assisted extractions are a few widely used methods to extract tea catechins.

2.4.2.1. Water extraction method:

The water-assisted brewing process can be either performed at a lower temperature (60-80 ^{o}C) with a longer extraction time (20 min) or at a higher temperature (95 ^{o}C) with a shorter extraction time (5-10 min) to avoid catechin degradation. The solvent used for extraction also plays a significant role in the process of catechin extraction. Reportedly, the application of deionised (DI) water to extract tea components provides the most significant yield rate of catechin with low caffeine [165].

2.4.2.2. Other extraction method:

- Polar-organic solvents (such as acetonitrile, acetone, acetic acid, ethanol, methanol, and ethyl acetate) have higher catechin extraction efficiency than water alone. However, such extracts are not safe for consumption; thus, the use of such organic solvents needs to be considered carefully regarding their final use.
- Microwave-assisted extraction (MAE) is a technique used for extracting soluble products into a fluid from a wide range of materials using microwave energy. Compared to conventional heating, MAE offers certain advantages, including shorter extraction time, use of less solvent, and higher extraction rate. In MAE, microwave treatment disrupts the structure of cells due to a rapid increase in internal cell temperature and pressure. However,

compared to conventional heating for large-scale applications, the MAE is not feasible and is more difficult to scale up.

- Sub-critical water extraction (SWE) technique employs hot water at a temperature ranging from 100 to 374 ^{o}C under high pressure (10 to 60 bar). Compared to conventional extraction techniques, SWE offers a higher extraction rate. However, this process is unsuitable for extracting tea components as the elevated temperature may degrade the tea catechin.
- Ultrasound-assisted extraction (UAE), is a technique used to extract natural bioactive components. UAE provides a greater solvent penetration into the cellular matrix and thus improves the mass transfer of the constituents into the solvent. Compared to the SWE technique, UAE is conducted at lower extraction temperatures, thereby reducing the risk of catechin degradation.
- Ultrahigh pressure extraction (UHPE) technique uses high extraction pressure (100 to 800 MPa) to extract bioactive. The ultrahigh-pressure technique is a promising method for effectively extracting catechins from tea. However, further studies are needed to optimize the conditions for extracting catechins from tea.

2.4.3. Concentration of the extracted constituent

After extraction, the next step is to concentrate the tea extract to partly remove the solvent and obtain crude concentrated catechin extract. The separation step is mainly carried out using filtration or centrifugation. After the removal of the insoluble tea materials, the tea infusion consisting of the soluble substances is concentrated by lowering the volume of the extraction solvent. The concentrated tea infusions are then further dried using a rotary evaporator, freeze dryer, or a spray-dryer. Reportedly, components such as Flavan-3-ols, such as catechins and epicatechins, the main phenolic compounds in teas, are highly unstable to processing conditions. Therefore, a non-thermal technique (such as a membrane separation process) should be employed to concentrate and dry tea extract to retain tea's beneficial properties.

The available literature on the concentration of black tea extract using the membrane process was found to be very limited. Marques et al. (2016) [166], attempted to optimize the process of concentrating tea extract using osmotic evaporation. The concentration process was carried out using a hollow-fiber membrane module (0.54 m^2) and 5M $CaCl_2$ as an osmotic agent. The effect of phenolic and anti-oxidant properties was also evaluated. The study claims to reach 40% w/w concentration in 5 h with a constant water flux and no significant change in phenolic/anti-oxidant properties of a final concentrated product.

2.4.4. Identification and quantification of tea catechin

The identification and quantification of tea catechins are employed to determine the catechin concentration, yield, and purity in the final product. High-performance liquid chromatography (HPLC) is one of the most widely used methods for determining tea catechin and it enables good separations. For this analysis, a reverse phase C18 column is generally used, and the mobile phase generally consists of an aqueous solution of acetonitrile or methanol with the addition of acids such as orthophosphoric acid and acetic or formic acid. The maximum absorbance wavelength of catechin is 210 nm and 269-280 nm. Therefore, UV and diode-array detectors have been widely used to determine individual catechins.

2.4.5. Application of extracted tea catechins in food and beverage processing industries

Catechin, epicatechin, and gallates of epicatechin are the major catechins with dietary importance for human health. Catechins are used as a natural anti-oxidant in oils and fats against lipid oxidation, as an antimicrobial agent, as functional food or dietary supplements, and also as a supplement for animal feed.

Due to their high lipid content, red meat and poultry are more susceptible to lipid oxidation. Tea catechins were found to be most effective against lipid oxidation of cooked meat. Reportedly, in a study against raw beef's lipid oxidation, tea catechins' anti-oxidant activity was superior to sodium ascorbate acid at the same concentration. The lipid oxidation of animal fats is more likely to occur during the extended storage period at refrigerated conditions. Tea catechins have the potential to be utilized in muscle food for the inhibition of lipid oxidation during storage. The anti-oxidant properties of catechins (200 mg L^{-1}) were higher than tocopherol at the same concentration. Tea catechins can scavenge DPPH radicals and chelate Fe^{2+}. Compared to rosemary, tocopherol, phospholipid, and ascorbyl palmitate, the catechin provides increased stability of peanut oil against lipid oxidation. The antimicrobial activity of EGCg against various strains of *Staphylococcus* and gram-negative rods, such as *E. coli, K. pneumonia*, and *Salmonella typhi*, was reported by Yoda et al. (2004) [167]. Tea catechins such as EGCG and epicatechin inhibit the growth of *Helicobacter pylori*, a common ulcer-causing bacterium.

Functional food can be defined as a food or food ingredient that provides a health benefit beyond satisfying traditional nutritional requirements. Tea catechins are considered an essential functional group for improving oral health. Tea polyphenols can potentially prevent dental plaque formation and treat hypertension. The anti-oxidative activity of catechins makes

catechins a potential candidate as a functional ingredient for food and beverages. Applying green tea extract (GTE) in foods such as cakes, cereals, biscuits, dairy products, ice cream, and confectionery provides a healthier appeal to the consumer regarding the overall product [168].

Thereby suggesting that the concentrated tea extract can be:

(i) Directly used as RTD beverages (as tea concentrate or tea powder) or

(ii) It can be indirectly used as a functional food by incorporating tea catechin in food (baked goods or beverages) to improve the product marketing potential.

2.5. Instant Tea

The formulation of instant ready-to-drink (RTD) tea was first reported in the early 20th century to cater to the RTD ice tea market [52,169]. With the increasing consumer demand for RTD, traditional tea brewing cannot meet the requirement of young consumer groups in expanding markets, which promotes the development of tea beverages. Reportedly, tea beverages can be classified into two categories, namely liquid tea beverages (tea concentrate, RTD tea beverage, tea wine, and kombucha) and solid (powdered) tea drinks (instant tea, solid milk tea). With the improvement of consumers' living standards, the sensory quality and health benefits of tea beverages are becoming more critical.

Black tea products such as instant tea have recently gained consumer acceptability due to their simplicity in preparation [169,170]. Generally, tea beverages are divided into three categories: RTD tea beverages, instant tea, and tea concentrate. Tea concentrate has been used as the raw material of RTD tea beverages, while in recent years, it has been used to make novel tea beverages (an instant drink made of tea products as the primary raw material and mixed with milk, fruit, and other materials on site) [171]. Instant tea powder can be a fully soluble tea solid that have emerged as a new and fast-growing product. Instant tea is manufactured from black tea by extracting the brew from processed tea leaves, tea wastes, or undried fermented leaves. The extract is concentrated using vacuum-drying, freeze-drying or spray-drying technique. The elevated temperature during spray-drying increases the chances of generating oxidation reactions leading to the formation of unflavoured molecules in the dried tea powder [172]. Sinjia et al. (2007) [173] developed a method for producing instant tea powder by drying tea extract using a vacuum drying technique.

The organoleptic appeal of tea correlates to the presence of essential volatile components (such as hexanal, geraniol, citral, cis-jasmon α-ionone, Nerol, and E-2-Z-4-hexadienal) in tea [174]. During the manufacturing of cold soluble instant tea, volatile chemicals with desirable aroma

notes can be escaped, thus affecting the aroma profile of instant tea and instant tea-based products. Thereby, research on developing novel technologies for preparing tea concentrates that are not detrimental to heat-sensitive biological compounds is urgently needed.

2.6. Literature Closure and Research Gaps

(i) Due to mild operating conditions, the FO process has been widely investigated as a potential candidate for liquid food concentration.

(ii) The availability of a suitable draw solute plays a vital role in the overall FO operation.

(iii) Low permeate flux is a significant concern in the FO process. Thus, the utilisation of a modified membrane in the application of liquid food concentration is needed.

(iv) The alternate strategies for draw solution regeneration are essential in realising FO-based concentration techniques' economic feasibility for liquid food concentration.

Chapter 03

Theory

Abstract: *In this chapter, the theory related to developing a one-dimensional mathematical model for the concentration of tea extract has been briefly described. Further, the application of these models in the process design and simulation is briefed with respect to tea extract concentration.*

In this study, the mathematical model for the unsteady-state one-dimensional FO process was developed by integrating a system of model equations such as:

(i) Tank model for unsteady mass balance equation across feed solution and draw solution tank,

(ii) Solution diffusion (SD) model for membrane active layer transport, and

(iii) Film theory model for mass transport in internal concentration polarisation (ICP) and external concentration polarisation (ECP) layer.

A one-dimensional mathematical model for the lab-scale FO process, the whole HFFO process is subdivided into three pieces of equipment: the HFFO membrane module, the draw solution tank, and the feed solution tank (Figure 3.1) [48].

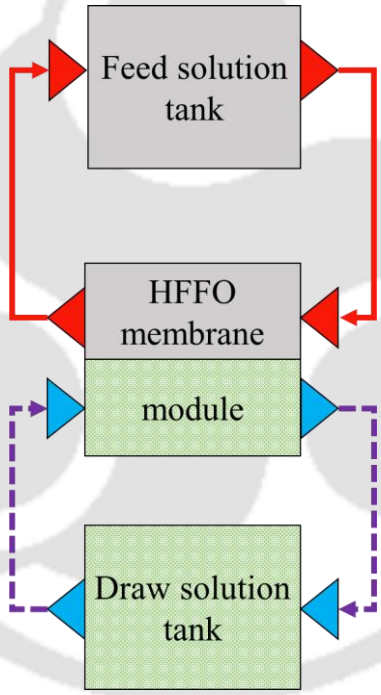

Figure 3.1 Flow sheet for lab-scale hollow fiber forward osmosis process modelling

3.1. Development of a One-Dimensional Mathematical Model for the Concentration of Tea Extract Using Forward Osmosis Process

In an osmotically-driven membrane process, the water (solvent) permeation flux (J_w) across a semi-permeable membrane that allows water passage but rejects solute or ion molecules. The term water flux (J_w) is related to pure water permeability (L_p), osmotic pressure gradient ($\Delta\pi$), and hydraulic transmembrane pressure gradient (ΔP):

$$J_w = L_p(\Delta\pi - \Delta P) \quad (3.1)$$

The term Δπ represents the osmotic pressure gradient at the surface of the active layer (AL) and the interface of the support and active layers.

The solute permeates across the membrane in the opposite direction of the water flux (i.e., from draw to feed solution). The reverse solute flux (J_s) is a function of the solute permeability coefficient (B) of the membrane AL and the solute concentration gradient at the membrane AL.

$$J_s = B(C_{dm} - C_{fm}) \quad (3.2)$$

where, C_{dm} and C_{fm} represents the concentration of DS and FS on the membrane active layer surface, respectively.

The specific reverse salt flux (SRSF, g L^{-1}) can be defined as a ratio of RSF (J_s, g m^{-2} h^{-1}) and water flux (J_w, L m^{-2} h^{-1}):

$$SRSF = \frac{J_s}{J_w} \quad (3.3)$$

3.1.1. Overview of hollow fiber forward osmosis (HFFO) membranes

In this work, an axial flow Aquaporin inside hollow fiber forward osmosis (HFFO) membrane module was used for batch-scale FO experimental studies. The flow configuration of the HFFO membrane module is shown in Figure 3.2. Depending upon the membrane orientation, the FS and DS are allowed to pass through either shell lumen side of the membrane module. Due to the continuous dilution and concentration of DS and FS, a non-uniform osmotic driving force is present along the length of the module. Unlike radial-flow HFFO mathematical model, feed and draw solution concentrations are expected to vary along the axial direction [175]. Thereby, a precise mathematical model for the axial flow HFFO model is vital to predict and optimize the overall HFFO membrane performance.

The mathematical model proposed in this work is primarily intended to be used for the experimental validation of liquid food concentration. Further, the validated model can be potentially used to optimize the HFFO membrane module design and operating condition.

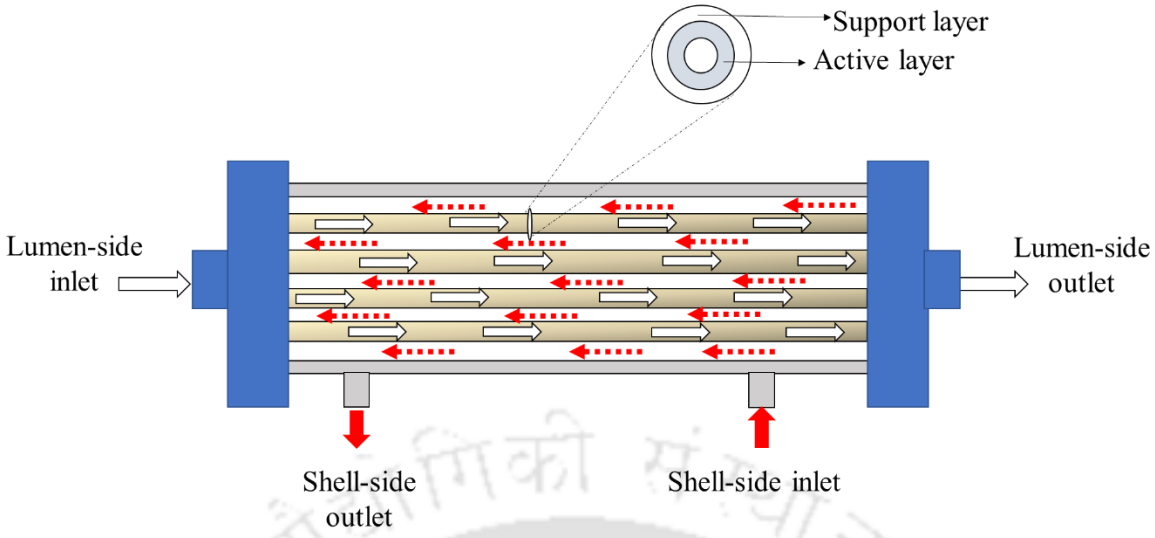

Figure 3.2 Hollow fibre forward osmosis membrane module in the counter-current flow configuration

3.1.2. Flux equation for FO membranes

The solute-diffusion (SD) model has been a widely used transport model to express solute and solvent diffusion through the membrane separation layer [176,177]. The SD model assumes that the solute and solvent are first adsorbed on the dense membrane separation layer and then diffused from high to low chemical potential. The solvent and solute flux through the membrane in the SD model is defined by water permeability (*A*) and solute permeability (*B*) coefficients. The governing equations for solvent flux (L m^{-2} h^{-1}) and reverse solute flux (g m^{-2} h^{-1}) is represented by the following equations [141]:

$$J_w = L_p[(\Delta\pi_{dm,NaCl} - \Delta\pi_{fm,NaCl} - \sum_{i=1}^{n}\pi_{fm,tea_i}) - (P_d - P_f)] \quad (3.4)$$

$$J_{s,NaCl} = B(C_{dm,NaCl} - C_{fm,NaCl}) \quad (3.5)$$

where, L_p, B, P, and C are solvent permeability coefficient (L m^{-2} h^{-1} bar^{-1}), solute permeability coefficient (L m^{-2} h^{-1}), trans-membrane pressure (bar), and concentration (g L^{-1}) of the draw and feed side respectively. The π_{dm} and π_{fm} represents the osmotic pressure at the active layer of the membrane surface on the draw and feed side, respectively. The experimental results concluded that the forward flux of the tea component is zero (i.e. $J_{s,tea} = 0$). The osmotic pressure plays a significant role in determining the overall FO performance. Therefore, the determination of appropriate osmotic pressure is crucial. Khraisheh et al. (2020)

[178] stated that the water activity (a_w) provides a better correlation of experimental data than the classical van't Hoff equation.

The van't Hoff equation assumes a linear correlation between the osmotic pressure and the solution concentration. The linear assumptions are considered accurate for low-concentration (or ideal) solutions. However, the deviation from the ideal behaviour is more prominent for high concentration. In this study, the bulk osmotic pressure (π) for FS and DS is calculated considering water activity (a_w) [179]:

$$\pi = -\left(\frac{RT}{V}\right)\ln(a_w) \tag{3.6}$$

where, *R*, *T*, *V*, and a_w represents the gas constant, temperature, molar volume, and water activity.

The water activity (a_w) is estimated using the Pitzer equation:

$$a_w = \exp\left(-0.01802\phi\sum_i M_i\right) \tag{3.7}$$

where, ϕ and *M* represents the osmotic coefficient and molality of solutes per kg of solvent, respectively.

3.1.3. Concentration polarisation

Concentration polarisation (CP) is inevitable in any membrane process and significantly influences solvent movement through the membrane[180]. Due to CP, the real osmotic pressure difference between the inlet FS and DS are much lower, thus resulting in the actual permeate flux being much lower than expected. FO membranes usually consist of an active layer (AL) and a porous support layer (SL). The membranes can be either used with (Figure 3.3) [71,181,182]:

a) Active-layer-facing-FS (ALFS or FO-mode): The ALFS generates concentrative ECP (CECP), thus resulting in FS solute deposition on the AL surface. Furthermore, DS dilution with SL results in dilutive ICP (DICP), reducing water and RSF from bulk DS to the interface of the membrane.

b) Active layer facing DS (ALDS or PRO-mode): The permeate flows through SL without hydraulic resistance in ALDS mode. However, since the solutes of FS may come along with water and get trapped in the porous SL. The accumulation of the FS solutes within the SL may

create concentrative ICP (CICP). Similarly, on AL, the accumulation of transported water molecules dilutes DS, thus generating dilutive ECP (DECP).

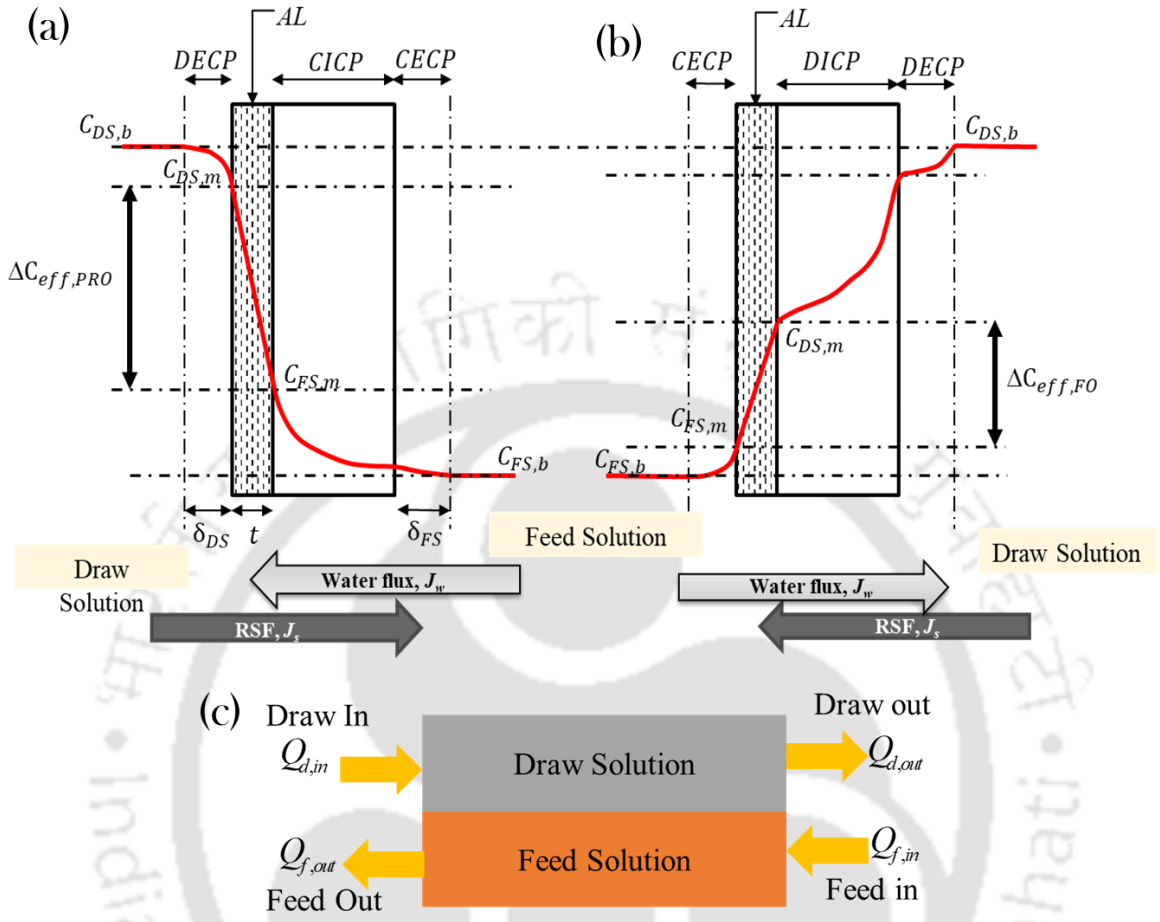

Figure 3.3 Solute concentration profile for (a) ALDS (PRO) mode, (b) ALFS (FO) mode [Note: osmotic pressure gradient, $\Delta\pi = \left(\pi_{D,b} - \pi_{F,b}\right)$ and effective osmotic pressure gradient, $\Delta\pi_{eff} = \left(\pi_{D,b} - \pi_{F,b}\right)$, and (c) Mass balance for feed and draw solution components across HFFO membrane module

Figure 3.3 (a) demonstrates the concentration gradient across a thin film composite membrane operating in ALDS mode (the porous support layer facing the feed solution). The effective driving force for osmosis exists only at the interface of the selective (active) layer. Theoretically, the feed solution from bulk must diffuse through the porous support layer to the interface between the active and support layer. As water permeates from the draw solution to the feed solution, it dilutes the draw solution on the porous support layer and draw side boundary layer resulting in dilutive internal and external CP. At the same time, solute diffuses

from bulk through porous support to the interface of support and the separation layer due to the concentration gradient from the dilution of the draw solution.

In ALDS mode, due to water permeation from FS to DS side. The DS becomes diluted at the vicinity of AL; this phenomenon is commonly termed as a dilutive external concentration polarisation (DECP). Whereas the membrane is permeable to water only, and the solute in the membrane accumulates inside the support layer of the membrane, this phenomenon is called internal concentration polarisation (ICP).

$$C_{dm} = \frac{J_S}{J_w}\exp\left[\frac{-J_w}{k_d} - 1\right] + C_{db}\exp\left[\frac{-J_w}{k_d}\right] \tag{3.8}$$

where, C_{dm} and C_{db} represents the concentration of DS on membrane surface and bulk. The term k_d, J_w, and J_s denotes the mass transfer coefficient of DS, water flux, and reverse solute flux.

$$C_{fm} = C_{fb}\exp\left[J_w\left(\frac{1}{k_f} + \frac{S}{D_d}\right)\right] + \frac{J_S}{J_w}\exp\left[J_w\left(\frac{1}{k_f} + \frac{S}{D_d}\right) - 1\right] \tag{3.9}$$

The term C_{fm} denotes the FS concentration at the selective support layer interface and can be expressed as the sum of the two components. The first component is expressed in terms of concentrative internal and external concentration polarisation, whereas the second component is associated with reverse solute flux (RSF).

The water and reverse solute flux were expressed in terms of the structural parameter (S), pure water permeability (L_p), solute permeability coefficient (B), and mass transfer coefficient (k).

The mass transfer coefficient 'k' for the DS and FS side of the membrane module was calculated using (3.10 and 3.11), where the term D, Sh and d_h represents the diffusion coefficient, Sherwood number, and hydraulic diameter, respectively:

$$k_d = \frac{DSh_d}{d_{i,\,fiber}} \tag{3.10}$$

$$k_f = \frac{DSh_f}{d_{o,\,fiber}} \tag{3.11}$$

Sherwood number (Sh) is a function of two other dimensionless numbers, Reynolds number (Re) and Schmidt number (Sc):

$$Sh_d = \alpha_d \, \mathrm{Re}_d^{\beta_d} \, Sc^{\gamma_d} \tag{3.12}$$

$$Sh_f = \alpha_f \, \mathrm{Re}_f^{\beta_f} \, Sc^{\gamma_f} \tag{3.13}$$

where, the terms α_f, α_d, β_f, β_d, γ_f, and γ_d are considered as the tuning parameters which are determined during model validation. The Schmidt number (*Sc*) for FS and DS can be expressed as:

$$Sc_f = \frac{\mu_f}{\rho_f D_f} \tag{3.14}$$

$$Sc_d = \frac{\mu_d}{\rho_d D_d} \tag{3.15}$$

where the term ρ, μ, and D represent density, dynamic viscosity, and diffusion coefficient, respectively.

The mass transfer coefficient is expected to vary with time as the FS becomes concentrated due to the changes in FS density and viscosity.

3.1.4. Mass balance equation for HFFO membranes

The mass balance across the FS tank can be represented as:

$$\left(Q_{f,in} - Q_{f,out}\right) = J_w A_m \tag{3.16}$$

$$\left(Q_{f,out} C_{f,out}\right) - \left(Q_{f,in} C_{f,in}\right) = J_{s,NaCl} A_m \tag{3.17}$$

$$\left(Q_{f,out} C_{f,out,tea_i}\right) - \left(Q_{f,in} C_{f,in,tea_i}\right) = J_{s,tea_i} A_m \tag{3.18}$$

Similarly, the equation (3.19 and 3.20) represents the net mass balance across the DS tank:

$$\left(Q_{d,in} - Q_{d,out}\right) = -J_w A_m \tag{3.19}$$

$$\left(Q_{d,in} C_{d,in}\right) - \left(Q_{d,out} C_{d,out}\right) = J_s A_m \tag{3.20}$$

where, the terms *C*, A_m, and *Q*, represent the concentration, active membrane area, and flow rate, respectively.

3.1.5. Tank mass balance equation

The unsteady state mass balance equation determines the change in volume and Concentration in FS and DS tanks during the FO process. The equation (3.27 to 3.30) depicts the mass balance for the FS tank:

$$\frac{dV_f}{dt} = \left(-Q_{f,out} + Q_{f,in}\right) \tag{3.21}$$

$$\frac{d\left(V_f C_{f,out,NaCl}\right)}{dx} = \left(-C_{f,out} Q_{f,out,NaCl} + C_{f,in} Q_{f,in,NaCl}\right) \tag{3.22}$$

$$\frac{d\left(V_f C_{f,out,tea_i}\right)}{dx} = \left(-C_{f,out} Q_{f,out,tea_i} + C_{f,in} Q_{f,in,tea_i}\right) \tag{3.23}$$

$$M_f = \frac{V_f}{\rho_f} \tag{3.24}$$

For an ideal solution, $\rho_f = \rho_{water} + C_f$

Similarly, the mass balance for DS can be represented using equation (3.25 to 3.27):

$$\frac{dV_d}{dt} = \left(Q_{d,in} - Q_{d,out}\right) \tag{3.25}$$

$$\frac{d\left(V_d C_{d,out,NaCl}\right)}{dt} = \left(Q_{d,in} C_{d,in,NaCl} - Q_{d,out} C_{d,out,NaCl}\right) \tag{3.26}$$

$$M_d = \frac{V_d}{\rho_d} \tag{3.27}$$

For an ideal solution, $\rho_d = \rho_{water} + C_d$

3.1.6. Methods for solving the model equation and membrane parameter estimation

For developing a one-dimensional mathematical model of the given HFFO membrane module, the n-number of the continuous stirred tank (CST)/finite volume units connected in series is assumed to be equivalent to plug-flow (PF) configuration. An individual model for CST was developed by solving equations (3.4 to 3.22), and by integrating the equation (3.23 to 3.27), a dynamic lumped system model of FS and DS was developed. The complete FO flow-sheet model was developed by integrating FS-tank, DS-tank, and HFFO model equations. The

Dymola software (DynaSim AB, Sweden) was used to develop the flow-sheet model and solve the model equation.

Further, the developed model was used to estimate the membrane transport parameters by minimising the error between the model and experimental data using the Dymola design library [26]:

$$Error = \sum_{t=0}^{t} \left[\left(\frac{M_{d,\exp} - M_{d,\mathrm{mod}}}{M_{d,\exp}} \right)^2 + \left(\frac{M_{f,\exp} - M_{f,\mathrm{mod}}}{M_{f,\exp}} \right)^2 + \left(\frac{C_{d,\exp} - C_{d,\mathrm{mod}}}{C_{d,\exp}} \right)^2 + \left(\frac{C_{f,\exp} - C_{f,\mathrm{mod}}}{C_{f,\exp}} \right)^2 + \sum_{i=1}^{8} \left(\frac{C_{f,tea_i,\exp} - C_{f,tea_i,\mathrm{mod}}}{C_{f,tea_i,\exp}} \right)^2 \right] \quad (3.28)$$

where, M and C denote the mass and concentration, whereas the subscript exp and mod represent the experimental and model outputs, respectively. The number of essential tea components is identified as 'i'= 8.

The lower and upper bounds for the estimated membrane parameters were:

0.07< L_p<0.99; 0.02< B <0.09; 0.00019< S < 0.00023; 0.01< α_f <1.85; 0.01< α_d <1.85;

0.01< β_f <2; 0.01< β_d <2; 0.32< γ_f <0.34; 0.32< γ_d <0.34

The number of CST units in the HFFO module is a critical parameter to minimise the overall simulation time. To estimate the optimal number of CST-unit, the HFFO module was simulated by increasing the number of CST from 1 to 20. The simulation results were analysed by comparing the improvement in the model prediction against the number of CST units.

Apart from those mentioned above, the following are the assumptions made while developing the given model [183]:

- The FS and DS behave like an ideal solution
- The temperature is constant throughout the experiments
- The permeate flux (J_w) is directed from FS to DS
- The reverse solute flux (J_s) is directed from DS to FS
- The membrane parameters are constant during the experiment
- The diffusion coefficient (D) is constant during the experiment
- Fouling does not occur
- The fluxes axial across the membrane are constant; no local dependencies are assumed

3.2.Process Flow-Sheet Simulation

To estimate the optimal process design for essential tea concentrate and FO performance. A series of simulation studies were reported in this section with different flow rates and DS concentrations. Figure 3.4 represents the different cases of FO process configurations, and Table 3.1 summarises the attributes of the given FO configurations.

Table 3.1 Attributes of different FO configurations

	No. of FO module	No. of pump	No. of FS tank/ Mode of circulation	No. of DS tank/ Mode of circulation
Case I	01	02	02/ Continuous	02/ Continuous
Case II	02	02	02/ Continuous	02/ Continuous
Case III (a)	02	03	02/ Continuous	04/ Continuous
Case III (b)	08	09	02/ Continuous	16/ Continuous
Case IV	01	02	01/ Recycle	01/ Recycle
Case V	02	02	01/ Recycle	01/ Recycle
Case VI	02	03	01/ Recycle	02/ Recycle
Case VII	02	03	01/Recycle	04/ Recycle
Case VIII	02	02	01/ Recycle	02/ Continuous

The trade-off between the net permeates flow-rate, specific energy consumption, and SRSF for the given FO membrane was analysed based on the decision variables, such as DS and FS flow rate of the inlet stream. To meet the conflicting nature of the objective function (that includes high permeate flux and low SRSF), a multi-objective optimisation (MOO) problem was formulated. The given decision variables include DS and FS flow rate (L h^{-1}), and the corresponding lower and upper bounds were: 25≤ Q_{DS} ≥60 and 25≤ Q_{FS} ≥60. The constraints for the given optimisation study involve feed solution volume reduction by >91%. The best-performing flow configuration was further investigated to check the feasibility of high-concentration reject brine (from a desalination plant) as DS for the concentration of liquid food extract using the FO process. The detailed methodology of process flow sheet simulation and optimisation is mentioned in Section 5.3.2.

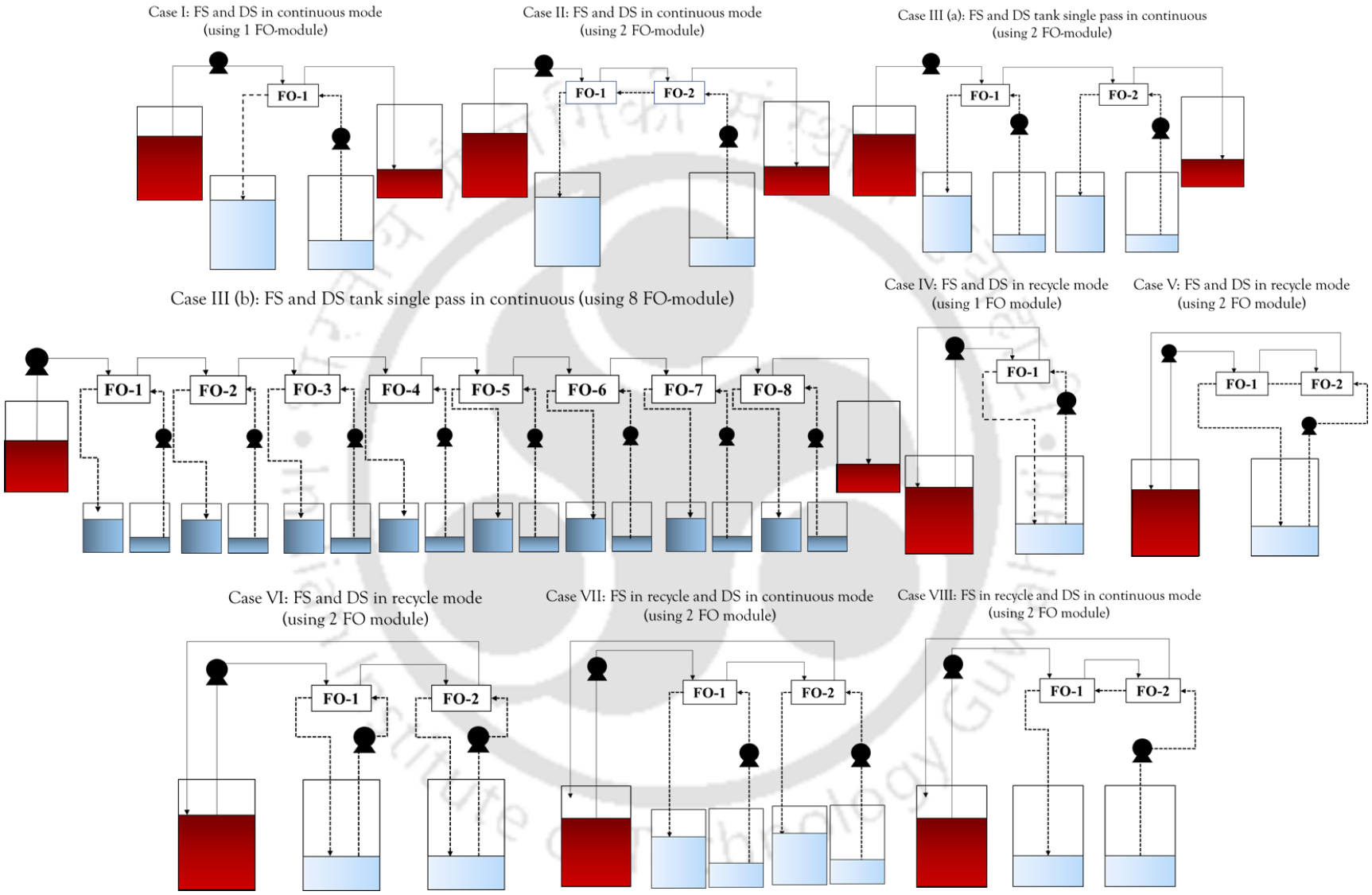

Figure 3.4 Different system process configurations for the preparation of tea concentrate using the forward osmosis process

Chapter 04

Materials, methods, and experimental procedure

Abstract: *This chapter details all the analytical procedures and protocols employed in characterising the samples. This section also details the methodologies and experimental procedures used for selecting suitable draw solutions and membranes for the concentration of tea extract using the FO process.*

4.1. Materials

Black tea leaves were generously supplied by Unilever India (Bangalore). Analytical grade inorganic salts (such as sodium chloride, sodium sulphate, magnesium chloride, and potassium chloride) were purchased from Himedia (India). For the synthesis of hydrogels, the polymers (such as polyvinyl alcohol 'PVA', poly (diallyl dimethylammonium chloride) 'polyDADMAC'), and monomers (such as acrylic acid and N-Isopropyl acrylamide 'NIPAM') were purchased from Sigma-Aldrich. The cross-linker (such as N, N′-Methylene bis-acrylamide solution 'MBA' and glyoxal), and initiator (ammonium persulphate 'APS') was purchased from Merck. HPLC-grade acetonitrile and methanol were purchased from Merck (India). The standards for essential tea components were purchased from Catechin (C), Epicatechin (EC), Epigallocatechin (EGC), Epigallocatechin gallate (EGCg), Epicatechin gallate (ECG), gallic acid, and caffeine anhydrous were purchased from Sigma Aldrich. The hollow fiber forward osmosis (HFFO) membrane module and flat-sheet membrane used in this were supplied by Aquaporin Asia Pvt. Ltd (Singapore) and DOW Filmtech (India). All the chemicals used in this study were of high grade and were further used without any modifications.

4.2. Methodology

4.2.1. Preparation of feed solution

For the preparation of the FS, a freshly brewed tea extract was prepared by brewing 100 g of dried tea leaves in 1000 mL of DI water at 95 ^{o}C for 10-15 min. The brewing was performed in a closed vessel under atmospheric conditions to minimise the degradation of essential tea components. The brewed tea extract was allowed to cool to room temperature and sieved using a cloth filter followed by a UF membrane (pore size: 0.4 µm) to remove suspended solids.

4.2.2. Selection of draw solution

4.2.2.1. Inorganic salt

For the preparation of DS, a certain amount of inorganic salts was dissolved in DI water at room temperature under atmospheric conditions. Table 4.1 summarises the physiochemical properties of inorganic salt used for the preparation of DS.

Since FO is a concentration-driven membrane separation process. The osmotic pressure plays a significant role in selecting appropriate DS for the given process. In this study, a different composition of DS was prepared by dissolving inorganic salts (monovalent or multivalent inorganic salts) at different compositions under atmospheric conditions. The osmotic pressure

of the prepared DS was measured in terms of osmolality using a freezing point ohmmeter (Osmometer basics, Type 7/7 / M/s Löser Messentechnik, Berlin).

Table 4.1 Physiochemical properties of inorganic salts used for the preparation of concentrated tea extract

	NaCl	$MgCl_2.6H_2O$	KCl	Na_2SO_4
Molecular weight (g/ mol)	58.5	203.31	75.55	142.04
Density (g/ cm^3)	2.17	1.569	1.98	2.66
Solubility (g/L) (at 25 ^oC)	360	2350	355	281
Food-grade	Yes	Yes	Yes	Yes
Taste and Odour	Salty	Bitter	Bitter-metallic	Bitter

4.2.2.2. Hydrogel

In this study, a series of thermo-responsive hydrogels were synthesised, and their feasibility as DS for the concentration of liquid food (tea extract) was determined based on their swelling capacity, FO performance, and, most notably based on their ability to regenerate.

4.2.3. Selection of suitable forward osmosis membrane

In this study, two commercially available hollow fiber forward osmosis membranes were used to investigate the role of the suitable membrane in the FO process. A Toyobo hollow fiber forward osmosis membrane (HFFO), supplied by Toyobo Co. Ltd, Japan (with an active membrane area of 30.5 m^2), whose cellulose triacetate (CTA) hollow fibers have been used extensively in various desalination industries. The Aquaporin embedded HFFO membrane (purchased from Aquaporin M/s, Denmark) with an effective area of 2.3 m^2 was used for the FO experiments. The support layer of the membrane is composed of a polyester (PE) mesh embedded on a polysulfone (PSF) substrate, and the active layer is formed by a polyamide (PA) dense selective layer with integrated aquaporin proteins coated on the lumen side of the hollow fibers [141]. Reportedly, the addition of aquaporin water channels into the rejection layer makes the membrane capable of rejecting difficult contaminants and preserving valuable components. The pore-forming protein is integrated into the PA active layer of the FO

membrane to facilitate gradient water diffusion, resulting in enhanced water permeability. The HFFO module specifications for both HFFO membranes are summarised in Table 4.2 [26,76].

Table 4.2 Specification of HFFO membranes

	Aquaporin inside HFFO membrane	Toyobo HFFO membrane
Manufacturer	Aquaporin A/s (Denmark)	Toyobo Co. Ltd, (Japan)
Module type	HF	HF
Membrane material	Aquaporin protein embedded in polyamide	Cellulose triacetate
Active membrane area	2.3 m^2	30.5 m^2
Number of fibres	13000	
Fibre dimension		
ID (µm)	195	85
OD (µm)	230	175
Pure water permeability coefficient, L_p ($L/m^2\,h\,bar$)	0.43	0.27
Solute permeability coefficient, B ($L/m^2\,h$)	0.05	0.08
Structural parameter (µm)	210	1024
pH	2−10	3-8
Maximum operating pressure		
Pressure (psi)	58	30
Temperature (^oC)	10-30	5-40
Flowrate (L/h)		
Shell side:	25	78
Tube side:	60	132
Free chlorine tolerance (mg/L)	< 0.1	< 0.1

4.2.4. Analytical methods

4.2.4.1. High-performance liquid chromatography analysis

The quality of concentrated tea extract (liquid food) was estimated in terms of the change in the concentration of the essential tea components. The change in the concentration of essential tea components was estimated using a high-performance liquid chromatography 'HPLC' (M/s Shimadzu, Singapore) system comprising the auto-sampler, pump, vacuum degasser, and diode array detector. A C18 reversed-phase (Ascentis® C18, 5 µm; dimension: 25 cm x 4.6 mm) was operated at room temperature using the isocratic method. For accurate detection of the tea components, a standard solution of catechin, epicatechin (EC), epigallocatechin (EGC), epigallocatechin gallate (EGCg), epicatechin gallate (ECG), caffeine, gallic acid, and L-theanine were prepared, ranging from 1 to 140 mg L^{-1} concentration. A calibration curve (concentration vs. area) was plotted and used to determine the concentration of essential components (Table A1.2). For HPLC analysis, 1 mL of the sample was filtered (0.2 µm filter) to remove particulate matter from the sample. The filtered sample was then diluted with DI water in a ratio of 1:100. For the given study, the selected components of the mobile phase were methanol/DI water/ Ortho-phosphoric acid (100/399.5/0.5) at 1.0 mL min^{-1} flow rate [184] at 210 nm for 50 mins [185].

4.2.4.2. Ion chromatography analysis

The change in draw solute concentration in the FS tank was estimated using ion chromatography (M/s Metrohm, Switzerland). The columns used for cation and anion analysis are Metrosep C4 (150/4.0) and Metrosep A Supp 5 (250/4.0). For cation (Na^+, K^+, and Mg^{2+}), the mobile phase is prepared by mixing 1.7 mM of Nitric acid, and 1.7 mM of DPA to 1 L of DI distilled water with a flow rate of 0.9 mL min^{-1}. For anion (Cl^- and SO_4^{2-}) the mobile phase is prepared by mixing 3.2 mM of sodium carbonate and 0.5 mM of sodium bicarbonate in 1 L of DI distilled water with a flow rate of 0.7 mL min^{-1}. The FS were diluted (1:100) and filtered using a 0.22 µ syringe filter to remove particulate matter from the sample. Using an auto-calibration mode, the anion and cation concentrations were estimated using four standard solutions (M/s Sigma Aldrich) at 0.5, 1, 5, and 10 mg L^{-1} concentrations.

4.2.4.3. Fourier transformed infrared (FTIR) analysis

Attenuated total reflectance Fourier transform infrared spectroscopy (ATR–FTIR, make: PerkinElmer, Inc., USA) was used to confirm the prepared hydrogel's structural confirmation.

The scanning was conducted using an ATR mode with a spectral range of 4000-400 cm^{-1} and a resolution of 4 cm^{-1}.

4.2.4.4. Field emission scanning electron microscope analysis

A field emission scanning electron microscope (FESEM) (Make: Zeiss, Germany, Model: Sigma 300) was used to determine the synthesis of hydrogel morphology. For morphological analysis of the synthesised hydrogel, the finely powdered samples were placed over a carbon tape, and the instrument was operated at 7 kV.

4.2.4.5. Energy dispersive X-ray (EDX)

The elemental composition analysis of the synthesised hydrogel was evaluated using energy dispersive energy X-ray (EDX) spectroscopy (Make: Zeiss, Germany, Model: Sigma 300). The analysis was performed on uncoated samples at 20 kV.

4.2.4.6. Contact angle

The water contact angle of the synthesised hydrogel samples was measured via the sessile drop method using a goniometer (Holmarc Opto-Mechatronics Pvt. Ltd.).

4.2.4.7. UV spectrophotometer

The total polyphenol content (TPC) and total theaflavin content was determined using a UV-spectrophotometer (Make: PerkinElmer, Singapore; Model: Lambda 45).

The total polyphenol content was determined according to the method described in the literature [186]. 1 mL of sample is mixed with 5 mL of 1:10 FC reagent in water, followed by the addition of 4 mL of 7.5 wt.% of Na_2CO_3. The reaction mixture was allowed to stand for 60 minutes, and the absorbance was measured at 765 nm in a UV-vis spectrophotometer.

Fo the determination total theaflavin (TF) in the given sample, a mixture of 6 g of sample and 250 mL of DI water is boiled at 90 ^oC for 10 min. The infusion is then filtered and allowed to cool to room temperature. The 6 mL of the prepared tea extract is mixed with an equal volume of 1% (w/v) disodium hydrogen phosphate (Na_2HPO_4). Then, 10 mL of ethyl acetate is added to the above solution mixture and shaken vigorously for 1 min. After shaking, it is observed that the solution gets fractionated. The top fraction of the solution is collected, and the absorbance is measured at 380 nm against the reference (1:1.5 ratio of ethyl acetate: methanol) solution.

4.2.5. Experimental Setup for HFFO module performance study

To understand the effect of membrane orientation on the overall FO performance for the preparation of concentrated tea extract. The initial experiments were performed in both FO and PRO modes against monovalent inorganic salt (NaCl, 50 g L^{-1}) solution as DS. Figure 4.1 demonstrates the schematic representation of the lab-scale experimental set-up in both FO (ALFS) and PRO (ALDS) modes of the FO process.

4.2.5.1. Single component inorganic salt solution as draw solution

Depending upon the membrane orientation, the FS and DS are pumped (Model: VND-380-SP1, M/s Lunar Motors, India) through the shell or tube side of the HFFO membrane module. The flow rate of FS and DS were maintained using a flow meter (Model: RAKD-41, M/s Yokogawa). Using a digital conductivity meter (HANNA edge ® M/s HANNA Instruments, India), the change in TDS of FS and DS was measured. The experiments were conducted at room temperature (26.5±1 ^{o}C). A digital weighing scale (M/s Weighing solutions and Instrumentation, Delhi, India) was placed under the feed tank and the draw tank to measure the change in permeate flux. 1 mL of the sample was collected from the feed and draw tank at regular intervals using a micro-pipette (M/s Tarsons Product Pvt. Ltd., India) and stored at the refrigerated condition for the analysis of change in concentration of FS and DS, respectively.

The permeate and reverse solute fluxes are estimated as given below:

$$J_w = \frac{\Delta V_{FS}}{A_m \times \Delta t} \tag{4.1}$$

where, ΔV_{FS} represents the change in volume (L) of FS in time 'Δt' (h) and A_m represents the membrane area (in m^2).

$$J_s = \frac{\Delta\left(V_{FS} \times C_{FS}\right)}{A_m \times \Delta t} \tag{4.2}$$

where, ΔV_{FS} and ΔC_{FS} represents the change in volume and concentration of feed solution in time 'Δt' (in h) and A_m represents the membrane area (in m^2).

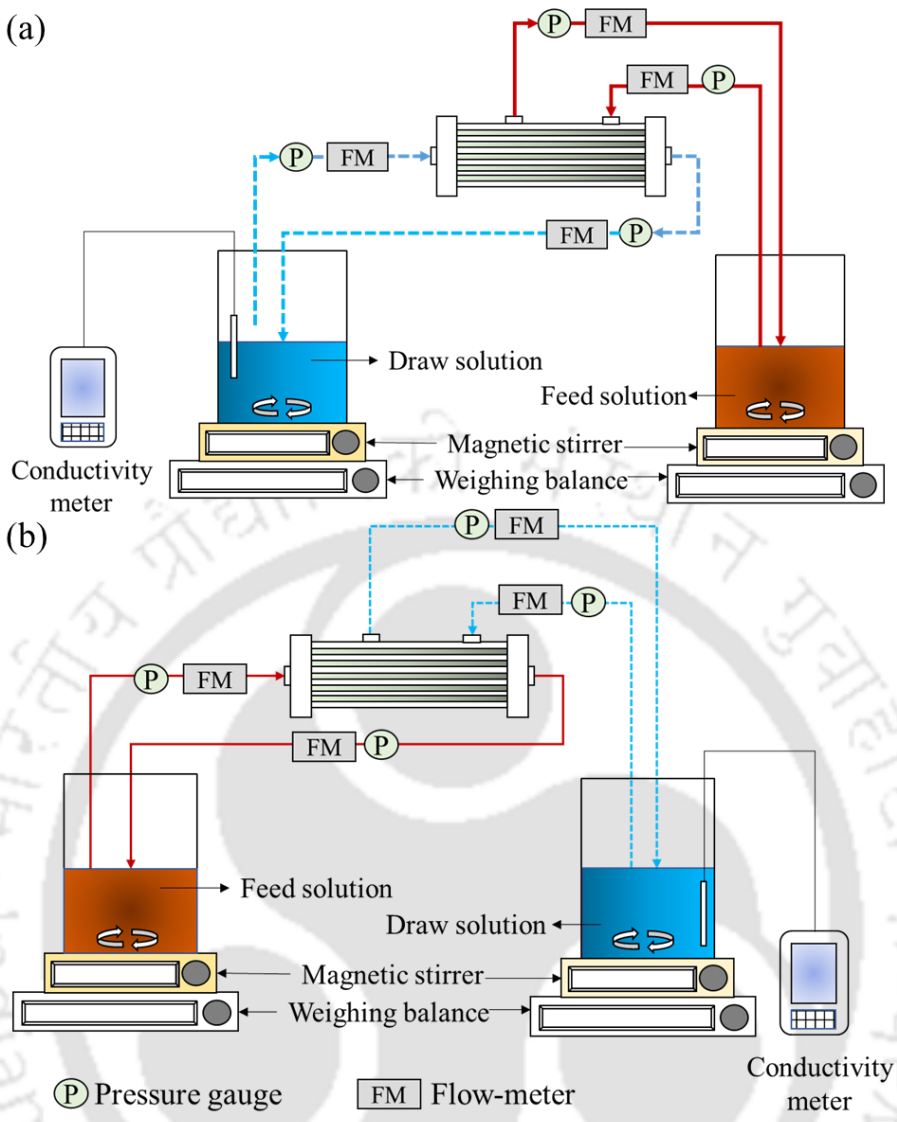

Figure 4.1 Schematic representation of bench-scale experimental set-up used for the preparation of 5-fold tea extract concentrate using (a) ALFS (FO) mode and (b) ALDS (PRO) mode

The FO experiments were designed and performed for 4 L of freshly brewed tea extract (FS) and 2 L NaCl (DS). Before each experiment, the HFFO membrane module was first stabilized by passing DI water through the lumen and tube side of the module. After stabilisation, the DS was pumped (25 L h^{-1}) through the module's shell side, keeping the module's lumen side closed. Similarly, the FS was pumped (60 L h^{-1}) through the pre-filter (pore size, 0.2 µm) before introducing it to the tube side of the membrane module by keeping the shell side of the module closed. After stabilisation, the FS and DS flow rate were maintained at 60 L h^{-1} and 25 L $h^{-1,}$ respectively, in counter-current mode. The TDS and mass of the feed and draw tank were measured to estimate the water flux and reverse solute flux using equations (4.1 - 4.2). The

specific amount of FS was manually collected at regular intervals of 1 min and stored under refrigerated conditions for further analysis. The FS and DS were recirculated to the respective tanks till the mass of FS reduced from 3.8 kg to 1.179 kg. When the mass of the FS tank reached 1.179 kg, the circulation of FS and DS to the membrane was terminated. After each experiment, the membrane module was properly rinsed using DI water. The shell and tube sides of the membrane were flushed simultaneously, maintaining the same flow rate as that used during the FO process. Then, keeping the shell side of the module closed, the tube side of the membrane module was flushed with DI water for another 25 min. To abolish the organic foulants deposited on the surface of the membrane, the given module was cleaned by rinsing them with 0.1 M NaOH for another 30 mins. After rinsing with NaOH, the membrane module was again rinsed using DI water until the TDS of the outlet stream from both the lumen and shell sides of the module became equivalent to that of the DI water. The membrane module was then stored at 4 ^{o}C till subsequent use.

4.2.5.2. Multi-component inorganic salt solution as draw solution

To investigate the effect of multi-component DS composition on the preparation of concentrated tea extract using the FO process. In this study, using a commercially available Aquaporin HFFO membrane, the DS and FS were circulated through the lumen and shell side of the membrane by maintaining flow rates at 60 L h^{-1} and 25 L h^{-1}, respectively, in counter-current mode (Figure 4.1 (b)). The FS and DS reservoir temperature was maintained at 25±1 ^{o}C. The DS tank comprises a mixture of inorganic salt (NaCl, KCl, $MgCl_2$, and Na_2SO_4) at specific compositions.

The permeate flux and RSF were calculated by measuring the volume and DS concentration change in the FS tank using (4.1 and 4.2). SRSF (g L^{-1}) reveals the amount of draw solute that can leach across the FO membrane to the feed side per unit of water recovered and is defined as the ratio of reverse solute flux (J_s, g m^{-2} h^{-1}) and water flux (J_w, L m^{-2} h^{-1}) [67]:

$$SRSF = \frac{J_s}{J_w} \tag{4.3}$$

4.2.5.2. Experimental setup for tea crystallisation using the forward osmosis process

Figure 4.1 (b) and Figure 4.2 demonstrates the experimental setup used for the preparation of concentrated tea extract using the FO process. The DS is prepared by dissolving an inorganic salt in DI water at room temperature (25±2 ^{o}C). The DS (60 L h^{-1}) and FS (25 L h^{-1}) were pumped through the tube side (active layer) and shell side (support layer) of the HFFO

membrane in counter-current mode. The FO performance is measured in terms of permeate flux (L m^{-2} h^{-1}) and RSF (g m^{-2} h^{-1}). Due to the osmotic pressure gradient, the solvent from low concentration FS to high concentration DS resulting simultaneous dilution and concentration of FS and DS, respectively. The FO performance was measured in terms of permeate flux, RSF, and SRSF estimated using equations (4.1 to 4.3).

In this study, the experiments were designed and performed for 6 L of freshly brewed tea extract and 2 L of DS. Before performing any experiments, the membrane module was stabilized, as mentioned in section 4.2.5.1. The change in weight and concentration of the FS tank was measured to estimate the water flux (L m^{-2} h^{-1}) and RSF (g m^{-2} h^{-1}) using equations (4.1 – 4.2). The FS and DS were recirculated to the respective tanks till the FS volume was reduced by 75% (FO-0^{th} cycle) (refer to Figure 4.1 (b)). Once the FS is reduced to 1.5 L, the recirculation of DS and FS to the membrane module is terminated and rinsed using DI water, followed by 0.1 N NaOH solution to abolish the organic foulant deposited on the membrane surface. The membrane module was then rinsed with DI until the TDS of the outlet stream for both the tube and shell side of the membrane module became equivalent to that of DI water (i.e., 0.45 mg L^{-1}). After the 0^{th} FO cycle, the chiller unit was integrated for further concentration, as shown in Figure 4.2.

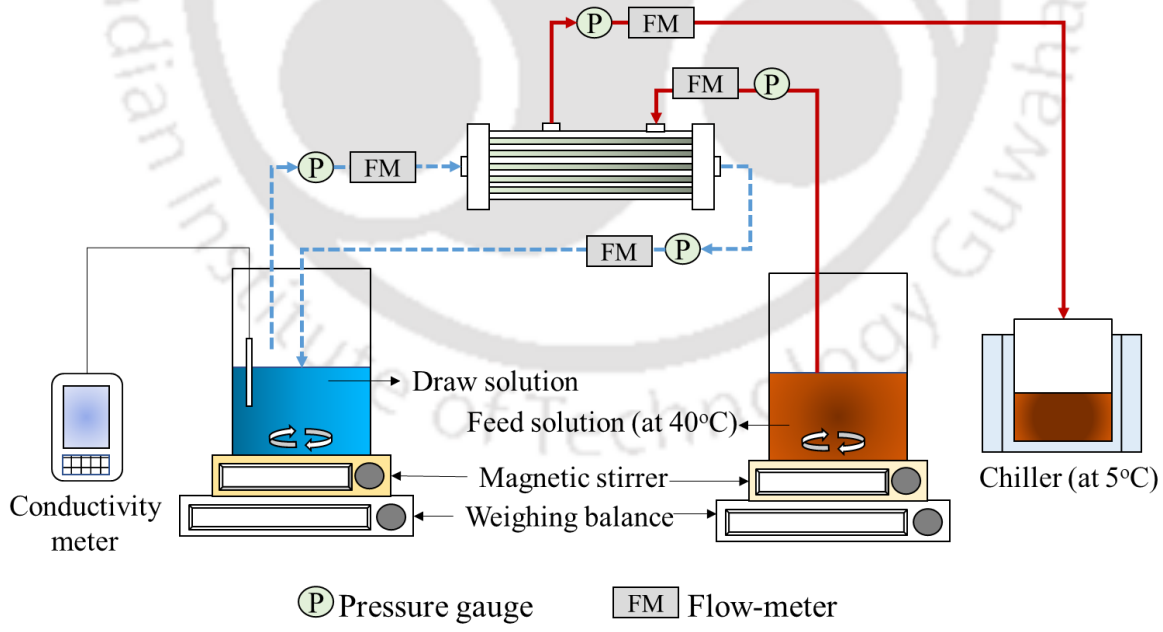

Figure 4.2 Schematic representation of a bench scale experimental setup used for the preparation of tea crystal using the freeze crystallisation technique

Figure 4.3 represents the overall integrated forward osmosis crystallisation technique for the preparation of concentrated tea extract. For the FO−1st cycle, the FS is further concentrated to 83.33%. In this stage, the inlet FS stream is maintained at 40 ^{o}C, and the outlet stream is maintained at –5 ^{o}C. Reportedly, the viscosity of the FS is expected to increase with an increased extent of concentration, thus resulting in higher chances of concentration polarisation on the membrane surface. The increased temperature of the feed stream ensures that the viscosity is reduced [187]. The change in temperature between FS streams also elevates the chances of tea crystal formation [188].

Figure 4.3 represents the overall integrated forward osmosis crystallisation technique for the preparation of concentrated tea extract. For the FO-1st cycle, the FS is further concentrated to 83.33%. In this stage, the inlet FS stream is maintained at 40 ^{o}C, and the outlet stream is maintained at -5 ^{o}C. Reportedly, the viscosity of the FS is expected to increase with an increased extent of concentration, thus resulting in higher chances of concentration polarisation on the membrane surface. The altered inlet and outlet FS stream temperature ensure reduced viscosity (Shin & Kim, 2018) and improved tea component recovery (Michaeli & Koschmieder, 2000). After each batch of FO process, the concentrated FS was centrifuged at 20000 rpm for 20 min. The pellet obtained are dried at 50 ^{o}C, whereas the supernatant solution for again recycled for the subsequent FO-cycle.

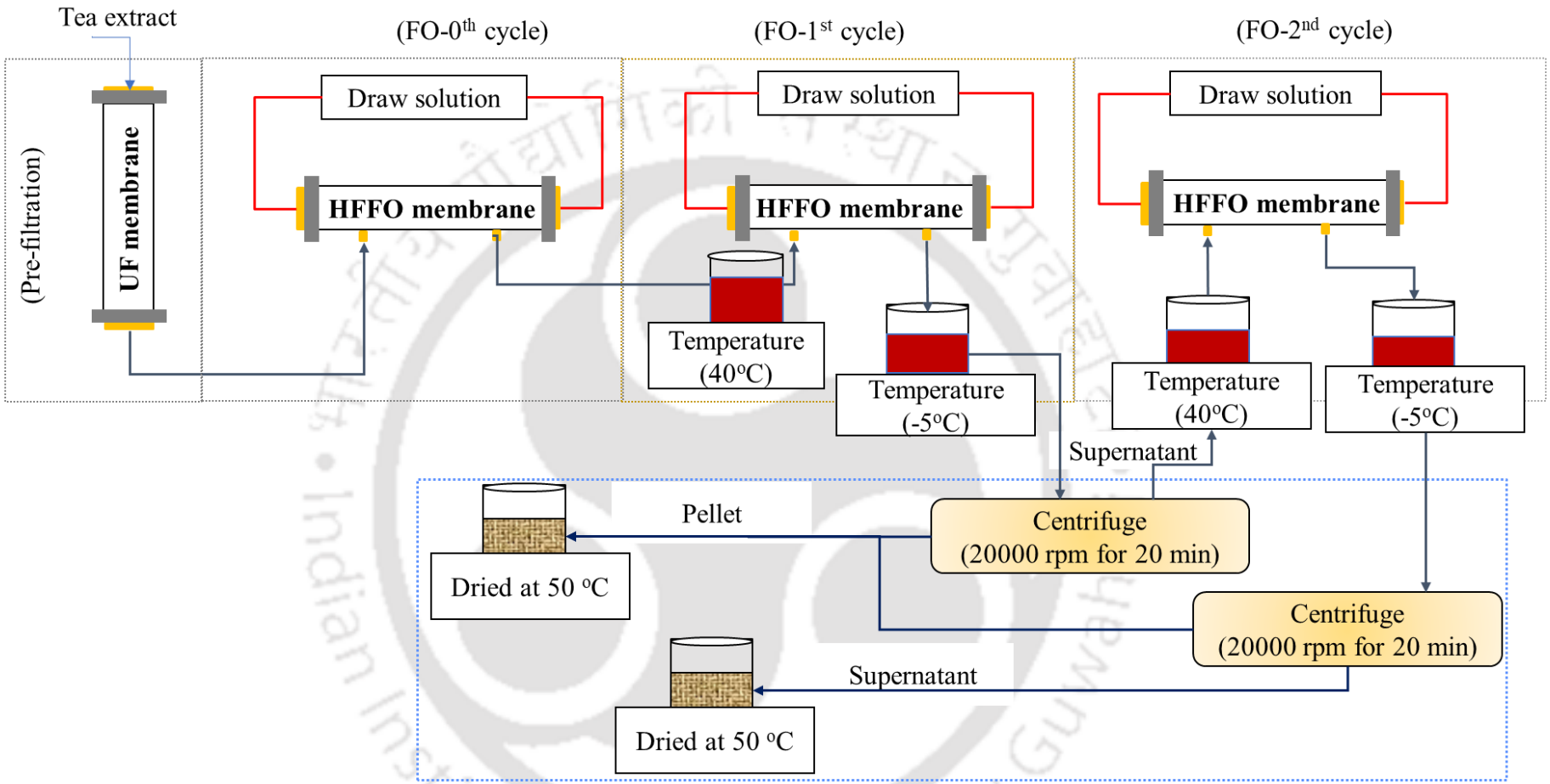

Figure 4.3 Schematic representation of the integrated forward osmosis and crystallisation process for the preparation of tea extract

4.2.6. Synthesis of hydrogel

4.2.6.1. PVA-polyDADMAC hydrogel

In this study, a series of hydrogels were synthesised to understand the effect of polymer (PVA and PolyDADMAC) and crosslinker (Glyoxal) concentration on the overall swelling capacity of the hydrogels (Table 4.3).

Table 4.3 Composition and swelling ratio of the prepared hydrogel

Code	PVA (wt.%)	PolyDADMAC (wt.%)	Glyoxal (wt.%)	Swelling capacity (g g^{-1})	Remark
H-3:3:1.5	10	10	5	13.59 ± 0.06	Gel formed with spongy white colour texture after drying
H-4:3:1.5	13.33	10	5	20.68 ± 0.06	
H-6:0:1.5	20	0	5	13.45 ± 0.02	
H-4:2:2	13.33	6.67	6.67	16.56 ± 0.05	Gel formed with spongy white colour texture after drying
H-3:3:3	10	10	10	11.77 ± 0.02	Gel formed with spongy pale-yellow texture colour after drying
H-6:0:3	20	0	10	11.15 ± 0.06	Strong network gel formed

The polymers were allowed to form an aqueous solution with 30 mL of DI water at 70 ^{o}C for 3 h. The crosslinker was added to the PVA-PolyDADMAC solution to maintain the same operating condition. After 45 mins, the resultant polymeric solution was allowed to cool down to room temperature and then poured into non-solvent ethanol (500 mL) for 24 h to remove the absorbed water. Then ethanol was decanted, and the product was cut into small, uniform-sized pieces. The resultant hydrogel was dried in an oven at 30 ^{o}C for 8 h. After drying, the hydrogel was placed in a desiccator till further use (Figure 4.4).

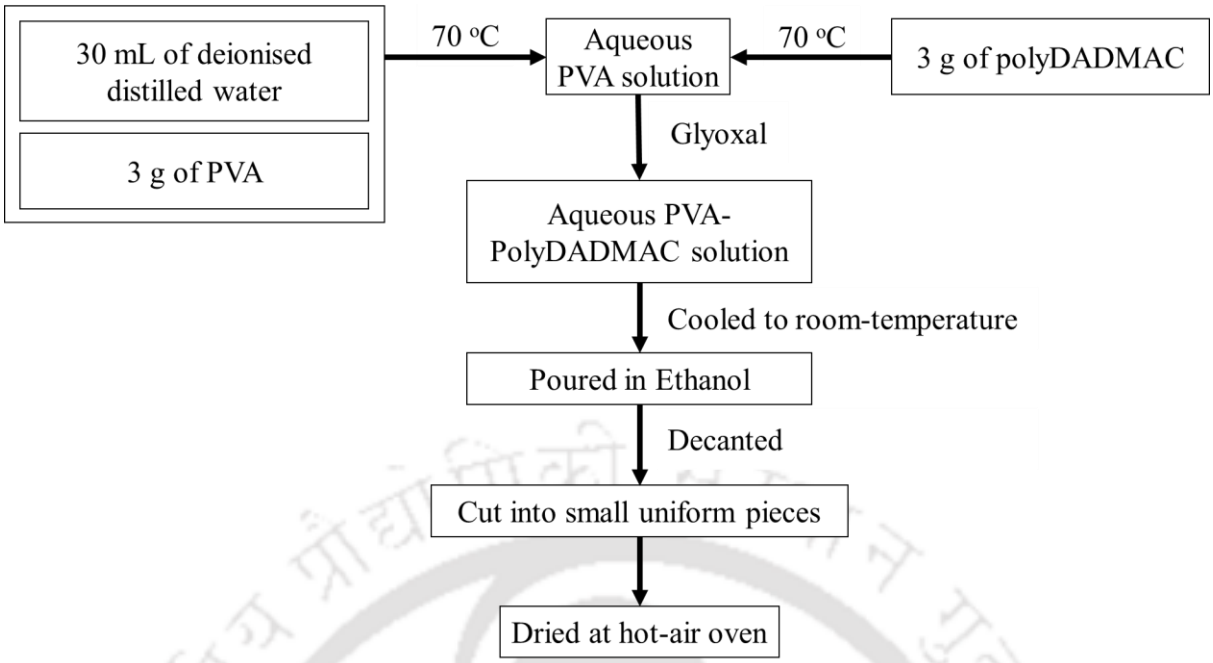

Figure 4.4 Schematic representation of the method of synthesising PVA-polyDADMAC hydrogel as draw solute for the forward osmosis process

4.2.6.2. Acrylic acid-NIPAM hydrogel

20 mL of potassium hydroxide (55% KOH) solution was added to 30 g of acrylic acid. The solution was stirred using a magnetic stirrer at room temperature. Then cross-linker (MBA) was added to the partially neutralised acrylic acid solution. After mild agitation, APS solution and potassium metabisulfite ($K_2 S_2 O_5$) solution were added. Finally, sodium bicarbonate ($NaHCO_3$) and acetone were added to the solution. The solution viscosity increased, and after 15-20 s of gelation, the solution was left undisturbed. In this stage, Due to the simultaneous action of the blowing agent, water evaporation, and gel formation, the polymeric solution changes its state from viscous liquid to foamy solid. After cooling to room temperature, the foam (polymeric network) was cut into small uniform pieces and dried at 70 °C for 18 h. After drying, the dried polymer was ground to a fine powder and stored in an air-tight container under desiccated conditions (Figure 4.5).

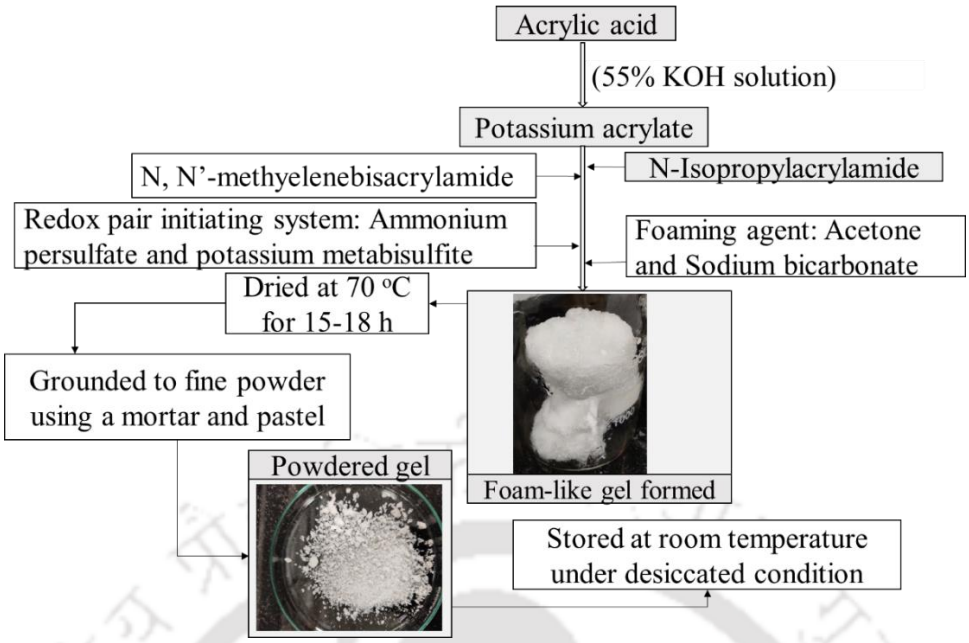

Figure 4.5 Schematic representation of the synthesis of the fast-swelling hydrogel as draw solute for the forward osmosis process

Due to the high monomer (acrylic acid), the neutralisation of acrylic acid with potassium hydroxide is an exothermic reaction, thereby accelerating polymerisation [189]. Sodium bicarbonate ($NaHCO_3$) reacts with the non-neutralised acrylic acid monomer group, resulting in the evolution of carbon dioxide (CO_2) gas. The acetone provides additional foam height due to the evaporation of volatile acetone at the elevated reaction temperature. Figure 4.6 represents the proposed reaction mechanism for the given synthesis.

For the synthesis of thermoresponsive hydrogel, apart from adding thermosensitive monomer (NIPAM) to the partially neutralised acrylic acid solution, the rest synthesis conditions were maintained to be the same as mentioned in Figure 4.5.

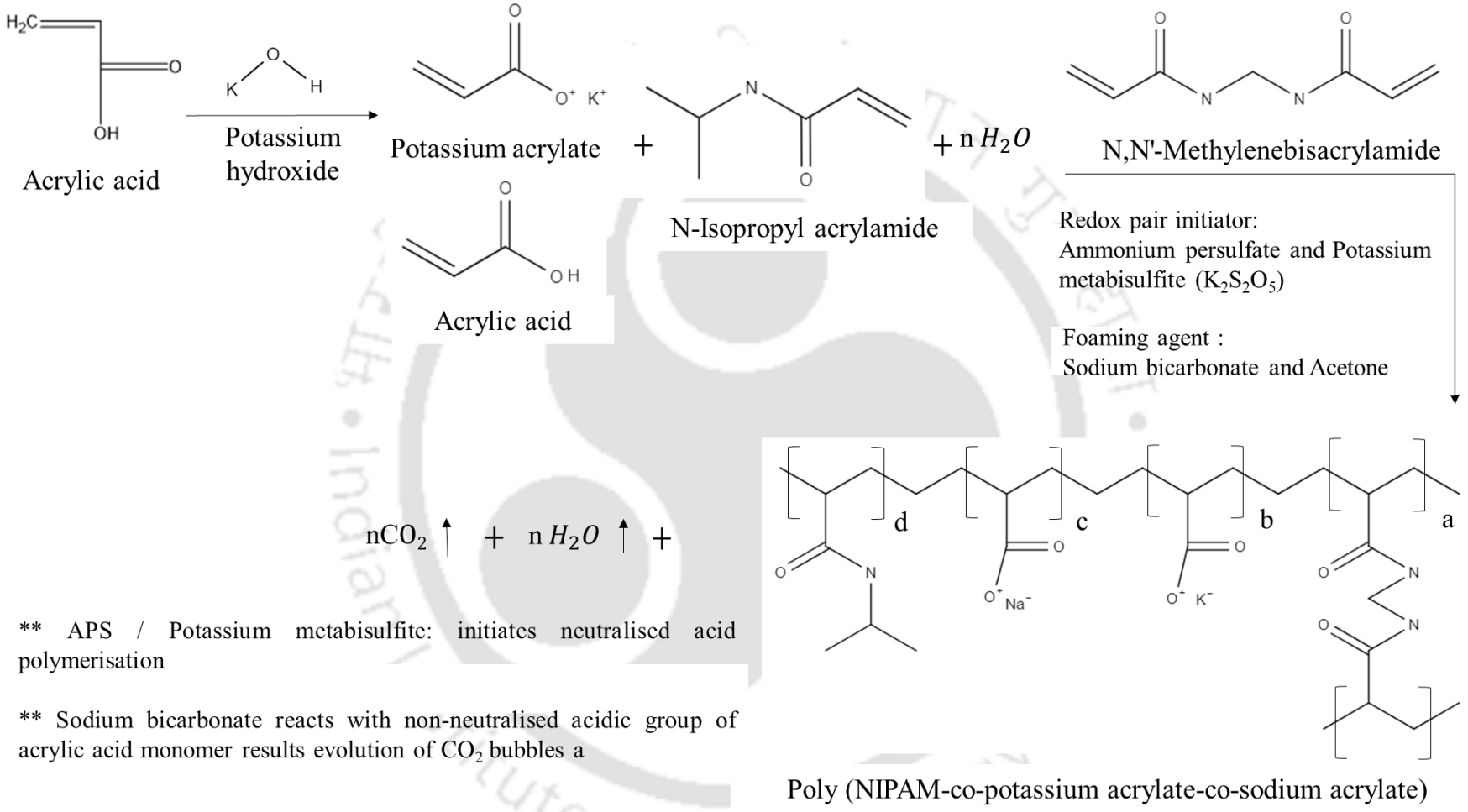

Figure 4.6 Proposed reaction mechanism for the fast-swelling hydrogel as draw solute for forward osmosis process

The performance of the synthesised hydrogel was estimated in terms of hydrogel swelling and deswelling capacity. The swelling capacity of the hydrogels was estimated to evaluate water absorption capability. Before each swelling study, the hydrogels were placed in a hot-air oven at 70 °C for 4 h to ensure complete dehydrated products. A certain amount of dry gel (1 g) was immersed in DI water for a certain time 't' to absorb and completely swell. Over the period of time, the swelling ratio (Q, g g^{-1}) of hydrogels was calculated using the following equation:

$$Q = \left(\frac{W_t - W_d}{W_d} \right) \tag{4.4}$$

W_d and W_t represent the weight (in g) of the dried and swollen hydrogel at a time '*t*', respectively.

The swelling ratio (Q, g g^{-1}) can be defined as the fractional increase in the weight of the hydrogel due to water absorption. Further, to evaluate the deswelling capacity of the synthesised hydrogel under the thermal influence. A specified amount of swollen hydrogel was placed under a blower at room temperature for the dewatering process. The hydrogel dewatering continued until a weight change between the two readings was constant.

4.2.7. FO experimental setup for performance analysis of hydrogel

4.2.7.1. Experimental Setup for batch FO process using hydrogel alone as draw solute

The feasibility of the prepared hydrogels as draw solute was investigated against 1000 mg L^{-1} NaCl as feed solution (FS). The membrane used during this investigation was obtained from Infinite water solution Pvt. Ltd. (DOW Filmtec membrane). A detailed discussion of the given membrane characterisations were discussed in section Appendix 3. For the given process, the given membranes were cut into a circular disk of 6 cm diameter and soaked in DI water for a minimum of 1 h prior to application.

Figure 4.7 represents the lab-scale forward osmosis set-up. In this set-up, 200 mL of the feed solution is poured into the cylindrical tube (diameter 6.5 cm and height 10.5 cm). The membrane is fitted at the bottom of the cylindrical tube such that the active layer faces the draw solute (ALDS). To maximise the contact area between the hydrogel and membrane, the thickness of the hydrogel layer was maintained at approximately 1 cm height. The bottom chamber ensures the removal of a water molecule from swollen hydrogel to maintain flux over 6 h of operation. The change in FS conductivity, weight, and setup was continuously monitored throughout the experiment.

The FO performance for the given process was measured in water flux, RSF, and SRSF using estimated using equations (4.5), (4.2), and (4.3), respectively.

$$Water\ flux, J_w = \frac{\Delta W_{FS}}{A_m \times \rho \times \Delta t} \quad (4.5)$$

where ΔW_{FS}, A_m, and ρ represent the weight change (in g) of FS over time 'Δt' (in h), membrane contact area (m^2), and density of the permeate water (assumed as 997 g L^{-1} at room temperature, at 25 ^oC) respectively.

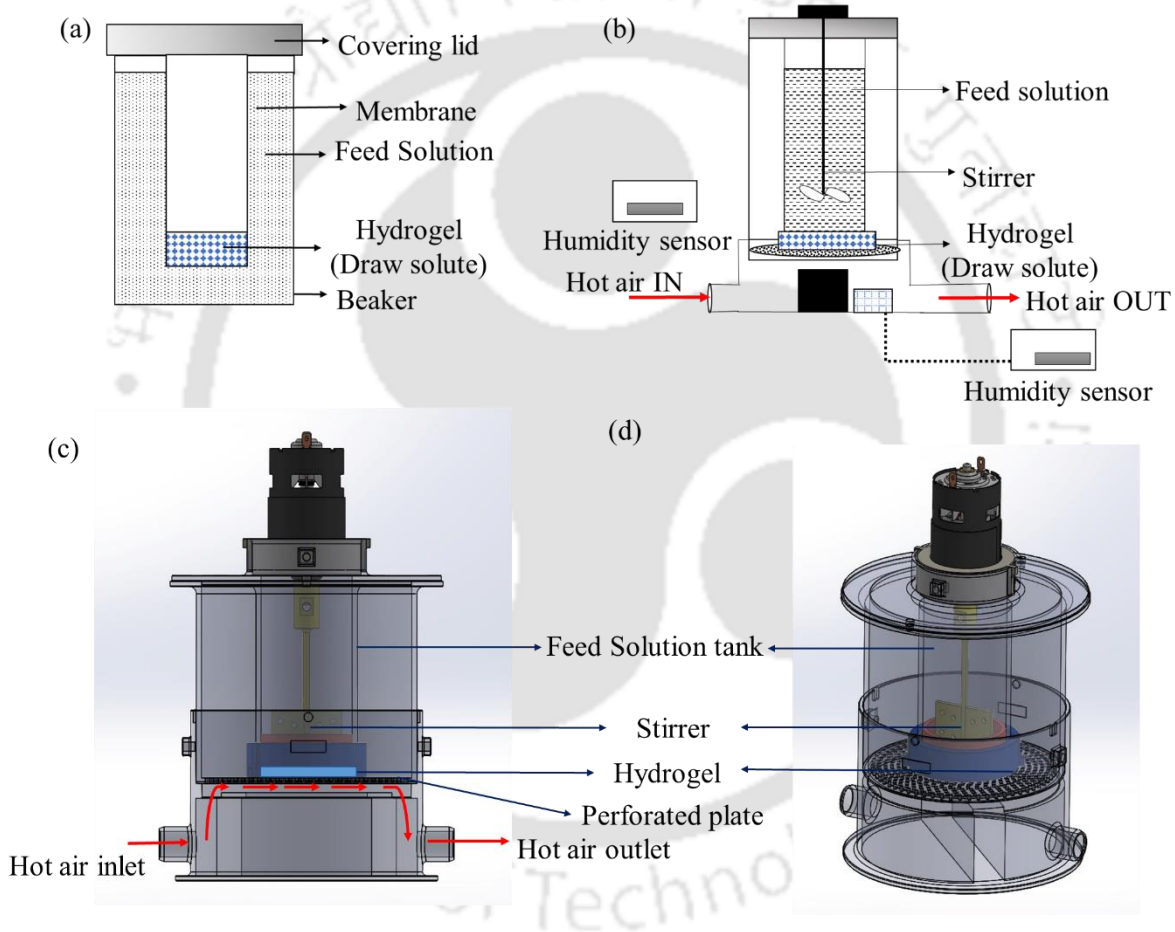

Figure 4.7 Schematic representation of a) test set-up without heat, b) lab-scale experimental FO set-up with thermal dewatering section, c) and d) design used for 3D printing of integrated FO set-up

4.2.7.2. Experimental setup for FO batch process using dual draw solute

The integrated FO membrane module (Figure 4.7) suggests that the regeneration of swollen hydrogel is possible using thermal energy. However, it was observed that complete dewatering of hydrogel under the thermal influence is not practical for large-scale applications.

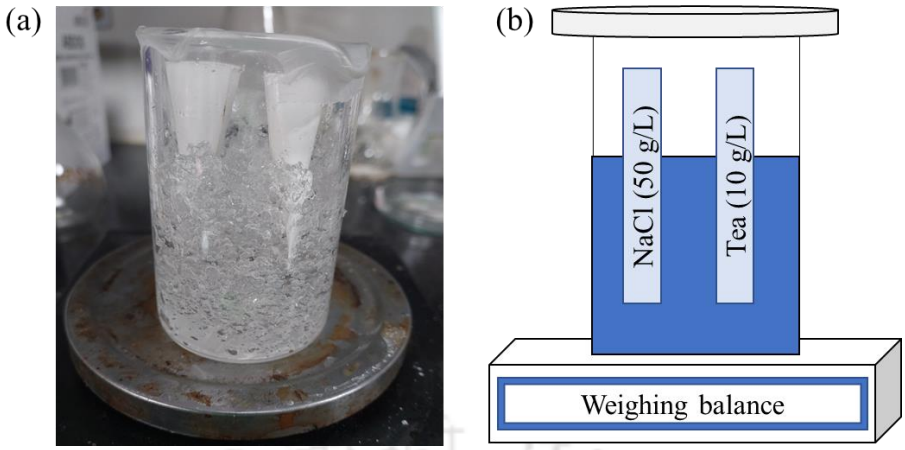

Figure 4.8 a) Test scale set-up, b) schematic representation of a test-scale integrated membrane module

The regeneration of swollen hydrogel using high concentration RO rejects brine solution (63,500 mg L^{-1}) was never explored, and according to our knowledge, and reportedly this is the first attempt of a concentration of liquid food (tea extract) using hydrogel as draw solute. Due to swelling and osmotic pressure, the solvent from low-concentration FS permeates to the osmotic agent (semi-swollen hydrogel). Similarly, due to the osmotic gradient between the high-concentration brine solution and hydrogel, the solvent is expected to permeate from the hydrogel to the brine solution.

Figure 4.8 provides a schematic representation of an integrated membrane module. The intention behind this set-up was to minimise the chances of hydrogel degradation due to thermal treatment (blowing air at 39-50 ^{o}C) to improve the life-cycle of hydrogel for improved commercial feasibility.

4.2.7.3. Experimental setup for continuous FO using dual draw solute

To determine the practical feasibility of the given study, a series of experiments was conducted using the 3-tier membrane module (Figure 4.9) using DI as FS (on the top tier) and high concentration NaCl solution (38.4 g L^{-1}, π = 30.27 bar) on the bottom tier. The middle tier consists of a 1.8 g of dried hydrogel semi-swollen using 10 mL of DI. The 3-tier were separated using a semi-permeable membrane (area: 0.005 m^2). The DI water and the highly concentrated NaCl solution were recirculated through the top and bottom tier of the membrane module at 45 L h^{-1} and 45 L h^{-1}, respectively, in counter-current mode.

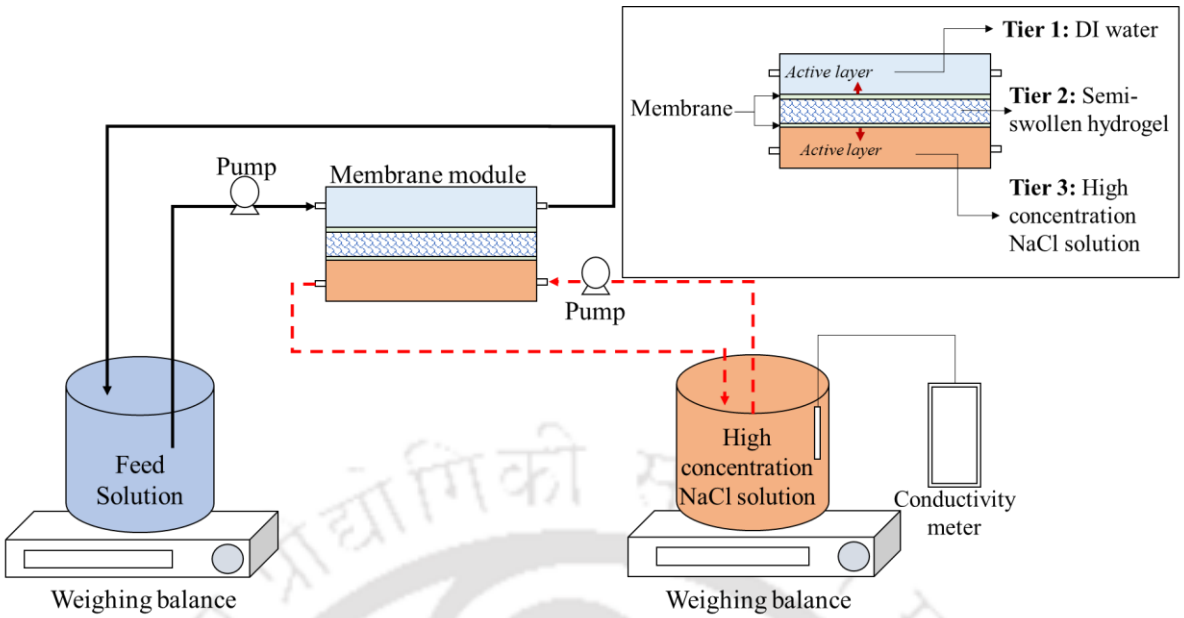

Figure 4.9 Schematic representation of the test scale experimental set-up using a 3-tier membrane module

The FO performance was measured in terms of permeate flux, RSF, and SRSF estimated using equations (4.1 to 4.3). In the first hour of the given process, a permeate flux and RSF of 27.81 ± 0.09 L m^{-2} h^{-1} and 0.081 ± 0.025 g m^{-2} h^{-1}, respectively. Over 6 h of the FO process, the permeate flux and RSF reduce 8.55 ± 1.22 L m^{-2} h^{-1} and 0.057 ± 0.026 g m^{-2} h^{-1}. The given trial study suggests the feasibility of the given 3-tier design of the membrane module. However, further investigation needs to be performed to enhance the FO performance. The effect of the flow rate of the FS/ high concentration NaCl, the thickness of the middle tier, and other factors need further investigation to enhance FO performance.

The concentrated brine discharged by the desalination plants are denser than ambient seawater and therefore sinks and flows along the sea bottom, causing. Therefore, the highly concentrated brine must be diluted and treated before being released into the environment. This design suggests that the highly concentrated RO-reject brine can be diluted and passed to the aquatic body without causing a significant environmental impact.

4.2.7.4. Experimental setup for regeneration of hydrogel using solar radiation

Hydrogels are polymeric networks capable of swelling and shrinking reversibly in response to changes in the external environment. The water content of the swollen hydrogel is one of the critical parameters for assessing the dewatering performance. The water content (W) of the swollen hydrogel can be determined using the equation (4.5):

$$W = \frac{(W_S - W_i)}{W_S} \times 100\% \quad (4.5)$$

where W_s and W_i represent the weight (in g) of swollen hydrogel (after 24 h) and initial hydrogel.

Stimuli-responsive hydrogels can exhibit switchable sol-gel transition upon application of external triggers using external stimuli such as electric, magnetic, solar, and temperature. The swollen gel after the FO process was placed in a glass funnel separated by a Whatman filter (Grade 42). The temperature (^oC) and relative humidity (% RH) was regularly measured using an infrared thermometer (HTC IRX-64 Digital Infrared Thermometer, Maker: HTC) and a humidity meter (HTC−1 high precision Humidity meter, Maker: HTC), respectively, at different exposure time. The dewatering efficiency (R) is calculated using:

$$R = \left(\frac{W_1}{W_0}\right) \times 100\% \quad (4.6)$$

where W_1 is the weight of water loss during the solar dewatering test (in, g), i.e., the difference in the weight of swollen hydrogel before and after exposure to the sunlight over a certain period of time; W_0 represents the weight of the water in the swollen gel before the dewatering test (in, g). In this study, the effect of solar stimuli was investigated for the effective dewatering of hydrogel used as a draw solute for the FO process (Figure 4.10).

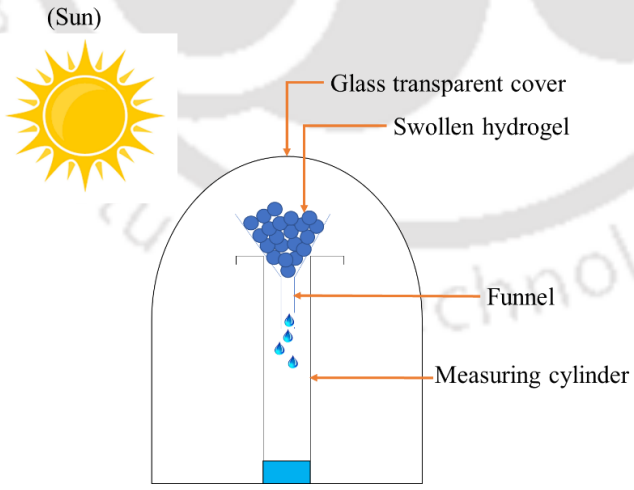

Figure 4.10 Schematic representation of the test scale set-up of hydrogel regeneration under solar-influence

Chapter 05

Results and discussions

Abstract: *This chapter reports a detailed discussion on the significant results obtained from different experiments and simulation studies are presented in this chapter.*

5.1. Performance Analysis of HFFO Membrane Module for Tea Concentration using:

5.1.1. Single-component inorganic draw solution

In this section, the performance of the FO experiments was reported using a freshly brewed tea extract and food-grade inorganic salt solution as feed and draw solution in ALDS mode (Figure 4.1 (a)). The efficiency of the FO process was determined in terms of water flux, SRSF, and the concentration of essential tea components in the final product.

5.1.1.1. Effect of membrane configuration on FO performance

In an osmotically driven membrane process, the water flux is dominated by the osmotic pressure gradient across the membrane. However, it is hugely impacted by the ICP across the membrane support layer. The mass transfer (water flux and RSF) in ALDS and ALFS modes can be broadly described as a function of DS concentration [67]. Thus, to understand the influence of membrane orientation on FO performance. In this study, except for the membrane orientation, other operating conditions, such as initial FS composition (black tea extract), flow rate configuration (counter-current), and membrane (Aquaporin inside HFFO membrane), were kept constant.

The ALDS mode enables higher permeate flux due to reduced concentration polarisation with SL. Figure 5.1 (a) illustrates that the water flux increases with increasing concentration of NaCl solution from 1g mol^{-1} to 2 g mol^{-1} when operating under both ALFS and ALDS modes.

SRSF (g L^{-1}) is defined as the ratio between the RSF and water flux and has been widely used to evaluate FO performances. According to Tang et al. (2010), in the FO process, the SRSF is only influenced by the intrinsic separation properties of the membrane and working temperature. Reportedly, the average SRSF in both ALDS-mode and ALFS-mode are almost the same, and a similar trend was observed while concentrating apple juice [137]. In ALDS mode, the ECP on the membrane AL is believed to reduce the RSF. Hence, the SRSF in ALDS-mode were expected to be slightly lower than in ALFS mode. A similar was observed in this study while concentrating tea extract using the FO process (Figure 5.1 (b)). Thereby suggesting that in the FO process, the selection of membrane orientation primarily depends on the feed solution and the degree of concentration.

In this study, the freshly brewed tea extract is prepared as mentioned in Section 4.2.1. Due to the low-fouling tendency of the prefiltered tea extract. In this study, the ALDS mode of membrane orientation is used for the concentration of tea extract using the FO process.

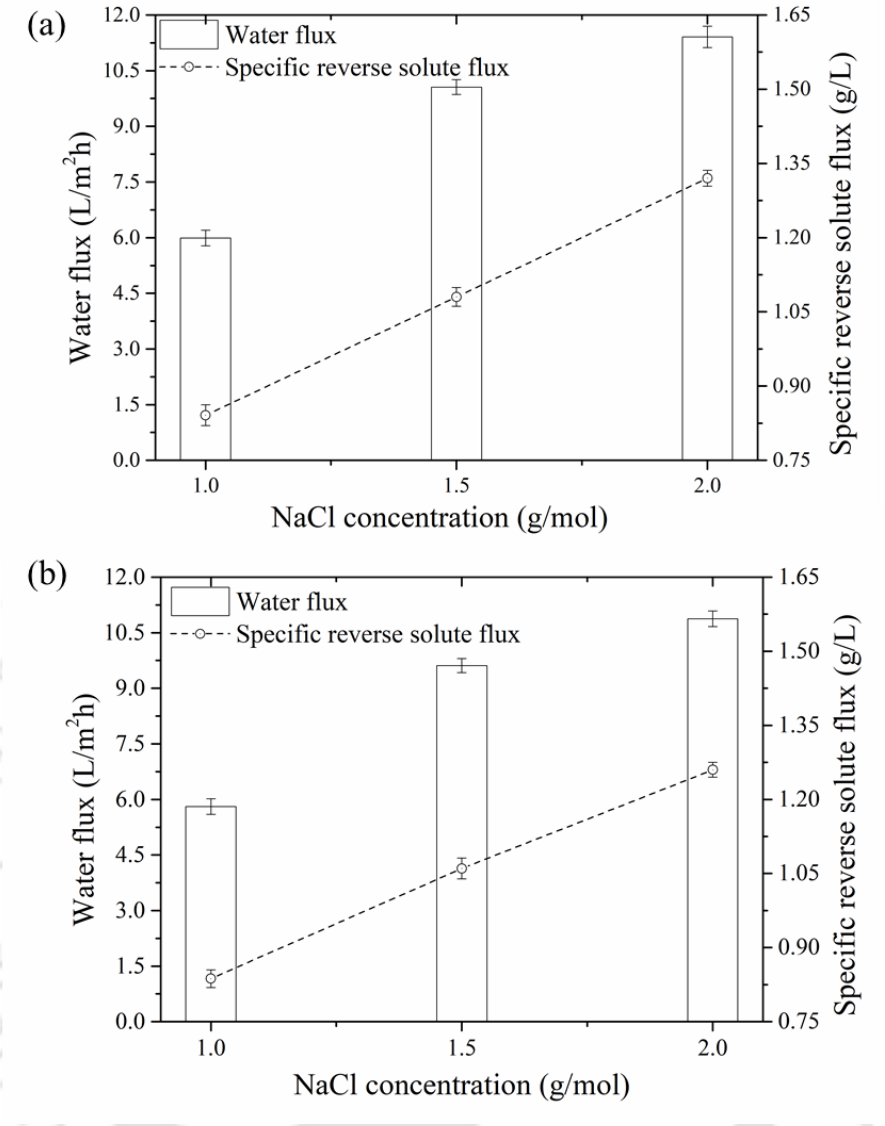

Figure 5.1 Water flux and reverse solute flux as a function of NaCl concentration in (a)ALDS (PRO) and (b) ALFS (FO) mode.

Furthermore, in the given HFFO (Aquaporin inside HFFO) membrane, the AL is on the inner surface (lumen-side) of the hollow fiber (HF) [76]. In ALFS mode, though the RSF was comparatively less than ALDS however, due to the small diameter of HF, the module was more susceptible to choking. Thus, resulting in increased transmembrane pressure across the lumen side of the membrane module. The increased pressure not only results in reduced FO performance but also causes damage to the module. Thus, to avoid this, after each set of experiments, the membrane modules were subjected to chemical cleaning (1% sodium hydroxide solution). The given membrane exhibits good resistance to chemical cleaning agents [190]. However, based on the overall time required for cleaning for reviving membrane

properties. It was found that the time required for cleaning the module with ALDS mode was comparatively less than ALFS. Thereby suggesting that if the AL (Aquaporin Inside^{TM} coating) was on the outer surface of the HFFO membrane (shell-side), then the ALFS mode could be efficiently employed for the given HFFO membrane module.

5.1.1.2. Effect of DS composition on FO performance

In the FO process, the water flux (J_w) can be described as a function of the concentration gradient between FS and DS across the dense AL of the membrane. Figure 5.2 demonstrates the average FO performance of the HFFO membranes in ALDS membrane orientation for the concentration of tea extract against single component inorganic salt as DS. The selection of an appropriate DS is a crucial component for the successful development of the FO process. Reportedly, the DS with the highest osmotic pressure are expected to provide superior FO performance (Figure 5.2). Compared to monovalent inorganic salt (such as NaCl), the divalent or multi-valent inorganic salts (such as $MgCl_2$ and Na_2SO_4) exhibits lower water flux and lower RSF. The SRSF for divalent or multi-valent inorganic salts was observed to be 12.5% to 18.5% lower than monovalent inorganic salt.

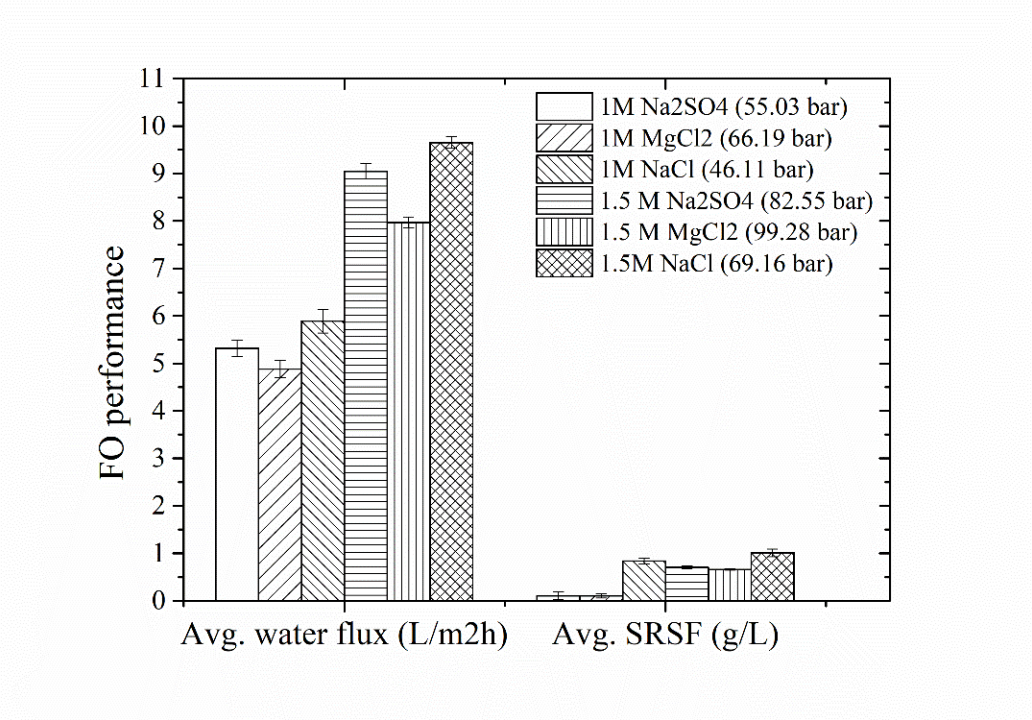

Figure 5.2 Overall performance of HFFO module of single component draw solution for concentration of tea extract using single component draw solution

The performance of different inorganic DS used for the preparation of concentrated tea extract and their effect on the concentration of essential tea components. The increasing concentration of tea components suggests that the FO process is capable of dewatering tea extract without compromising with its final product quality (refer Figure 5.9).

Summary on performance analysis of single-component draw solute for the concentration of tea extract using forward osmosis process

The present study demonstrates the FO process's feasibility for the tea extract concentration. This study aims to determine the role of appropriate DS selection and its influence on the final tea concentrate. The catechins and epicatechin, the main phenolic compounds in tea, and the increasing trends of the given components confirm the feasibility of the FO process using Aquaporin inside the HFFO membrane. In liquid food processing industries, the RSF is a critical factor that needs to be carefully observed. As it not only influences the FO performance but also results in altered taste and degraded quality of the final product. Reportedly, compared to monovalent inorganic salt, the RSF effect of di- and multi-valent inorganic salts was observed to be less, but the permeate flux was also significantly less. Thus, providing scope for developing an appropriate DS composition with enhanced permeate flux and reduced RSF for liquid food concentration.

5.1.2. Multi-component inorganic draw solution

This work aims to identify an appropriate food-grade multi-component draw solute composition with enhanced permeate flux and reduced RSF. This study also highlights the role of the membrane in an efficient FO process. The objective of this study was to identify an multi-component DS mixture with enhanced water flux and reduces RSF. The performance of the selected DS composition was evaluated in terms of their FO performance and their ability to retain essential tea components in the final concentrated product.

5.1.2.1. Selection of multi-component draw solution composition

The selection of appropriate DS is a crucial component for the successful development of the FO process. In this study, DS was selected based on osmotic pressure. Since the DS with the highest osmotic pressure results in the highest permeate flux [89]. Figure A1.1 summarises the details of the osmotic pressure of different possible multi-component inorganic salt compositions. Based on osmotic pressure details, the S10 (62.39 bar), S5 (60.24 bar), and S8 (59.41 bar) were identified as DS01, DS02, and DS03, respectively for FO process used for further studies.

This section assessed the performance of identified multi-component DS compositions (DS01, DS02, and DS03) in terms of permeate flux, RSF, and SRSF. The feasibility of the identified multi-component inorganic salt solutions was investigated as a potential DS for the concentration of liquid food (tea extract) using the FO process.

5.1.2.2. Effect of multi-component DS composition on FO performance

In this section, to evaluate the feasibility of the selected multi-component inorganic salt solution as DS for preparation of concentrated tea extract. The freshly brewed tea extract was concentrated using the Aquaporin HFFO membrane module (area 2.3 m^2). The overall experimental time was finalised based on the time required to concentrate tea extract from 4000 mL to 475 ± 2 mL (i.e., 8.42 times).

To understand the mechanism of multi-component DS composition on the FO performance. The effect of permeate flux and RSF was also investigated using single-component DS (Table 5.1). Since, water flux (J_w) is a function of the osmotic pressure gradient between DS and FS. To compare the effect of DS composition on permeate flux, the osmotic pressure of the mixed-salt DS and single-salt DS was maintained to be almost constant (60.56 ± 1.21 bar).

Table 5.1 Composition and osmotic properties of single-component and multi-component inorganic salt

Salt type	Sample ID	NaCl	Na_2SO_4	$MgCl_2$	KCl	Osmolality (mosmos/ kg H_2O)	Osmotic pressure (bar)
		(mol/L)					
Multi-component salt	DS01	0.25	0.5	1	0.25	2811	62.39
	DS02	0.5	0.5	1	0	2714	60.24
	DS03	0.25	0.25	1	0.5	2677	59.41
Single-component salt	DS04	0	0	1	0	2718	59.53
	DS05	1.5	0	0	0	2827	61.93
	DS06	0	1.2	0	0	2699	59.13
	DS07	0	0	0	1.5	2797	61.26

In this study, since other operating conditions (such as FS concentration, membrane area, and module type) were constant, the osmotic pressure of DS should be the only determining candidate responsible for flux.

The water flux is expected to increase with an increase in osmotic pressure [191], and a similar trend was observed in Figure 5.3. Thus, implying that for both single- and multi-component DS, the water flux is a function of osmotic pressure. Due to the high concentration gradient across the membrane, a sharp decline in the permeate flux was observed at the beginning of the experiment, with a transition of almost constant flux with time. Internal concentration polarisation (ICP) is critical in any osmotically-driven membrane process and is responsible for the declining trend of the water flux reduction in the FO process [72]. Several pieces of literature reported a similar trend of declining permeate flux, citing the reduced concentration gradient between the DS and FS due to the permeation of solvent from feed to draw solution and the leaching of draw solute to feed solution as a significant concern. Apart from a reduced concentration gradient between FS and draw solute, considering the situation where FS is not DI, the phenomenon of fouling is equally responsible for the declining trend of flux (Figure 5.3) [192,193].

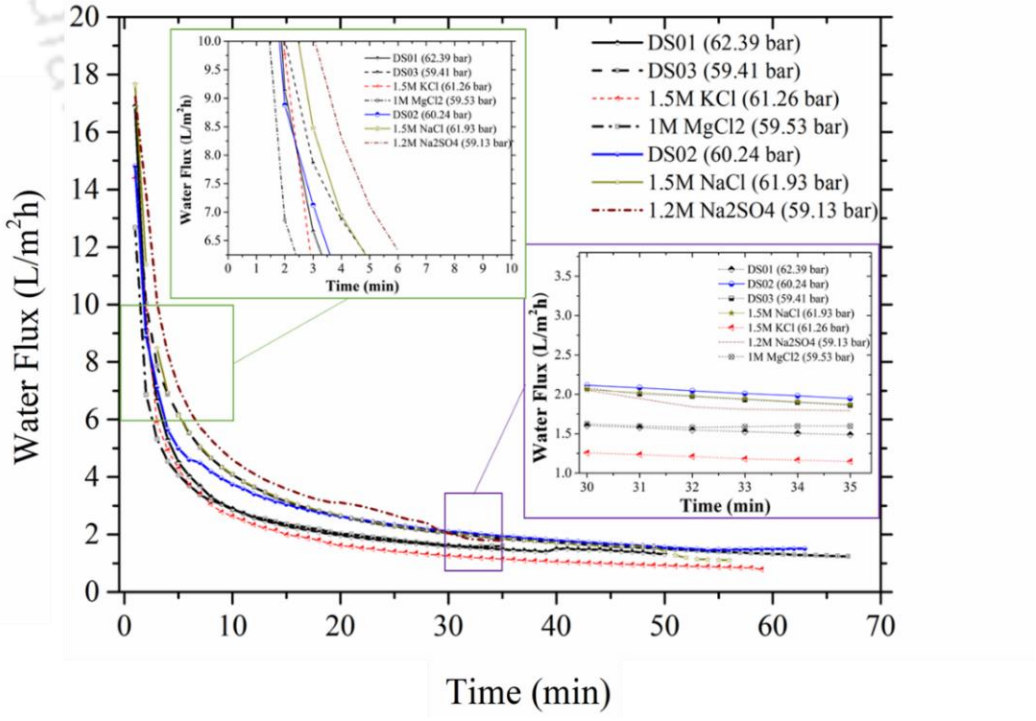

Figure 5.3 FO performance of the mixed-salt and single-salt DS for preparation of concentrated tea extract using Aquaporin-inside HFFO membrane module (area, 2.3 m^2)

The major drawback of using inorganic salts as DS is RSF. The RSF is believed to be proportional to the solute concentration gradient at the active layer interface of the membrane between the DS and FS [180]. SRSF (g L^{-1}) is a crucial index parameter used to evaluate the reverse solute permeation with respect to water flux. The higher SRSF reflects the higher DS leakage from the draw to the feed side of the module, thereby reducing the overall FO performance.

Compared to single-component DS, the RSF in the case of multicomponent DS behaves differently, as each solute in the multi-solute DS can behave differently due to different solute compositions. In multi-component DS, due to the incorporation of divalent ($MgCl_2$) or higher (Na_2SO_4) inorganic salts, the problem of RSF was reduced by 42−45% compared to monovalent inorganic salt (such as NaCl). The large hydrated radius and lower diffusion coefficient of Mg^{2+} resulted from the reduction in RSF of the given multi-solute DS composition (Table 5.2). The low diffusivity of magnesium-ion prevents sodium- and chloride-ions from diffusing through the pore at a high rate. The lower diffusion coefficient of magnesium salt resulted in an increment of ECP (external concentration polarisation) on the DS side of the membrane, resulting in a reduction in permeate flux of the multi-solute DS compared to the single-salt DS.

Table 5.2 Hydrated ion radius and diffusion coefficient of ions

Ion	Radius of hydrated ions (nm)	Diffusion coefficient ($\times 10^{-9}$ m s^{-1})
Na^+	0.36	1.334
K^+	0.315	1.957
Mg^{2+}	0.395	0.706
Cl^-	0.27	2.032
SO_4^{2-}	0.3	1.06

The RSF for multi-component DS was reported lower than individual salts (NaCl and KCl) due to the higher radius of hydrated ions of Mg^{2+}. For a given multi-component draw solute, the resistance encountered for its diffusion across the membrane SL depends on the ratio of structural parameter to the diffusion coefficient of the solute. Thus, compared to individual

inorganic salt solution, the multi-component exhibited superior FO performance. The high diffusion coefficient of KCl could be the main reason for the improvement of the overall permeate flux (J_w) as it reduces the ECP effect on the DS side. Whereas, the RSF trend was reduced due to low diffusion coefficient and higher hydrated radius of $MgCl_2$ salt.

The previous results demonstrated that compared to single-component DS, the multi-component DS provides superior FO performance against DI water (as FS). A similar trend was observed when the given multi-component DS (DS01, DS02, and DS03) compositions were used to concentrate freshly brewed tea extract using FO process. For the preparation of liquid food concentrate, the accumulation of solutes from DS may result in altered taste and nutritional value, eventually reducing the overall consumer acceptability. Compared to DS01 (osmotic pressure, 62.39 bar), the DS02 (osmotic pressure, 60.24 bar) and DS03 (osmotic pressure, 59.41 bar) exhibited lower RSF due to the absence of KCl and improved composition of Na_2SO_4 salt, respectively. Interestingly, even with high osmotic pressure, the DS01 provides significantly lower SRSF suggesting that among all selected DS compositions, the DS01 (osmotic pressure, 62.39 bar) is most suitable considering its ability to achieve higher water flux (16.91 L m^{-2} h^{-1}) while maintaining low RSF (0.86 g m^{-2} h^{-1}).

5.1.2.3. Effect of multi-component DS component on the concentration of essential tea components

The quality of the concentrated tea extract was measured in terms of the concentration of essential tea components. The change in concentration of essential tea components was measured using HPLC-UV. The change in concentration of essential tea components represents the improved quality of the final tea concentrate (Table 5.3). The essential tea components were almost identical for all three multi-component DS compositions. Thus, suggesting that the movement of solvent molecules from DS to FS is principally driven by the osmotic pressure gradient and not by DS composition. Apart from RSF, the DS composition has no significant impact on FS composition. In this case, since the osmotic pressure was maintained to be the same, the concentration trend was also the same.

Table 5.3. Effect of multi-component DS composition on the quality of concentrated feed solution

	Increased concentration of essential tea component (%)						
	EGCg	EC	EGC	ECG	Catechin	Caffeine	Gallic acid
DS01	465.15 (±1.04)	325.84 (± 0.88)	485.33 (± 1.01)	424.90 (± 0.90)	294.11 (± 0.21)	193.36 (± 0.18)	197.77 (± 0.99)
DS02	449.21 (± 0.15)	314.73 (± 1.00)	480.50 (± 1.04)	413.56 (± 1.11)	292.41 (± 1.44)	187.53 (± 1.04)	195.79 (± 1.03)
DS03	234.89 (± 0.91)	297.87 (± 0.74)	428.45 (± 0.88)	390.22 (± 0.75)	290.78 (± 1.01)	188.34 (± 1.02)	191.45 (± 1.01)

EGCg: Epigallocatechin gallate; EC: Epicatechin; EGC: Epigallocatechin; ECG: Epicatechin gallate

5.1.2.4. Role of a suitable HFFO membrane in an efficient membrane separation process

The appropriate selection of DS and FO membranes plays a significant role in improving the overall FO process. Xu et al. (2017) [21] reported that the availability of a suitable FO membrane is crucial for developing the FO process. RSF, high CP, and poor mechanical strength are a few frequently encountered problems in food processing industries using FO membranes. Compared to the pressure-driven membrane process, the FO process tends to exhibit lower chances of membrane fouling. However, fouling is still inevitable while concentrating liquid food, impacting the overall FO membrane performance and shelf-life.

Due to CP, the boundary layer forms near the membrane active layer in any membrane process. Since most FO membranes are asymmetric, the active layer is embedded in the support layer. Therefore, CP results in a reduction in water flux and increased RSF. This CP layer is expected to form on both sides of the active layer. For example, i) the accumulation of solute on the support layer facing FS/DS and is called external concentration polarisation (ECP) and, ii) the accumulation of solute in the support layer embedded with the active layer and is termed as internal concentration polarisation (ICP) [194,195].

Reportedly, the support layer dramatically influences the severity of ICP. The membrane with a lower *S*-value for the FO process is usually preferred to reduce ICP severity. Suwaileh et al. (2018) [16] state that in order to lower the ICP effect, a support layer should have low tortuosity and high porosity. Reportedly, the structural parameter of the Aquaporin HFFO membrane is

three times lower than Toyobo HFFO membrane. Thus, the flux of the Aquaporin HFFO membrane is expected to be higher than the Toyobo HFFO membrane. However, the experiments are performed in the batch FO process to study the relationship between the structural parameter (*S*) and water flux. In another aspect, the solute transport through the active layer is the function of material properties such as zeta potential and hydrophilicity.

The zeta potential is an essential and reliable indicator of the surface charge of membranes, and knowledge of it is essential for the design and operation of membrane processes. The hydrophilicity of the membrane was determined based on the contact angle. The contact angle of CTA (contact angle, 60.27 ± 1.27°) is typically lower than the Aquaporin (AqP)-embedded polyamide active layer (contact angle, 41.22 ± 2.24°). The smaller contact angle for the AqP membrane than the CTA membrane is due to the improved surface hydrophilicity via embedding aquaporin molecules into the polyamide active surface. Reportedly, a reduction in contact angle enhances water permeability and anti-fouling performance [196].

To evaluate the effect of a membrane on the overall FO membrane performance, a series of experiments were performed using a laboratory-scale batch FO system (Figure 4.1 (a)). This study continued until the FS volume (RO water, TDS: 103.30 mg L^{-1}) was reduced to 60 ± 2% of the initial FS volume. Figure 5.4 represents the osmotic flux performance of the Aquaporin-inside-HFFO membrane compared with the Toyobo membrane using mixed DS composition (refer to Table 5.1) against RO water as FS.

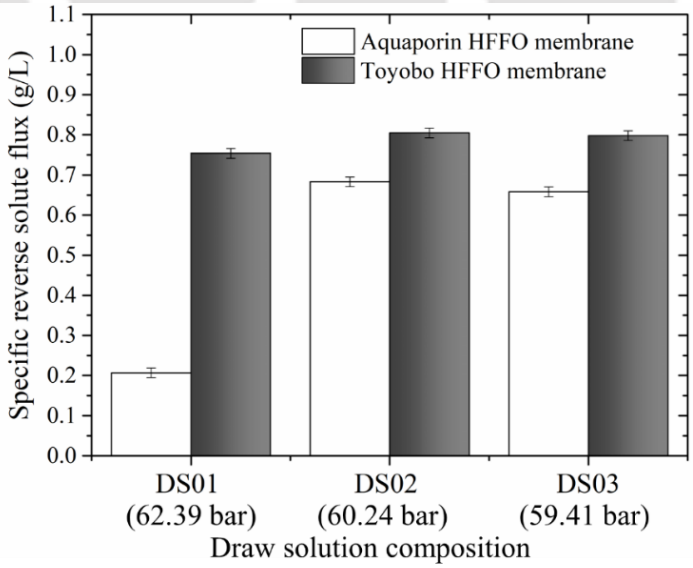

Figure 5.4 Comparison of Aquaporin and Toyobo HFFO module performance in terms of specific reverse solute flux (SRSF, g L^{-1}) using multi-component DS against RO water (103.30 mg L^{-1}) as feed solution

Due to a higher osmotic pressure gradient, the permeate flux for both Aquaporin inside HFFO membrane and Toyobo HFFO membrane exhibited higher flux against DS01 than DS02 and DS03. However, in the case of RSF, the trend was not the same. For the Toyobo HFFO membrane, the RSF was almost the same in all mixed DS compositions. The larger membrane area may affect permeation flow, but the main reason for equal RSF in the Toyobo membrane is probably due to low permeate flux. Since the RSF is primarily driven by the type of DS used and the concentration of DS at the membrane surface [197]. In contrast to RO processes, where the mass transfer is only directed from the FS toward the permeate, the RSF occurs in the FO process. This counter-directed diffusion is expected to pose a steric hindrance to feed solute transport, contributing to higher solute rejection.

Compared to Toyobo membranes, the aquaporin membranes exhibited lower SRSF with about 7.7 to 9.8 times higher water flux. The modules offered by Toyobo membranes are based on outer-selective CTA fibers, whereas Aquaporin A/s manufactures inner selective biomimetic thin-film composite (TFC) hollow fiber membranes. The AQP-incorporated proteoliposomes were immobilized on the inner surface of an HF membrane substrate and subsequently coated by a polyamide layer formed by a non-gas-assisted interfacial polymerisation process. Due to the particular structure and geometry of the HF membrane module, the Aquaporin membranes offer high water flux (L m^{-2} h^{-1}) and lower RSF (g m^{-2} h^{-1}). The *S*-value of the Aquaporin inside HFFO membranes was determined to be 210.5 ± 55.5 µm as one of the lowest *S*-value for TFC hollow fiber membranes [76].

Since structural parameter '*S*' is a property of the support layer of the FO membrane and is an indicator of the mass transfer resistance within the supporting structure of the membrane, an FO membrane with a high structural parameter and draw solute with a lower diffusion coefficient (*D*) is expected to result in significant ICP in the FO process [84]. Reportedly, instead of using DS with a superior diffusion coefficient, the high structural parameter (*S*) of the Toyobo membrane was primarily responsible for the comparatively lower flux (1.89 L m^{-2} h^{-1}) and higher SRSF (1.23 g L^{-1}) value than Aquaporin inside the HFFO membrane (water flux, 16.53 L m^{-2} h^{-1} and SRSF, 0.19 g L^{-1}). Reportedly, even when the RSF of the Aquaporin HFFO membranes was about 1.35 times higher than Toyobo HFFO membranes. Due to higher permeate flux, the SSF of the Toyobo HFFO membrane was almost 6.45 times higher than the Aquaporin HFFO membrane. Additionally, in the case of Aquaporin inside the HFFO membrane, the zeta potential at pH 5.3 to 6.5 was found to be more negative [198,199]. Thus, suggesting that compared to the Toyobo membrane, the negative zeta potential of the

Aquaporin HFFO membrane was more effective in rejecting the negatively charged essential tea components.

5.1.2.5. Integration of forward osmosis process with crystallisation technique for preparation of concentrated tea extract

The present research proposed an innovative approach for preparing instant tea using the integrating forward osmosis (FO)-crystallisation technique. In this study, the freshly brewed tea extract was concentrated to 93.67% using a mixed-component inorganic draw solution (refer Table 5.1).

(i) Effect of draw solution composition on the final tea powder

To understand the effect of DS composition in the final tea powder after FO 1st and 2nd cycles. The XRD and FTIR analysis were performed to get a brief overview of the effect of integrated FO-crystallisation technique on the essential tea components. The XRD analysis of the dried pellets obtained after the FO−1st and 2nd cycle confirms the formation of essential tea catechin crystallisation. Reportedly, being a crystalline compound, the catechin compound has a maximum XRD peak at 2θ = 15^{o} and another significant peak at 2θ = 24.84^{o} [200]. The same was confirmed with all dried pellets obtained after FO−1st and FO−2nd cycles. However, the peak intensity was significantly lower in the sample obtained after drying the final supernatant.

To characterise and recognise the molecules of black tea concentrate FTIR spectroscopy was used. Reportedly, the FTIR bands of tea extract solution consisting of polyphenols emerged at 3388 cm^{-1}, 1636 cm^{-1}, and 1039 cm^{-1}, and these are related to O−H/ N−H, C=C, C−O−C stretches, correspondingly [201]. Figure A1.2 reveals the presence of 3401 cm^{-1}, 2916 cm^{-1}, 1661 cm^{-1}, 1628 cm^{-1}, and 1029 cm$^{-1,}$ which corresponds to the O−H/ N−H (stretching modes of polyphenols), C−H (stretch in alkane), −C=N ring stretching, C=O (bond stretching in polyphenols), and C–O (stretching in amino acid), respectively exhibiting the given process is capable of retaining essential tea components [186,200,202,203]. The FTIR spectra reveals that despite the DS composition used for concentration of tea extract. The integrated FO-crystallisation technique proposed in this study was capable of retaining essential tea components.

The FESEM image (Figure 5.5) of the pellet obtained after 1st cycle FO process reveals the crystalline nature of the final product compared to the FESEM image obtained after drying the DS01 2nd cycle supernatant.

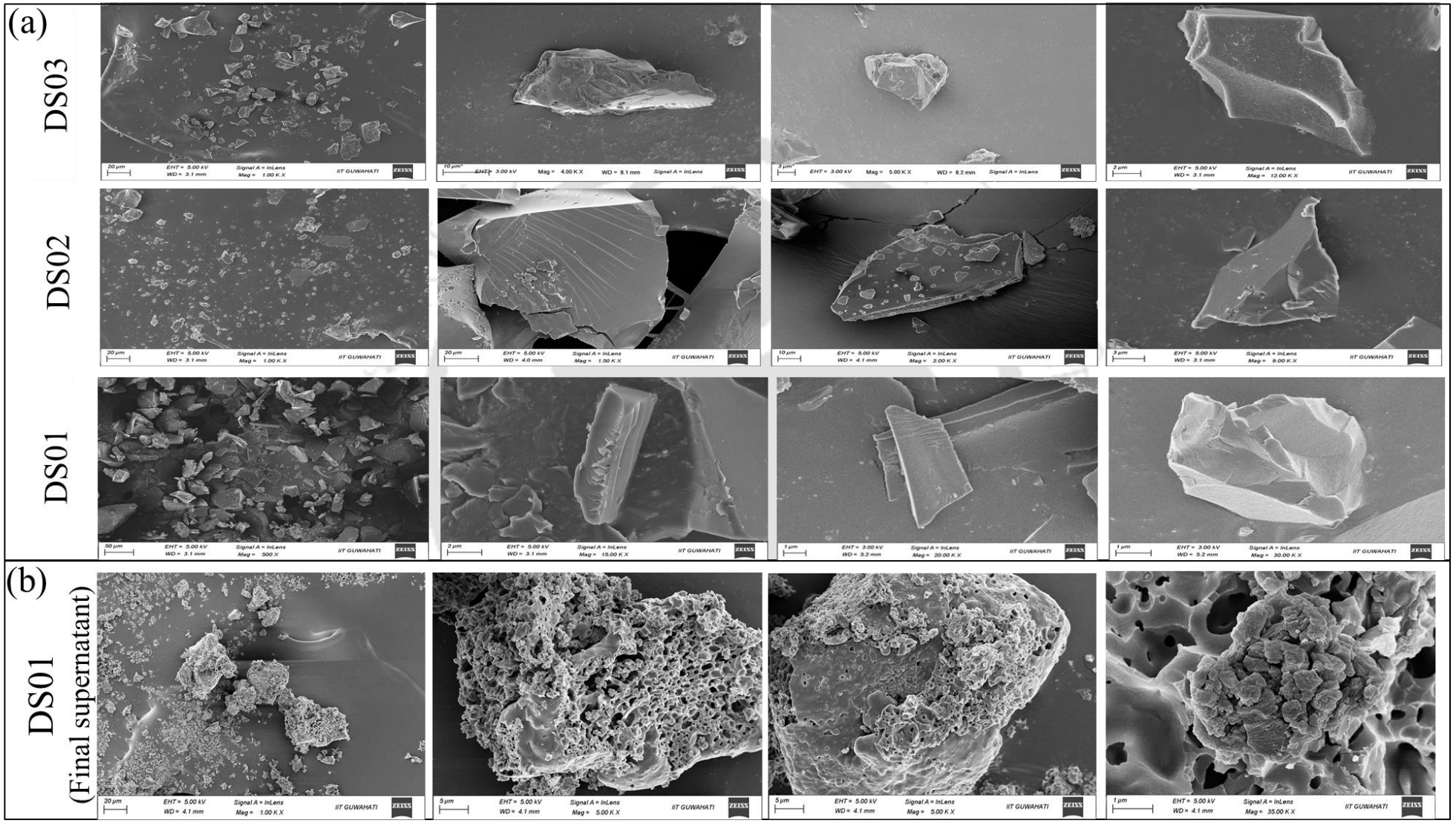

Figure 5.5 FESEM images of the final tea powder obtained after a) 1st cycle and b) 2nd cycle supernatant against different DS-composition

While brewing black tea, the tea extract consists of two fractions: water soluble and insoluble. The water-soluble fraction (such as catechin, caffeine, thearubingin, and TF) are responsible for the final concentrated product's taste, aroma, and strength. Therefore, the determination of the 'water-soluble fraction' of tea is one of the essential qualities which needs to be determined to evaluate the quality of the final product.

The effect of DS composition on tea components (tea catechins, caffeine, and L-Theanine) was estimated using HPLC analysis. The concentration of the EC, EGC, ECG, EGCG, catechins, caffeine, and L-Theanine was determined by injecting standard for all components at a concentration ranging from 5–50 mg L^{-1} concentration, and the peak area responses were obtained. A standard graph for each component was prepared by plotting concentration versus area (Table A1.2). Further, the quantification was carried out from the integrated peak areas of the sample and the corresponding standard graph.

Table 5.4 tabulates the effect of different DS compositions on the tea extract concentrated using integrated FO-crystallisation techniques. Maintaining other operating conditions constant, it was found that when FS (tea extract) is reduced by 93.67%, irrespective of the DS composition of the net amount of tea component (major catechin, caffeine, gallic acid, and L-theanine) composition is maintained to be almost identical with a slight deviation.

Table 5.4 Effect of DS composition on FS properties

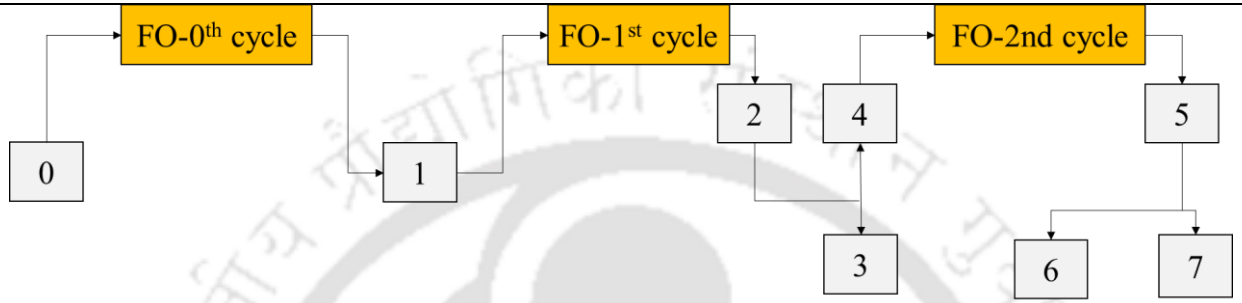

		0	1	2	3	4	5	6	7
DS01	Catechin (in g)	10.12	10.08	9.97	4.87	5.1	4.97	4.77	0.20
	Caffeine (in g)	12.18	12.15	12.13	6.88	5.25	5.21	4.19	1.02
	L-theanine (in g)	10.64	10.61	10.58	7.11	3.47	3.39	3.24	0.15
	Net weight (in g)	32.94	32.84	32.68	18.86	13.82	13.57	12.2	1.37
DS02	Catechin (in g)	10.15	10.12	9.91	4.64	5.27	4.97	4.77	0.20
	Caffeine (in g)	12.19	12.15	12.11	6.91	5.2	5.17	4.21	0.96
	L-theanine (in g)	11.14	10.61	10.59	7.16	3.41	3.39	3.27	0.12
	Net weight (in g)	33.48	32.88	32.61	18.71	13.88	13.53	12.25	1.28
DS03	Catechin (in g)	10.11	10.07	9.92	4.61	5.31	4.97	4.77	0.20
	Caffeine (in g)	12.19	12.15	12.18	6.88	5.19	5.17	4.17	1.00
	L-theanine (in g)	10.56	10.61	10.64	7.11	3.39	3.36	3.21	0.15
	Net weight (in g)	32.86	32.83	32.74	18.6	13.89	13.5	12.15	1.35

Catechins and their oxidation products are responsible for most of the sensory characteristics of black tea liquors [204]. The ability to retain net theaflavin (TF%) depicts that the FO process can essentially retain all the essential tea components (Figure 5.6 (a)). A high concentration of phenolic components was observed in freshly brewed tea extract, and the TPC content was found to range between 137.78 mg GAE per g and 164.37 mg GAE per g of sample for extract prepared from the tea bag and loose tea leaves, respectively (Figure 5.6 (b)).

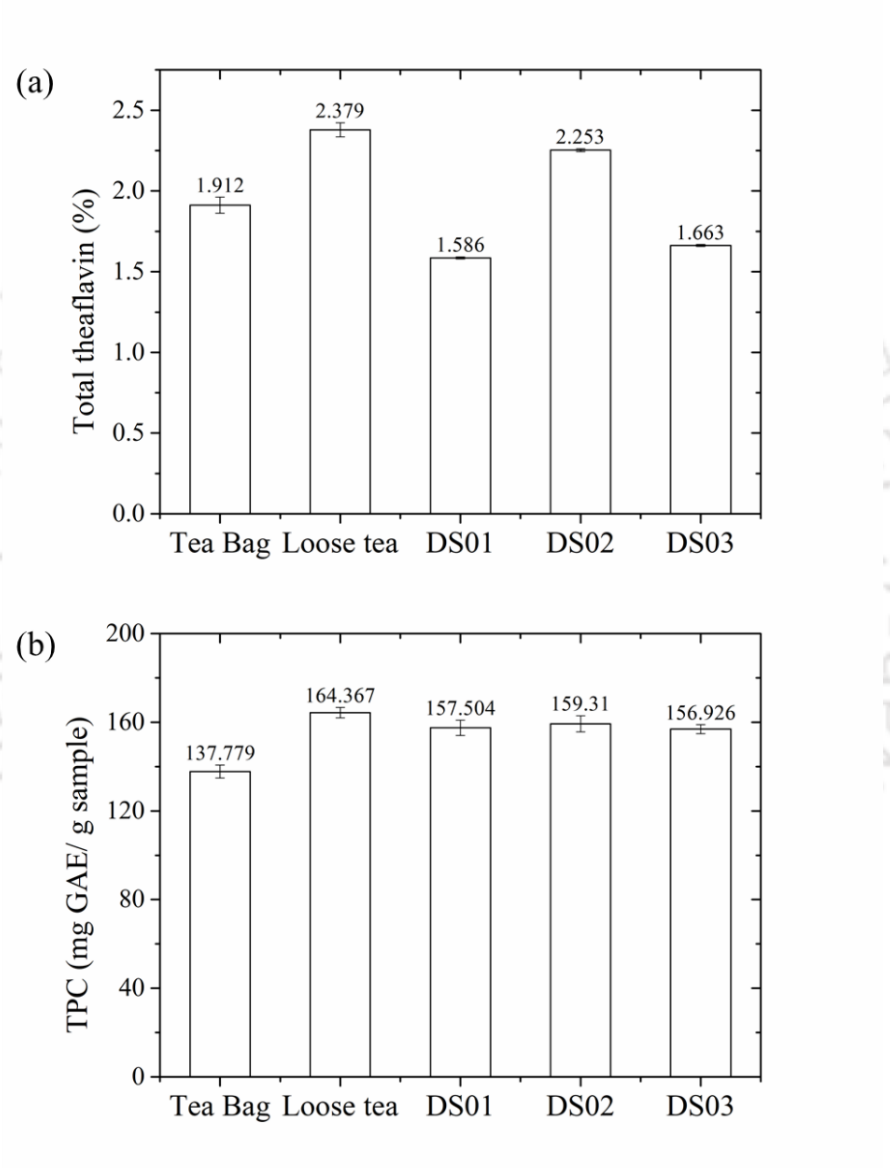

Figure 5.6 Effect of DS composition on a) Total theaflavin (%), and b) total polyphenol content (TPC, mg GAE/ g sample)

This study suggests that irrespective of the DS composition, the amount of final tea powder recovered from the given process was almost the same (26.36 ± 0.16 g). The recovered tea

crystal's cold and hot-water solubility was observed to be 88.11% and 94.75%, respectively. Thereby suggesting that the final product can be either directly used as a ready-to-drink (RTD) tea product or can be further purified to isolate essential tea components.

(ii) Effect of the process on the FO membrane properties and cleaning

The HFFO membrane module after each set of experiments reduces fouling and improves membrane performance. Chemical cleaning is a widely accepted and implemented industrial practice for cleaning membrane modules. The water permeability test was performed after each batch of experiments using 1% NaOH solution at room temperature to understand the effect of chemical cleaning on the membrane performance. Reportedly, the hydroxide ions in the alkaline solution promoted the disintegration of the fouled layer mainly by breaking the chemical bonds between the membrane and foulants (Zhang et al., 2019).

In literature, the stability of an aquaporin-based biomimetic membrane was tested against different chemical cleaning agents. The authors validated that the given membrane exhibited good resistance to the wide range of cleaning agents and performed well in a long-term FO operation [190,207]. The same was observed in the given study. The results (Figure 5.7) suggest that when 27 batches of experiments were performed (i.e., when 169 L of water permeated through the given membrane). Though the pure water permeability (L m^{-2} h^{-1} bar^{-1}) changes from 0.844 L m^{-2} h^{-1} to 1.106 L m^{-2} h^{-1}, the RSF trend change was only about 0.024% due to Aquaporin on the membrane AL.

The increased pure water permeability value indicates the change in water flux is either due to operation or chemical cleaning. Thereby suggesting that accompanied by an appropriate cleaning mechanism, the given process can be effectively utilised in liquid food and beverage processing industries.

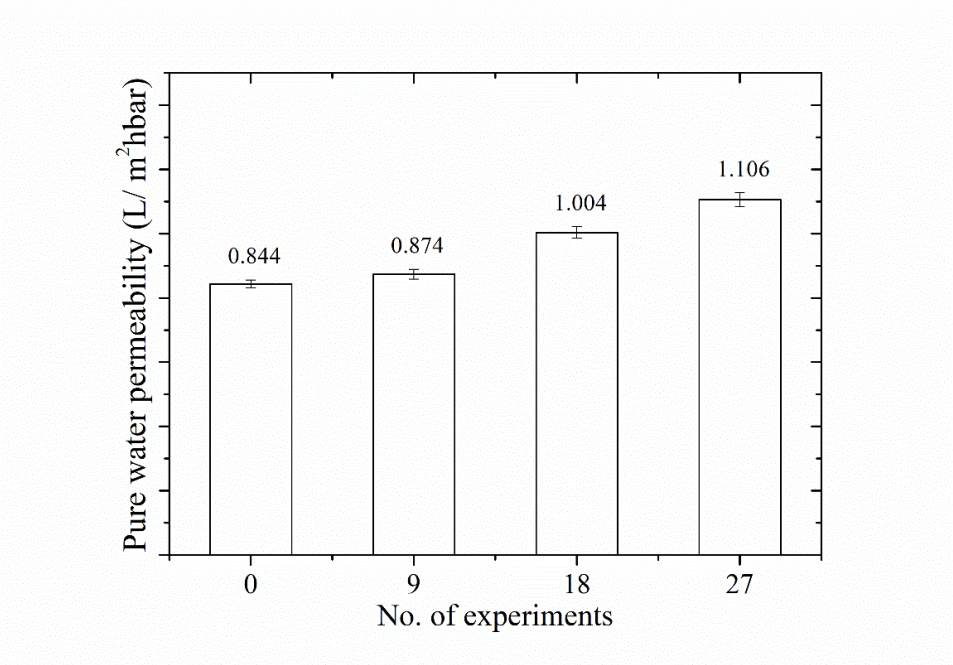

Figure 5.7 Variation in pure water permeability coefficient of the commercial Aquaporin inside HFFO membrane module with respect to continuous membrane operation

5.1.2.6.Concentration of tea extract: Forward osmosis vs Rotary vacuum evaporator

Compared to the conventional multi-stage evaporation process, the rotary-evaporation method is considered a gentle method of concentrating liquid food by removing the solvent (water) at reduced pressure by mechanically rotating a flask in a controlled temperature water bath. Thus, making the rotary-evaporation process ideally suitable for heat-sensitive materials.

To evaluate the effectiveness of the FO process, freshly brewed tea extract was concentrated up to 8-fold using an integrated FO-crystallisation process (refer to Section 5.1.2.5) and rotary-evaporation techniques. The quality of the final tea concentrate was evaluated based on the concentration of essential tea components. The low operating temperature and time in the FO process support the retention of heat-sensitive essential tea components, suggesting the FO process's feasibility for the concentration of black tea extract. Table 5.5 reveals that the FO process can retain essential tea components similar to the rotary evaporation technique.

Table 5.5 Comparison between the black tea extract concentrated using conventional rotary evaporation and forward osmosis process (multi-component DS composition 'DS01')

Method of concentration	Concentration of essential tea component (g L^{-1})						
	EC	EGC	EGCg	ECG	Catechin	Gallic acid	Caffeine
Rotary evaporation	3.678	7.132	1.576	0.700	0.347	1.676	0.859
Forward osmosis	3.754	7.652	3.112	1.150	1.78	3.054	2.08

EC: Epicatechin; EGC: Epigallocatechin; EGCg: Epigallocatechin gallate; ECG: Epicatechin gallate

In this study, for the preparation of 4 L of 100 g L^{-1} black tea extract, 400 g of dried tea leaves was used. Considering 2.25 g of tea leaves used for brewing 240 mL of tea extract, it can be assumed that using 400 g of tea leaves, about 178 cups of tea can be brewed. Table 5.6 represents a qualitative comparison between conventionally brewed tea extract and tea extract powder (about 9.4 g) obtained by concentrating tea extract to its maximum capacity using the FO process. To brew 178 cups of black tea using 9.4 g of black tea powder, a 0.05 g of tea powder was mixed with 240 mL of DI at 90 ^{o}C. The quality of tea extract obtained by both the conventional brewing process and tea powder was evaluated in terms of the concentration of essential tea components. Among all the essential tea components, the EGCG has been reported as the richest catechin in tea and has shown the most potent antioxidant activity in catechins, stronger than vitamins C and E [208]. EGCg is most susceptible to epimerisation and oxidation by light, oxygen, brewing methods, storage conditions, and packaging. As a result, all commercially available ready-to-drink (RTD) tea has low EGCg concentration than freshly brewed tea extract. Owing to the gentle operating condition of the FO process, the higher ability to concentrate tea extract with low or no significant loss of essential tea components exhibits the FO process as an efficient process of concentrating tea or any liquid food- beverage while retaining the essential thermolabile aromatic and nutritional component.

Table 5.6 Comparison of the synthesised tea concentrate with the conventionally brewed black tea extract

Component	Brewed tea (*), in mg L^{-1}		This study (**), in mg L^{-1}		Allowable range (per day)
	Per serving (240 mL)	Net consumption (5 cups per day)	Per serving (240 mL)	Net consumption (5 cups per day)	
EC	1.01	5.05	4.152	20.76	200-250 mg
EGC	17.64	88.2	191.53	957.65	
EGCg	1.95	9.75	2293.31	11466.55	338 mg
ECG	17.96	89.8	59.181	295.91	
Catechin	111.27	556.35	1311.92	6559.60	
Caffeine	17.4	87	16.88	84.40	< (300- 400) mg
Gallic acid	89.06	445.3	1071.58	5357.90	5 g per kg body weight
Sodium-ion	9	45	20	100	< 2300 mg
Chloride-ion	8	40	18	90	(3100-3600) mg

EC: Epicatechin, EGC: Epigallocatechin; EGCg: Epigallocatechin gallate; ECG: Epicatechin gallate

(*) 2.25 g in 240 mL DI, brewed at 90°C for 10 min

(**) 0.05 g dried concentrated tea extract mixed with 240 mL DI, heated at 90°C

Catechins are thermo-sensitive flavonoid derivatives that play a significant role in determining the taste of brewed tea extract. Therefore, the stability of tea catechin in an aqueous solution is one of the significant advantages of using the forward osmosis process for the preparation of concentrated tea extract. The FO process can be successfully used to concentrate black tea extract, and the concentrated final product can be either directly used for the preparation of ready-to-drink (RTD) tea beverages or as flavouring agents/ additives in beverage and food processing industries. The concentrate can also be further used to extract catechins for

pharmaceuticals, biotechnology, and related industries [162,163]. The high catechin concentration in the final concentrated products suggests that an effective separation of high-value catechins can be further purified and used as pharmaceuticals and for similar purposes [154,209].

Summary on performance analysis of multi-component draw solute for the concentration of tea extract using forward osmosis process

For the preparation of liquid food concentrate, the RSF can result in altered taste, which may eventually reduce consumer acceptability. Therefore, an optimized balance between permeate and RSF needs to be established. This study focuses on identifying a suitable multi-component inorganic salt solution as a draw solution (DS) with enhanced permeate flux and reduced RSF. The study also highlights the role of FO membrane and structural parameters on the overall process performance. It was found that the Aquaporin HFFO membrane with a lower S-value gave superior FO performance than the Toyobo membrane. Using the multi-component DS composition, freshly brewed tea extract was concentrated to supersaturated condition. The effect of draw solution composition on the quality of the final product was determined in terms of change in essential tea component concentration. This study demonstrates the feasibility of an integrated FO-crystallisation technique for the preparation of tea crystals. The final product can be either directly used as an RTD beverage or further purified to isolate essential tea components for other related industries.

5.2. Simulation and Design Analysis of HFFO Membrane Module

5.2.1. Model simulation and validation for single component inorganic draw solution for concentration of tea extract

The model equation for the FO process was solved using Modelica language in the Dymola software tool. The model parameters were estimated by minimising the error between the model and experimental output. The error function can be defined as the square of absolute error between the experimental and model data (refer to equation 3.28).

Here, the number of essential tea components was identified as ‘i’=6 (i.e., EGCg, EGC, EC, ECG, Caffeine, and Gallic acid). The model parameters (Table 5.7) were able to predict the performance of the Aquaporin HFFO membrane module for the preparation of concentrated tea extract within the maximum error of 12.12% for change in mass and concentration of DS and FS tank, respectively. Figure 5.8 and Figure 5.9 represents the effect of single-component DS on FO performance and essential tea component concentration, respectively.

Table 5.7 Overview of the estimated HFFO membrane module parameters while concentrating tea extract using FO process

	Description	Value					
		1M NaCl	1.5M NaCl	1M Na_2SO_4	1.5M Na_2SO_4	1M $MgCl_2$	1.5M $MgCl_2$
L_p	Pure water permeability coefficient ($L\ m^{-2}\ h^{-1}\ bar^{-1}$)	0.884	0.899	0.889	0.889	0.889	0.889
B	Solute permeability coefficient ($L\ m^{-2}\ h^{-1}$)	0.072	0.099	0.074	0.088	0.072	0.072
S	Structural parameter (µm)	210	210	210	210	210	210
α_f		0.044	0.045	0.043	0.045	0.048	0.051
α_d		0.063	0.077	0.074	0.083	0.075	0.076
β_f		1.958	1.594	1.799	1.957	1.795	1.795
β_d		0.781	0.787	0.785	0.856	0.784	0.784
γ_f		0.320	0.327	0.322	0.334	0.328	0.329
γ_d		0.329	0.329	0.329	0.329	0.329	0.330

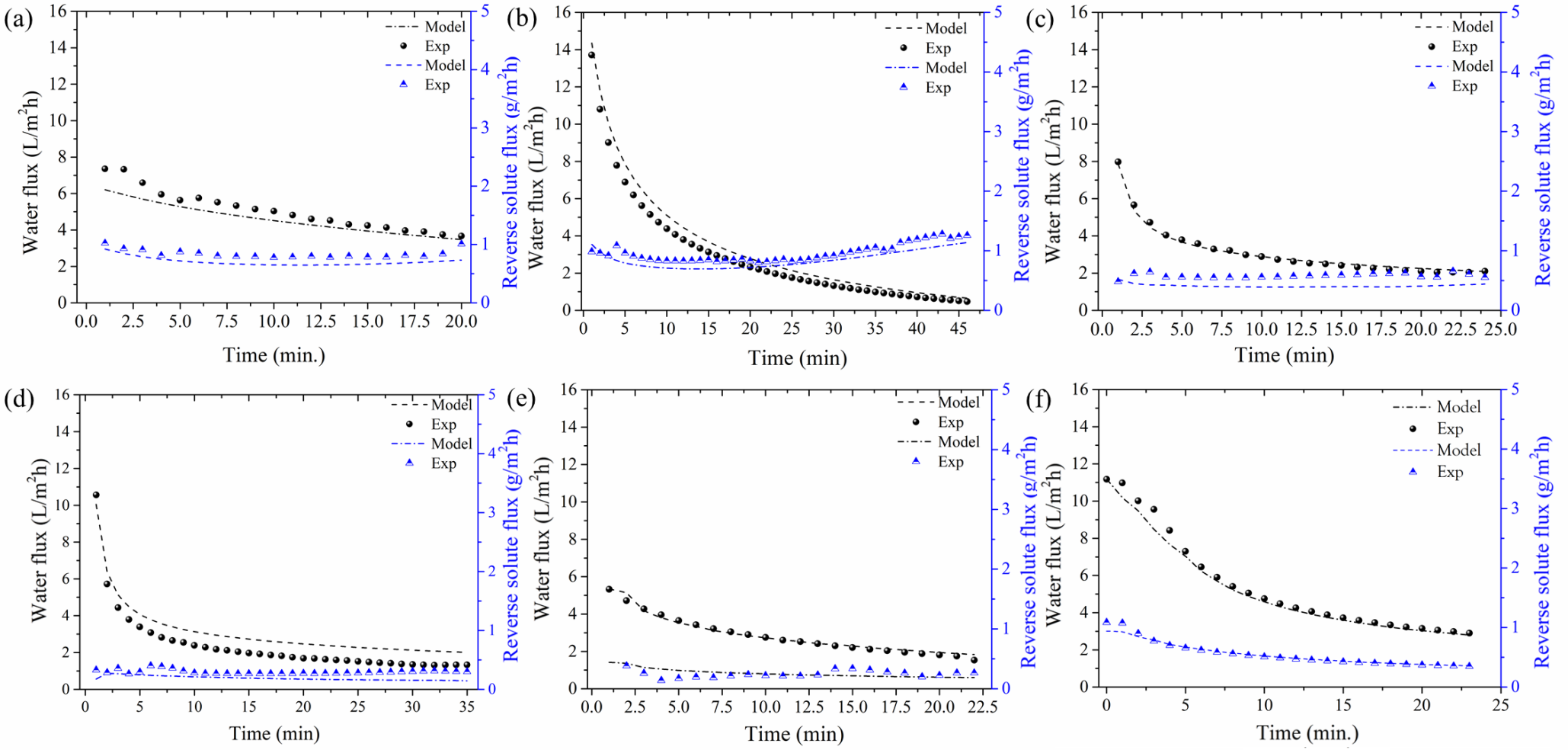

Figure 5.8 Performance (permeate flux and reverse solute flux) of HFFO module using (a) 1M NaCl, (b)1.5M NaCl, (c) 1M $MgCl_2$, (d) 1.5M $MgCl_2$, (e) 1M Na_2SO_4, and (f) 1.5M Na_2SO_4 as DS for preparation of concentrated tea extract

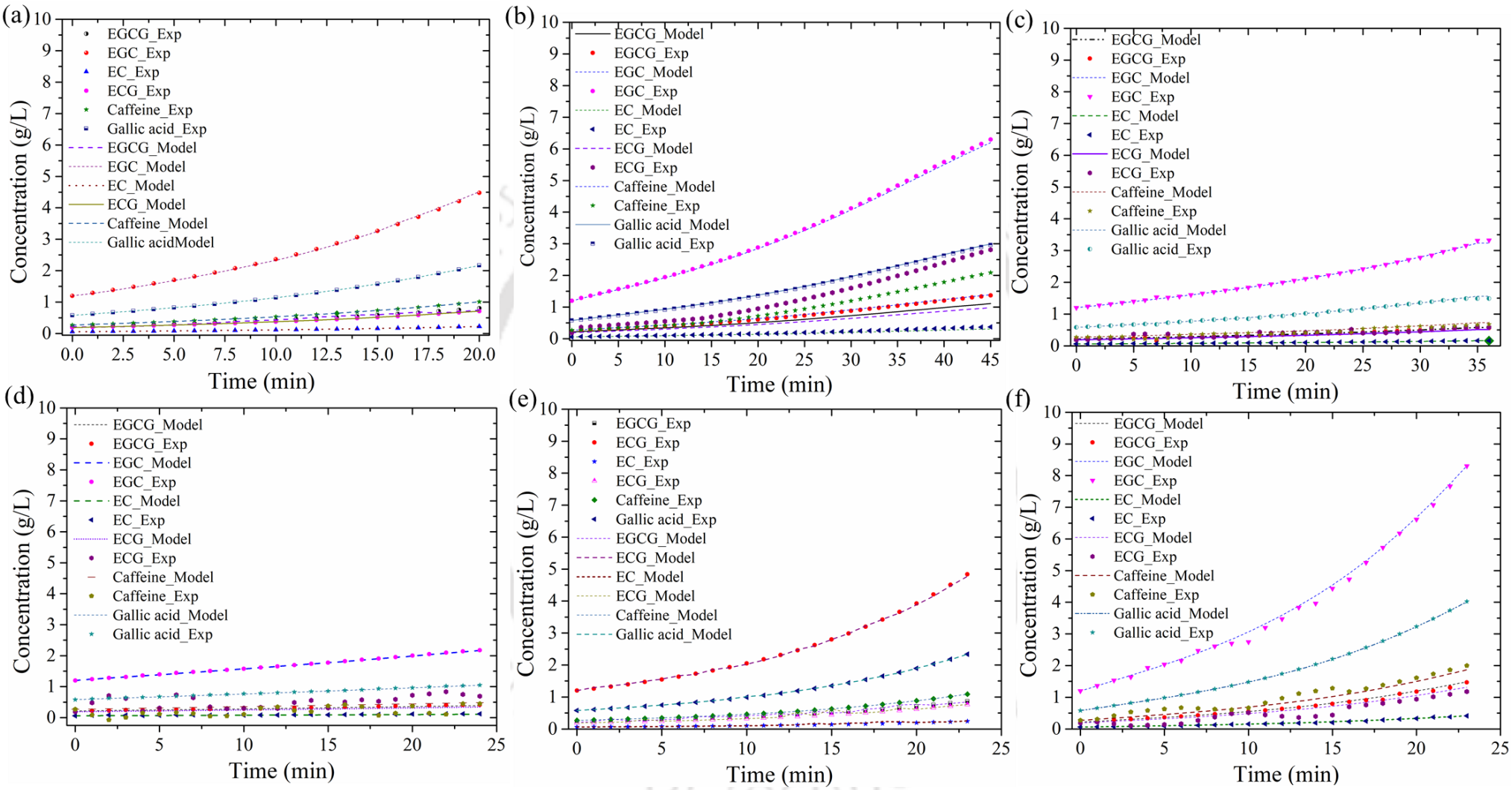

Figure 5.9 Variation in essential tea component concentration when (a) 1M NaCl, (b)1.5M NaCl, (c) 1M $MgCl_2$, (d) 1.5M $MgCl_2$, (e) 1M Na_2SO_4, and (f) 1.5M Na_2SO_4 are used as DS for preparation of concentrated tea extract

5.2.2. Process flow-sheet simulation for the concentration of tea extract

The above study suggests that the FO process is a viable technique for the concentration of brewed tea extract and the developed model was able to predict the performance of the given FO process. Thereby to evaluate the commercial feasibility of the given process for large-scale application. A series of simulation studies in ALDS mode were performed using the same one-dimensional mathematical model. Otherwise mentioned, the initial DS (NaCl) concentration was maintained as 65.6 g L^{-1} (at 25 ± 1 ^{o}C) and FS is freshly brewed black tea extract (refer to section 4.2.1.).

5.2.2.1. Feed and draw solution in continuous mode

In this study, FS and DS are circulated through the FO module in continuous mode. Reportedly, the performance of HFFO membrane modules strongly depends on the FS and DS flow rate [210]. Thus, in order to understand the role of the operating flow rate (of both FS and DS). While maintaining other operating conditions (such as membrane module, membrane area, initial FS/ DS composition, and temperature), only the operating (FS, and DS) flow rates were varied.

Figure A1.1 represents the effect of FS and DS flow rates on the different FO flow-sheet configurations on the overall FO performance (in terms of SRSF). The increased flow rate resulted in increased flux proving the dominance of ECP on the active side of the membrane. Theoretically, the increased flow rate configuration is attributed to the reduction of the ECP by reducing the mass transfer coefficient with the flow. Reportedly, with the introduction of higher feed velocity, a thick layer of the fluid at the AL gets disturbed. As a result, the diffused salt from DS can be more effectively transported to the bulk of FS, and the net driving force (osmotic pressure gradient between the feed and draw side of the AL) is enhanced. The same was observed in the given study, suggesting as when the FS flow rate is increased from 25 L h^{-1} to 50 L h^{-1}, a subsequent reduction of SRSF was observed for 27.65% (for case I), 30.33% (for case II), and 30.94% (for case III (a)). Similar to the FS flow rate, the applied DS flow rate also influences the performance of the HFFO module. Keeping the FS flow rate constant, the DS flow rate was changed from 60 L h^{-1} to 25 L h^{-1}. The impact of the DS flow rate on the FO performance can be theoretically explained by the more severe effect of the DS flow rate on dilutive internal and external concentration polarisation. The dilution of DS with permeate water significantly reduces the available driving force along the length of HFFO membrane modules. It suggests that the higher the DS flow rate, the lower would be the dilution obtained

in the module. Ideally, the DS should be operated at a higher flow rate. However, a higher flow rate also results in high-pressure build-up across the membrane, resulting in mechanical damage to the fiber. Therefore, the low or moderate DS flow rate is more suitable for extending the membrane lifetime, and as a result, in this study, the DS flow rate was not exceeded beyond 60 L h^{-1}.

When the FS and DS flow rate is changed from 25/60 to 45/45, the SRSF was found to be significantly reduced by 26.81% (case I), 58.85% (case II), and 29.74% (for case III (a)). Using the given Modelica model, to determine the improved values of model parameters (FS and DS flowrates) by multi-criteria optimisation based on simulation runs were performed: (i) to minimize SRSF and (ii) maximize the net flux (J_w). Thereby suggesting that further flow-sheet configuration would be performed using two FS/DS flow rate configurations (i.e., 25/60 and 45.14±0.08/ 45.21 ±0.29). Further, the function of the sweep-two parameter is to be used to study the dependence of response with respect to two parameters at the end of the integration interval (Figure 5.10).

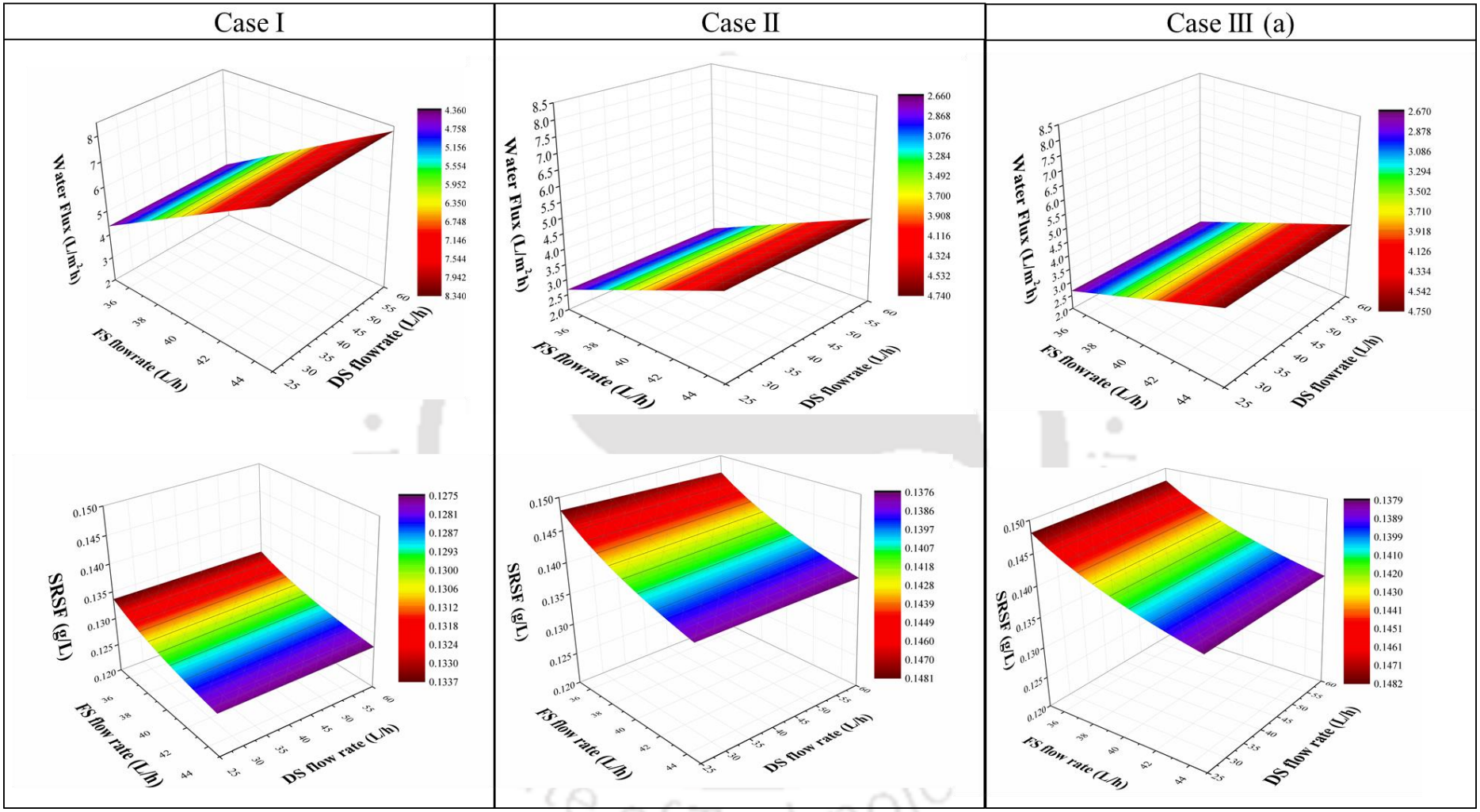

Figure 5.10 Effect of feed and draw solution flow rate on the overall FO performance against different flow-sheet configuration

5.2.2.2. Feed and draw solution in recycle mode

In this case, a single HFFO membrane (case IV) and two HFFO modules (case V) are placed in series. The FS and DS are re-circulated through the FO module in counter-current mode. Maintaining other condition operating conditions same, it was observed that by implementing 2 FO membrane modules (case V) instead of 1 FO membrane module (case IV), the time required to reduce the FS (tea extract) by 93.542±0.822% could be significantly reduced by 7.5 times. In case VI, similar to case V, the FS and DS are re-circulated through two HFFO modules placed in series. However, instead of one HFFO module, two separate DS tank was recycled through the module separately. As discussed in the previous section, the DS and FS flow rate significantly impact the overall FO performance, and the same trend was observed in this study. Therefore, case VI flow sheet configuration with FS and DS flowrate at 45.14 L h^{-1} and 45.21 L h^{-1}, respectively, was most suitable for dewatering liquid food using the FO process.

5.2.2.3. Feed solution in recycled mode and draw solution mode in continuous mode

The best-performing process flow configuration (case VIII) is further modified in this section. Here, the FS is recycled, whereas the DS is passed through the 2 HFFO modules in continuous mode. Due to the higher concentration gradient between the two solutions, the flux is much higher and, as a result, compared to other cases, where the time required to reduce volume by 93% was significantly lower compared to other cases. The DS can either be pumped continuously through the 2 HFFO membrane modules (case VII) or pumped separately through both HFFO modules using two pumps (case VIII). Similar to previous cases, the effect of FS and DS flow rates was investigated on the overall membrane performance.

The simulation data reveals that in both case VI and case VII, the time taken to reduce FS volume by 94.49 ±1.07% was almost the same for both flowrate configurations. In this section, it is observed that when the flow rate of FS/DS is changed from 25/60 to 45.14/45.21, the SRSF is reduced by 57.74% (case VII) and 66.87% (case VIII), respectively. Based on SRSF and SEC data, Case VIII was identified as the best-performing process flow sheet (Table 5.8).

Table 5.8 Overview of the optimised FO process condition [FS flow rate: 45.14 L h^{-1} and DS flow rate: 45.21 L h^{-1}]

	I	II	III (a)	III (b)	IV	V	VI	VII	VIII
Time (min.)	–	–	–	–	10.5	6.5	3.75	2.39	3.01
FS volume reduced (%)	27.54	43.15	88.18	93.11	93.18	93.15	93.16	93.14	93.16
SRSF (g L^{-1})	0.17	0.13	0.14	0.597	1.57	1.57	3.06	0.22	0.21
SEC (kWh m^{-3})	0.50	0.61	0.88	4.14	1.57	1.57	3.06	3.11	1.59

5.2.2.4. Implementation of seawater and reject brine as potential draw solute for the concentration of tea extract

In this section, the effect of implementing fresh seawater and high-concentration reject brine as draw solute for the concentration of liquid food solution was investigated. Considering the best-performing process flow sheet (Case VIII) configuration, the FS is recycled, and the DS is circulated in continuous mode. The principal objective of this study is to utilize high-concentration seawater as DS for the preparation of concentrated tea extract (93.22±0.18%). As discussed in section 3.9, the given objectives can be achieved when the FS and DS flow rate is maintained at 45.14±0.08 L h^{-1} and 45.21±0.08 L h^{-1}, respectively. Due to higher water flux, the concentration process was rapid, along with simultaneous seawater dilution. Herein, Table 5.9 tabulates the effect of DS concentration on the overall process performance when seawater and red seawater are used as DS.

The study suggests that when the reject brine stream of red seawater is utilized as DS (105.175 g L^{-1}), the solvent transport from DS to FS (tea extract) is significantly higher due to high concentration. Thus, the resulting FS volume to reduce by 93.10% in just 2.18 min, with minimal SRSF (0.19 g L^{-1}). This study also suggests that the reject brine is diluted while concentrating the FS from 105.17 g L^{-1} to 32.18 g L^{-1}.

Table 5.9. Comparison of FO performance while using seawater and red seawater as draw solute [FS flow rate: 45.14 L h^{-1}, and DS flow rate: 45.21 L h^{-1}]

		1.5 M NaCl	Seawater		Red seawater	
			Fresh	Brine reject	Fresh	Brine reject
Time (min.)		3	4.50	2.80	4.00	2.00
FS volume reduced (%)		94.05	93.68	93.26	91.98	93.35
SRSF (g L^{-1})		0.21	0.19	0.19	0.21	0.14
DS concentration	Initial	65.6	35	70	42.07	105.17
(g L^{-1})	Final	25.92	17.16	25.03	19.50	81.38

Summary of simulation and design analysis of the HFFO membrane module

The developed one-dimensional module was validated using the batch experimental data and could predict DS and FS tank mass and concentration. The estimated model parameters, such as pure water permeability (L_p), solute permeability (B), and structural parameter (S), were found to be like the literature-reported values. Additionally, a series of simulation studies were performed to understand operating conditions' role (flow rate) on the overall FO performance. The objective of this simulation study was to improve the overall FO performance (by maximising the water flux and minimising the SRSF). The feasibility of seawater and high-concentration reject brine as DS was also investigated. Due to high concentration, the reject brine (from the seawater desalination plant) can result in rapid dewatering with minimal SRSF (0.185 g L^{-1} to 0.207 g L^{-1}) along with simultaneous seawater dilution.

5.3. Performance Analysis of Hydrogel as Draw Solute for Forward Osmosis Process

5.3.1. Characterisation of the synthesised hydrogel

5.3.1.1. PVA-PolyDADMAC hydrogel

The morphology of the synthesised hydrogel was observed using FESEM at 500 and 1000X magnification (Figure 5.11). At the 0^{th} cycle (before the experiment), the FESEM image exhibits an uneven surface with a porous structure on the cross-sectional surface of the synthesised hydrogel (Figure 5.11 (a, b). After the 12^{th} cycle of FO and dewatering, the performance of the synthesised hydrogel got reduced. The same was represented using the

comparatively smooth surface of the gel with the reduced porous structure on the cross-sectional surface of the hydrogel. The reduced membrane performance was due to the surface morphology of the synthesised hydrogel due to repetitive cycles of swelling and deswelling (Figure 5.11 (c, d). The change in surface morphology of the hydrogel subsequently reduced water flux in the FO process. The reduction of FO performance could also be from DECP due to the reduced swelling capacity of the hydrogel on the membrane surface. The synthesized hydrogel consists of a loosely cross-linked polymeric network. Due to repeated swelling (in the FO process) and dewatering (for regeneration), the strength of the polymeric chain was expected to break, resulting in a subsequent loss of its porous texture. The FESEM image of the new and used membrane (after 10^{th} cycles) exhibited the deposition of loose hydrogel particles on the membrane surface (Figure A2.1).

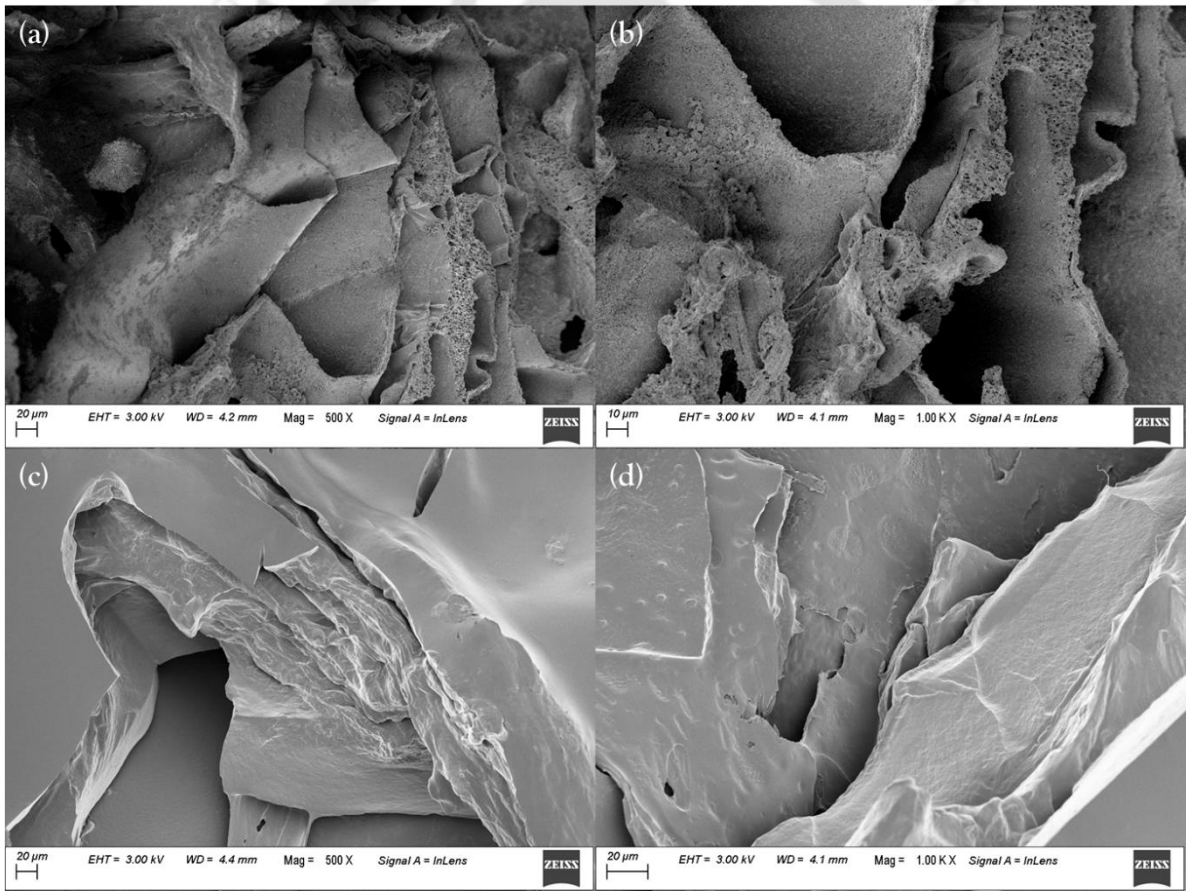

Figure 5.11 FESEM image of hydrogel before FO experiment (a) at 500X, (b) at 1000X, and after FO experiment (c) at 500X, (d) at 1000X

X-ray powder diffraction (XRD) is a rapid analytical technique used for phase identification of crystalline material. The surface characterisation of hydrogel has a significant effect on water absorbency. The change in crystallinity of hydrogel from cubic (0^{th} - 3^{rd} cycle),

tetragonal (7^{th} cycle), orthorhombic (9^{th} cycle), and monoclinic (10^{th} cycle) can be considered primarily responsible for the reduced water absorption capacity of the synthesised hydrogel.

The ATR-FTIR spectra for 0^{th}/ 5^{th}/ 7^{th}/ 9^{th}/10^{th} cycle are shown in Figure 5.12. The ATR-FTIR was used to provide information on functional groups near the surface of an internal reflection element. Here, the 0% transmittance means the sample has absorbed all radiation, whereas 100% transmittance means the sample absorbed the same amount of radiation as the reference.

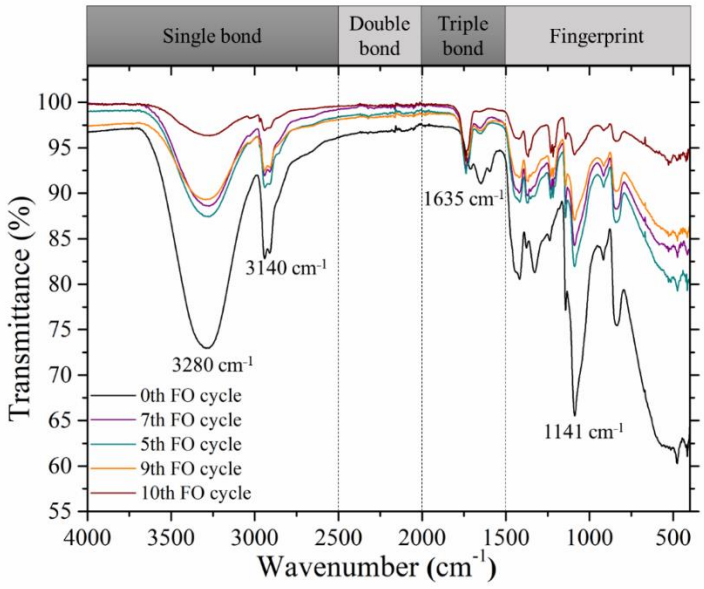

Figure 5.12 FTIR spectroscopy image of the synthesised hydrogel after each cycle

The peak observed between 3000 cm^{-1} to 3500 cm^{-1} was related to –OH stretching of PVA and aliphatic secondary amine of PolyDADMAC. According to a study reported by Mwangi et al. (2013) [211], the –OH group of solvent (in our case, water) can potentially result in a peak between 3382 cm^{-1} and 3332 cm^{-1}. The increment of transmittance from the 0^{th} to 10^{th} cycle represented the reduction of the swelling capacity of the hydrogel. The C–O (crystallinity) at 1141 cm^{-1} represents the increased crystallinity in terms of transmittance (%T). The characteristic C–C of the conjugated carbon atoms of the polyelectrolyte (polyDADMAC) at 1635 cm^{-1} was found to be the same with no significant change. The given result implied that each cycle's FO performance change was primarily due to a change in surface morphology and not due to the leaching of the component from the hydrogel [212,213].

The swelling properties of the synthesised polymeric hydrogel are among the most critical parameters that need to be considered. An interior osmotic pressure gradient can control the swelling capacity of the hydrogel (this is related to the number of ionic functional groups,

cross-linking points, the interaction between polymer-solvent, and hydrophilicity). The hydrogel composition with the highest swelling ratio can eventually result in a high water (permeate) flux. The swelling ratio was determined in 3 h. The concentration of PVA and PolyDADMAC used in hydrogel formulation significantly impacted the overall FO performance of the prepared hydrogel. Reportedly, keeping polyDADMAC and cross-linker glyoxal composition the same, it was observed that with an increase in PVA concentration from 10 wt.% to 13.33 wt.%, the swelling ratio increased from 13.45 g g^{-1} to 20.68 g g^{-1} (Table 4.3).

In hydrogel preparation, cross-linking agent prevents the dissolution of the hydrophilic polymer chains in an aqueous environment. As the cross-linker concentration increased from 5 wt.% to 10 wt.%, the swelling capacity decreased from 13.45 g g^{-1} to 11.77 g g^{-1}. A higher concentration of cross-linking agents resulted in diminished polymeric network space and reduced water absorption capacity [214,215].

5.3.1.2. Acrylic acid hydrogel

The FESEM image of dry hydrogel particles exhibits interconnected capillary channels (Figure 5.13). These interconnected capillary channels are formed due to the action of the foaming agent used during hydrogel synthesis. The literature suggests that such capillaries are connected through the pores on the gel surface [30, 31]. Compared to conventional gels, where the diffusion of water governs the swelling through the glassy polymer. In the given case, these open channels aid the fast absorption and exclusion of water. The interconnected capillaries are expected to accelerate the water diffusion in the hydrogel and thus can act as an additional driving force to accelerate solvent diffusion [216].

This section investigated the effect of cross-linker concentration and degree of neutralisation (DON) on the synthesised hydrogel. The swelling properties of hydrogel represent its ability to absorb water, which is used to achieve high water flux [116]. The cross-linking density plays a significant role in determining the absorption properties of the hydrogel. To investigate the effect of cross-linker (MBA) concentration on hydrogel swelling capacity, a set of hydrogels was synthesised as mentioned in section 4.2.6.2. Reportedly, the network density increases when the amount of cross-linking agent is high. Hence the hydrogel's swelling capacity decreases. However, when the amount of cross-linking agent is too low, the networking degree of hydrogel is too low to form a three-dimensional polymeric network. Thereby, the appropriate determination of cross-linking agent is critical to synthesise a hydrogel with a high swelling capacity [214,217]. Supposedly, keeping other component's composition constant, when only

the concentration of cross-linking agent (MBA) is changed from 0.005 g to 0.14 g, the swelling capacity reduces from 332.33 g g^{-1} to 82.33 g g^{-1}, respectively (Table 5.10).

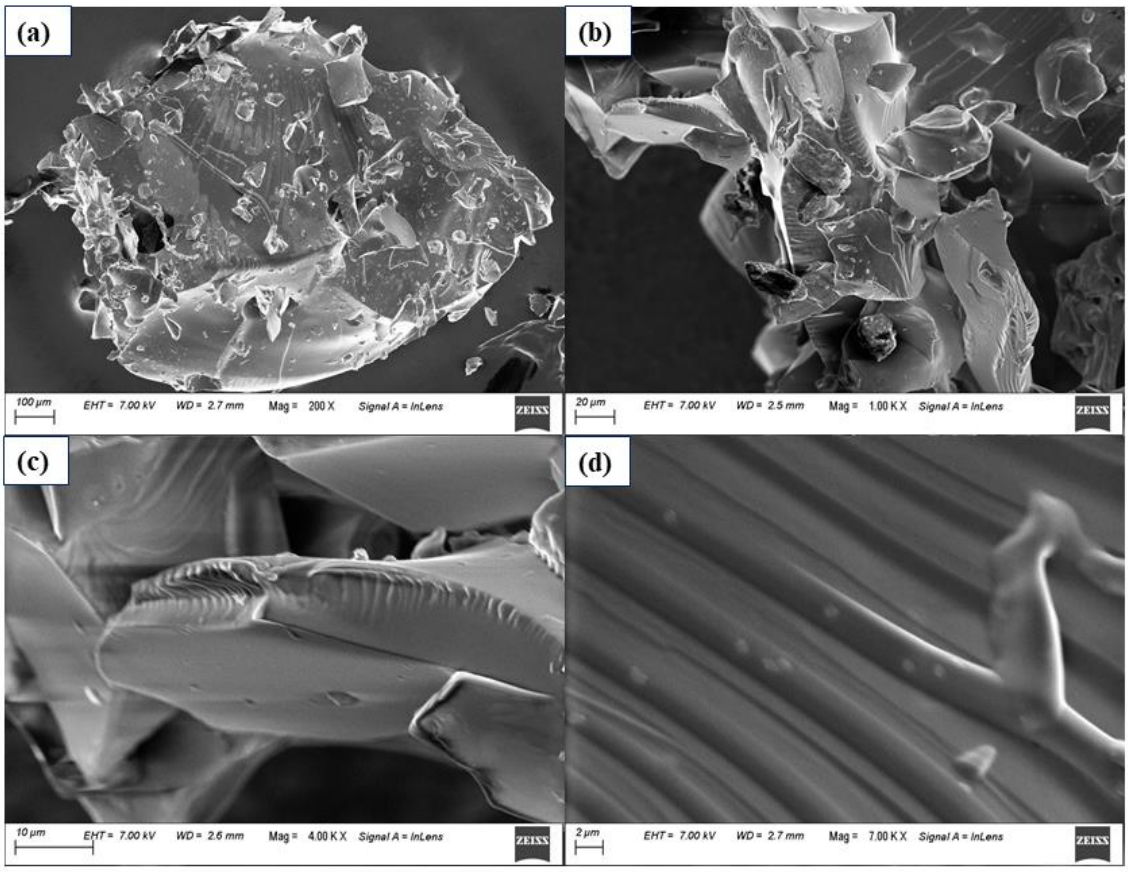

Figure 5.13 FESEM image of synthesised hydrogel at a)200X, b)1000X, c) 4000X, and d) 7000X magnification

During the neutralisation of acrylic acid using potassium hydroxide, the negatively charged carboxylic group attached to the polymeric group is expected to produce an electrostatic repulsion, subsequently leading to network expansion [218,219]. The EDX spectra (Figure A2.2) represent an increase in DON from 45% to 90%, the potassium elemental composition increases from 12.1 wt.% to 21.5 wt.%, and sodium elemental composition reduces from 3.2 wt.% to 1.6 wt.%. Due to increased DON, the amount of potassium acrylate increases and thereby lowering the availability of the non-neutralized group of acrylic acid for reaction with sodium bicarbonate. The electrostatic repulsion is primarily responsible for hydrogel synthesis's high or low absorption capacity. A similar trend was observed in this study; when the DON% of neutralisation of acrylic acid was improved from 45% to 75%, the swelling capacity improved from 114.44 ± 1.008 g g^{-1} to 332.333 ± 1.012 g g^{-1} (Table 5.10). When hydrogel is synthesised using partially neutralized acrylic acid, the carboxyl anions are

expected to be exposed to water resulting in rapid swelling of hydrogels [220]. However, no significant improvement in swelling capacity was observed when the DON was improved beyond 75%.

Table 5.10 Effect of hydrogel composition on swelling capacity

	MBA, g	NIPAM, g	DON, %	Swelling capacity, g g^{-1}
C005_45%	0.005	-	45	114.44 ± 1.008
C005_60%	0.005	-	60	197.454 ± 1.011
C005_75%	0.005	-	75	332.333 ± 1.012
C005_90%	0.005	-	90	144.55 ± 1.004
C1	0.140	-	75	82.332 ± 1.112
C2	0.015	-	75	223.641 ± 1.045
C3	0.005	-	75	332.333 ± 1.012
C4	0.005	0.016	75	334.812 ± 0.887
C5	0.005	0.200	75	365.671 ± 0.117

Though the incorporation of NIPAM does not play a significant role in improving the swelling capacity of the hydrogel. However, taking into consideration of the thermo-responsive behavior of NIPAM. For further studies, the performance of synthesised hydrogel 'C1', 'C3', and 'C5' (refer to Table 5.10) was selected.

5.3.2. Effect of different stimuli on hydrogel regeneration

In hydrogels, the swelling and deswelling rate are considered critical properties. It ensures the continuous regeneration and repeatability of the given synthesised hydrogel. As the swelling capacity of the hydrogel reduces, the flux also reaches saturation. The swelling rate of the synthesised gel was identified to be too high. It was observed that the flux of hydrogel could be significantly enhanced if the trapped water in the hydrogel network could be removed efficiently. To evaluate the effective regeneration of the synthesised hydrogel, the dewatering efficiency of the swollen hydrogel were evaluated under different stimuli.

5.3.2.1. PVA-PolyDADMAC hydrogel

During the swelling process, the water molecules diffuse into the polymeric network, and as a result, the polymer chain starts relaxing. After each FO process, the hydrogels (osmotic agents) were regenerated by blowing hot air (40 ^{o}C). The change in the weight of hydrogel was accurately measured using a digital weighing balance. The process of dewatering hydrogel

continued till the weight change became constant. After the regeneration of the osmotic agent (hydrogel), the dried osmotic agent was subjected to another cycle of the FO process, followed by DS regeneration. This swelling and deswelling of the synthesised hydrogel continued until the change in water flux (L m^{-2} h^{-1}) became constant. Figure 5.14 (a) represents the change in average flux with each cycle of FO (swelling) and deswelling (regeneration). Additionally, the application of hot air (40 ^{o}C) increased the crystallinity and, as a result, reduced the swelling capacity of the hydrogel. Figure 5.14 (b) represents each cycle's change in flux (in the first 60 min). The surface morphology of the hydrogel also changed from a porous to a crystalline structure (Figure 5.14 (c)).

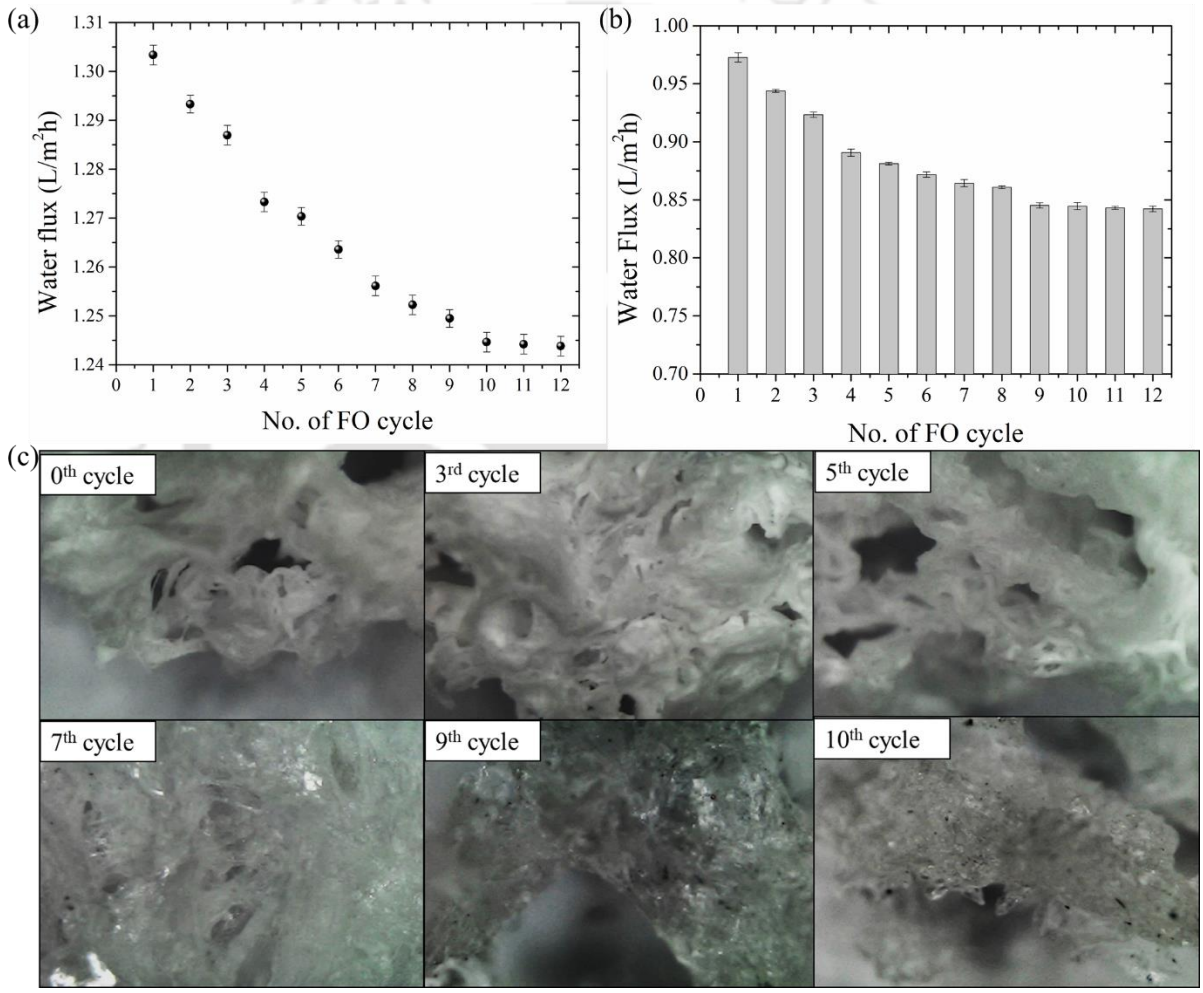

Figure 5.14 a) Change in average water flux with each FO and regeneration cycle, b) change in flux over the first hour of FO process, and c) digital microscopic image to determine the change in morphological structure with each cycle, at 100X

The study suggests that the water flux can be recovered to 86.6% of the initial flux after 12-time of the hydrogel (draw solute) regeneration. Thereby suggesting that instead of

implementing thermal influence (hot air) for draw solute regeneration. The performance of the given hydrogel can be further improved by implementing a non-thermal regeneration technique.

5.3.2.2. Acrylic acid-NIPAM hydrogel

(i) Temperature

To investigate the effect of temperature on the synthesized hydrogel's deswelling capacity, a certain amount of swollen hydrogel was placed in a hot plate under atmospheric pressure. The effect of temperature on deswelling capacity was determined in terms of drying rate (g m^{-2} h^{-1}) at a temperature ranging between 45−95 ^{o}C (Figure 5.15).

The initial deswelling trend of 'C1' and 'C3' at 75 ^{o}C was almost similar to 45 ^{o}C, and 55 ^{o}C. This signifies that cross-linker concentration has no significant effect on the deswelling properties of the hydrogel. However, while maintaining the concentration of cross-linking agent similar, the deswelling trend of hydrogel 'C5' was found to be superior than 'C3'. The improved dewatering performance of hydrogel 'C5' was due to the incorporation of NIPAM-monomer to the polymeric network. NIPAM-monomer exhibits a lower critical solution temperature (LCST) [64,221]. The LCST in PNIPAM results from the realignment of water molecules around the hydrophobic (alkyl) and hydrophilic (acrylate) group in polymeric chains resulting in the release of water due to collapsed hydrogel network. Due to the incorporation of thermo-responsive monomer 'NIPAM', at 45 ^{o}C the initial drying rate of hydrogel 'C5' (309.55 g m^{-2} h^{-1}) was found to be superior than 'C3' (182.16 g m^{-2} h^{-1}).

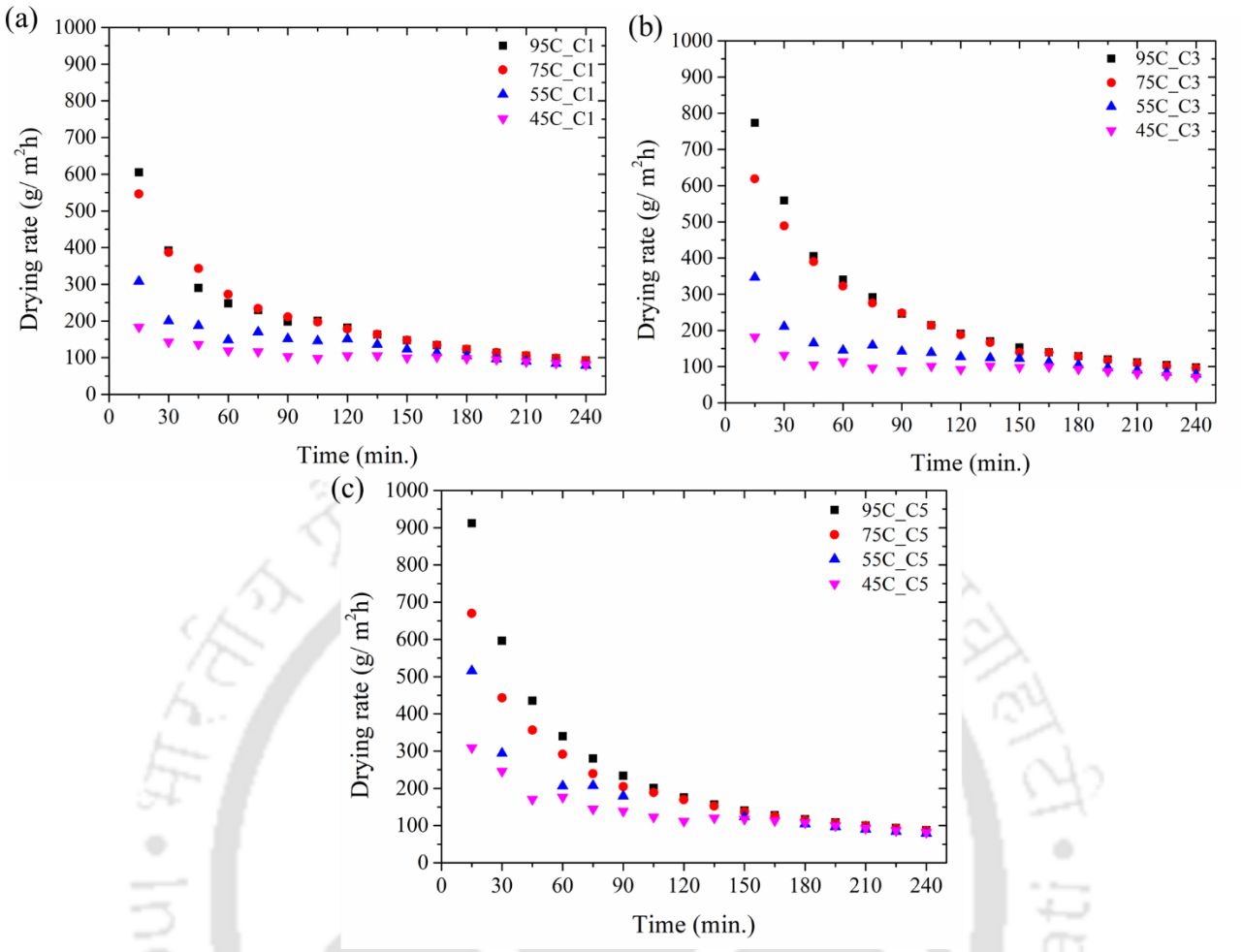

Figure 5.15 Effect of temperature on deswelling capacity of the given hydrogel with (a) C1, (b) C3, and (c) C5

(ii) High-concentration reject brine

This section explored the regeneration of swollen hydrogel using high concentration RO rejects brine solution (63,500 mg L^{-1}). Due to swelling and osmotic pressure gradient between the feed and draw solution, the solvent from low-concentration FS permeates to the osmotic agent (semi-swollen hydrogel). Similarly, due to the osmotic gradient between the high-concentration brine solution and hydrogel, the solvent is expected to permeate from the hydrogel to the brine solution. Figure 5.16 represents a brief overview of NaCl concentration's effect on the synthesised hydrogel's deswelling. In this study, the swollen hydrogel after the FO process was placed inside a membrane module and in a beaker consisting of different concentrations of aqueous NaCl. As the concentration of NaCl solution is improved from 10 g L^{-1} to 70 g L^{-1}, due to improved osmotic pressure gradient, the solvent molecules from hydrogel move more efficiently toward high-concentration brine (NaCl) solution.

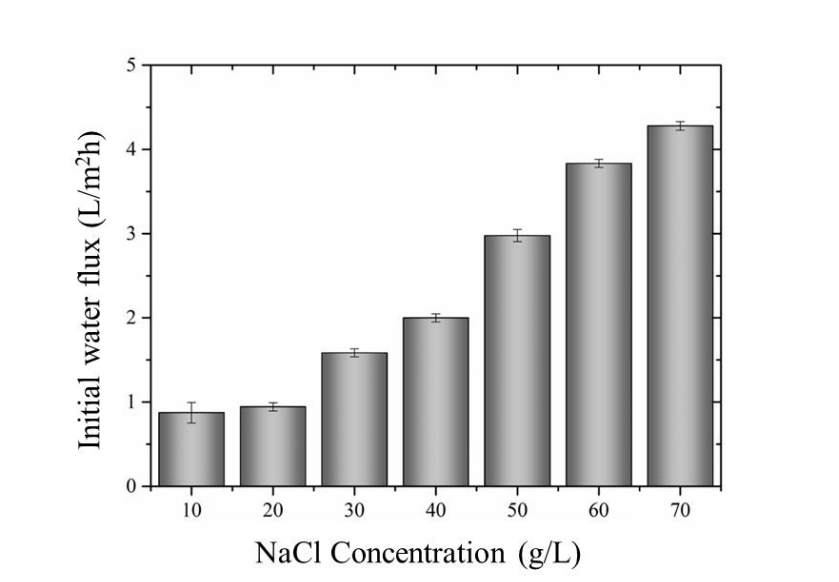

Figure 5.16 Performance of the synthesised swollen gel against different NaCl concentration

(iii) Solar radiation

To investigate the effect of solar energy on hydrogel regeneration, a certain amount of swollen hydrogel was dewatered under the sun for 6 h. According to the literature, Assam's average solar energy potential is 4.290 kWh m^{-2} day^{-1} to 4.660 kWh m^{-2} day^{-1} [222]. The amount of water released from the polymeric network was collected carefully for further analysis. Interestingly, a dewatering efficiency of 81.36% was achieved in 6 h of span (at $33^{o}C$). The concentration and osmotic pressure of the collected water were analysed using Ion chromatography (IC) and a freezing point osmometer. The FTIR analysis spectra (Figure A2.3) represent the peak observed in rinsed water after each dewatering cycle as the peak observed in DI. The FTIR spectra of the water collected at 1^{st} to 5^{th} rinse exhibited the FTIR spectra as DI implying no significant leaching of polymeric particles. The osmolality of the rinsed water reduces from 3 mosmos kg H_2O (for 1^{st} rinse) to 1 mosmos kg H_2O (for 5^{th} rinse) with a change in concentration of sodium ion, potassium ion and chloride ion from 1.844 mg L^{-1} to 0.785 mg L^{-1}, 0.643 mg L^{-1} to 0.273 mg L^{-1}, and 2.275 mg L^{-1} to 1.213 mg L^{-1} respectively. In context to other reported hydrogel composition and their FO performance, the modest performance of our synthesised hydrogel reveals it can be potentially used for the actual application.

5.3.3. Forward osmosis performance of the synthesised hydrogel

5.3.3.1. Batch FO process using hydrogel as draw solute

(i) PVA-PolyDADMAC

Figure 5.17 represents the FO performance of the prepared hydrogel (as draw solute) against 5000 mg L^{-1} NaCl solution at room temperature (26 ± 0.05 ºC). Compared to other hydrogel compositions, the hydrogel '3:3:1.5', with superior swelling capacity (refer Table 4.3), exhibited an improved trend of permeate flux. In 360 min, the water flux changed from 1.30 L m^{-2} h^{-1} to 0.68 L m^{-2} h^{-1}. The concentration of cationic polyelectrolyte polyDADMAC and PVA played a significant role in determining the overall performance of the hydrogel. As the FO process proceeded, a decrease in water flux was observed with time. This decreasing trend of water flux was evidently due to the decreased concentration gradient between FS to draw solute due to the swelling of hydrogel.

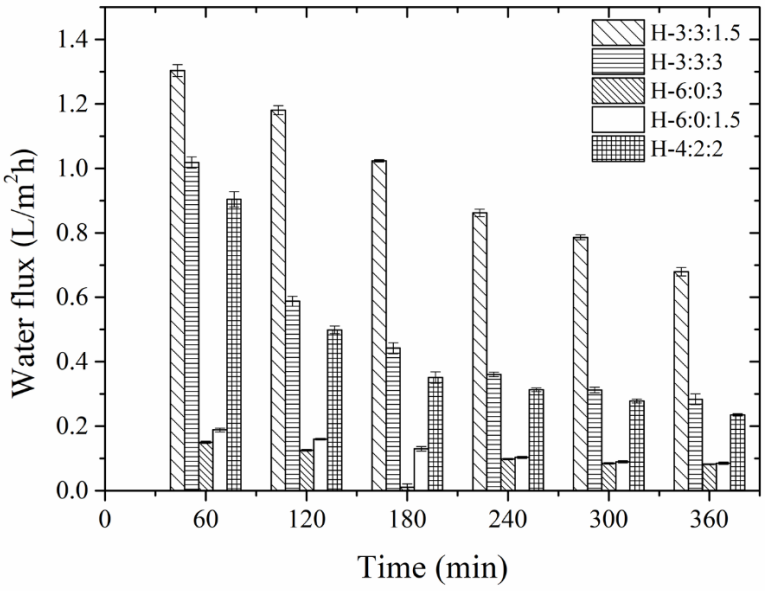

Figure 5.17 Effect of hydrogel composition on the overall forward osmosis performance against 5000 mg L^{-1} NaCl solution

Figure 5.18 represents the overall performance of the best-performed draw solute against different NaCl (5000 mg L^{-1} and 2500 mg L^{-1}) concentrations and DI as FS. As the FS concentration increased, the corresponding flux decreased. The solution with NaCl concentrations of 5000 mg L^{-1}, 2500 mg $L^{-1,}$ and DI as FS against hydrogel (with composition 3:3:1.5) as draw solute. In the first hour, the flux was observed as 1.30 L m^{-2} h^{-1}, 1.81 L m^{-2}

h^{-1}, and 1.91 L m^{-2} h^{-1}, respectively. The decreased flux with time was attributed to the reduced osmotic pressure gradient across the membrane.

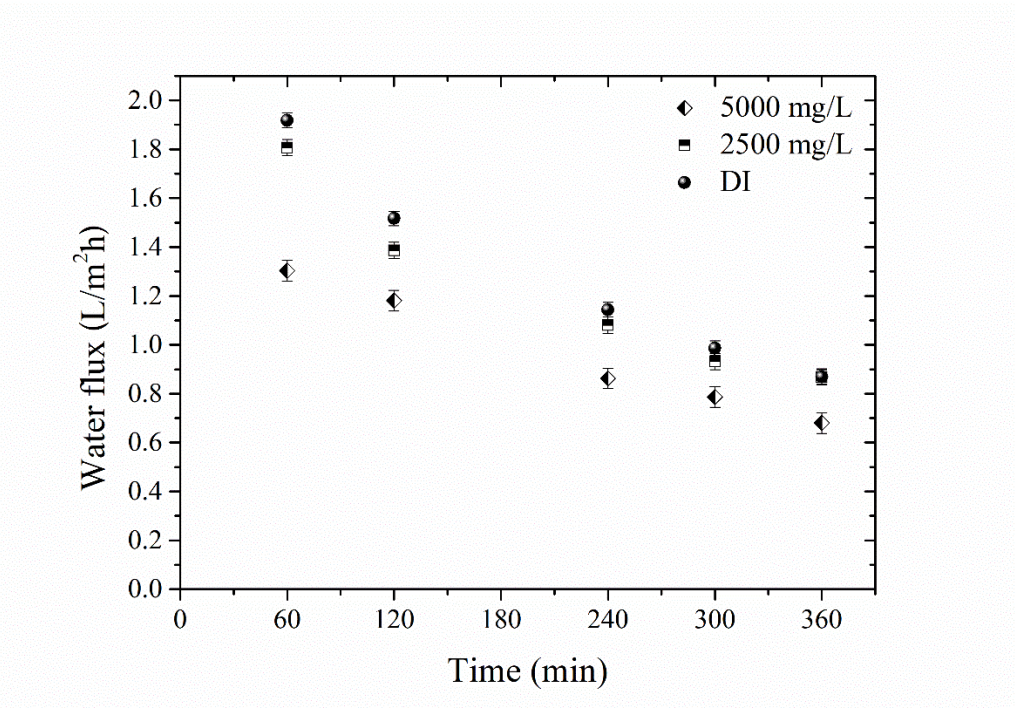

Figure 5.18 Effect of feed solution (NaCl) concentration on the overall FO performance against H-3:3:1.5 hydrogel as DS

Along with permeate flux (L m^{-2} h^{-1}), the RSF also plays a significant role in determining the overall feasibility of the synthesised hydrogel. In this case, the NaCl solution is replaced by DI water. The change in conductivity of the DI water was used to estimate the RSF (0.11 g m^{-2} h^{-1}) using equation (4.2).

(ii) Acrylic acid-NIPAM hydrogel as draw solute

Figure 5.19 represents the FO performance of the synthesised hydrogel against 5000 mg L^{-1} NaCl aqueous solution as feed solution. Owing to high swelling pressure, the initial flux of 'C3' (5.8 ± 0.154 L m^{-2} h^{-1}) was observed to be superior than C2 and C1. As the FO process proceeds, the swelling pressure of polymer hydrogels decreases with increasing their degree of swelling, resulting in the observed decrease in water flux. Due to the diffusion of solvent from feed to draw solute (hydrogel), the swelling capacity of hydrogel gradually reduces, and eventually, the FO performance also reduces. To overcome the given issue, the solvent from the polymeric network must be simultaneously removed to retain the swelling capacity of the synthesised hydrogel. The improved initial flux of hydrogel 'C3', 'C4', and 'C5' can be attributed to the lower cross-linker concentration that eventually enhanced the swelling

capacity. Reportedly, the swelling of hydrogel is driven by osmotic pressure originating from the dissociation of the ionic group and the solvation force generated by the hydrogen bonding interaction between the hydrogel network and the H_2O molecule. Potassium polyacrylate is highly hydrophilic, and with the incorporation of NIPAM, the hydrogel's deswelling properties also improve significantly. After a certain period of FO, the polymeric network entraps the permeated water and becomes swollen. Thus, due to reduced swelling and osmotic pressure of hydrogel (osmotic agent), its water permeation rate also reduced. To avoid this, the hydrogel needs to be continuously dewatered using thermal treatment (~30 to 40 ^{o}C), ensuring the regeneration of the given batch of hydrogel for further FO process. Over 6h, using thermal dewatering treatment (i.e., by blowing hot air), the NIPAM-incorporated hydrogel-maintained flux of 2.454 L m^{-2} h^{-1} compared to 1.668 L m^{-2} h^{-1} of hydrogel without NIPAM.

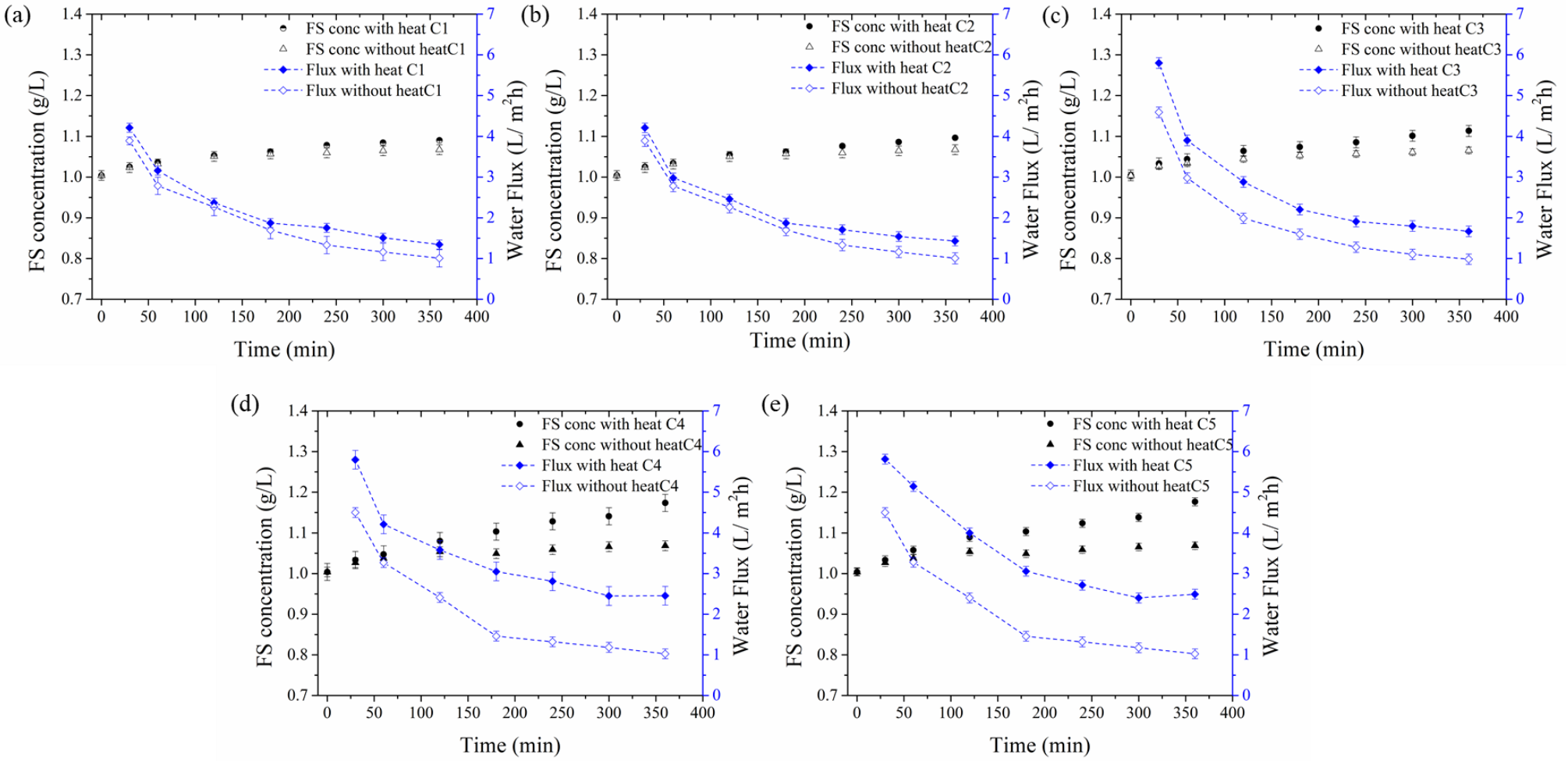

Figure 5.19 Average water flux of 5-cycle of forward osmosis process using a) C1, b) C2, c) C3, and d) C4, e) C5 as draw agent against 5000 mg L^{-1} NaCl as Feed Solution

In most studies, it is assumed that hydrogels are insoluble in water. However, the chances of reverse solute flux are almost negligible for applying the synthesised hydrogel in the food and beverage processing industries. The leaching of loose polymeric components could be possible due to the continuous swelling and deswelling of hydrogel over the 5-cycle of the FO process. To investigate the effect of leaching, the FO process was performed using C5-hydrogel (as DS) against 1000 mg L^{-1} NaCl (Figure 5.20 (a)) and DI (Figure 5.20 (b)) water as FS.

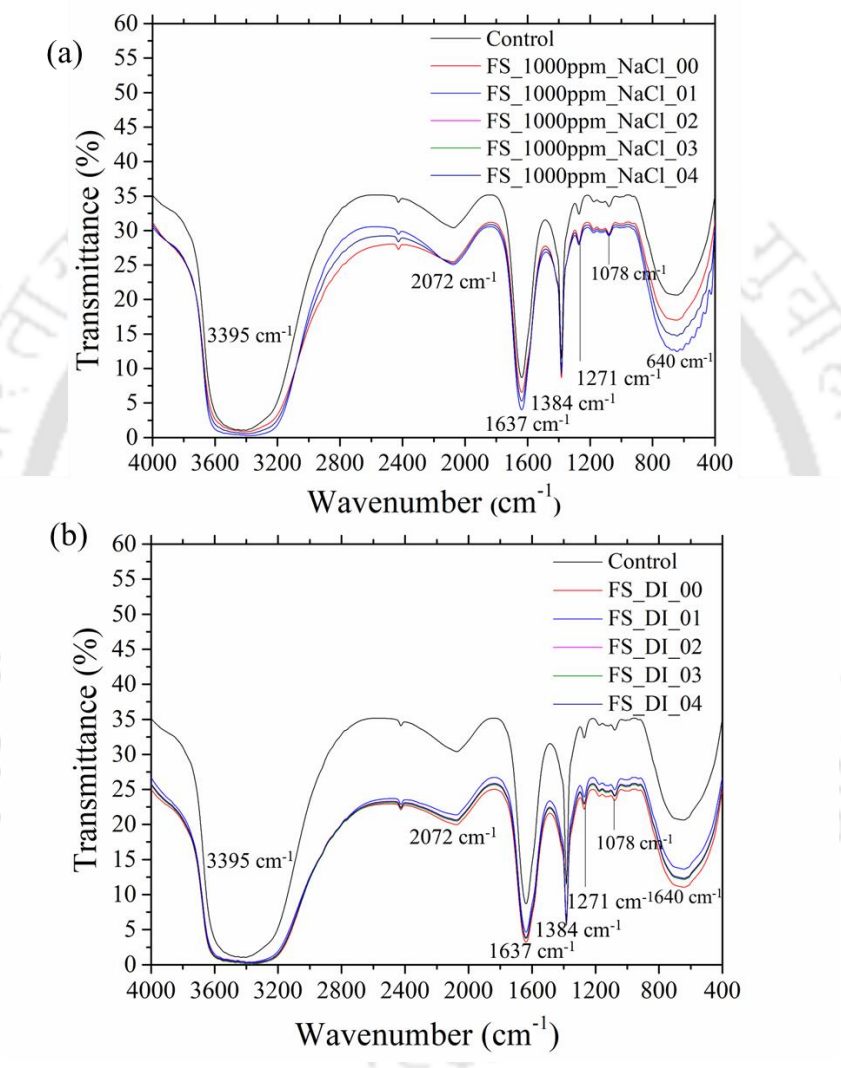

Figure 5.20 FTIR spectrum of FS a) NaCl solution, and b) DI water after each FO cycle against 'C5' as DS

Based on the flux data, the hydrogel 'C5' was designated as the best-performed gel due to its improved dewatering capacity. Further, using the 'C5' hydrogel, the effect of FS concentration on FO performance was investigated. Figure 5.21 represents the average flux data against *FS* concentrations ranging from 500 to 5000 mg L^{-1} NaCl.

Conventionally, FO occurs when the osmotic pressure gradient between the feed and draw solution is positive ($\Delta\pi > 0$) at the same hydrostatic pressure. The average flux (L m^{-2} h^{-1}) in the first 30 min reduces from 5.714 to 0.329 L m^{-2} h^{-1} as the FS (NaCl, aqueous solution) increases from 500 to 5000 mg L^{-1} at 25 ± 1 ºC.

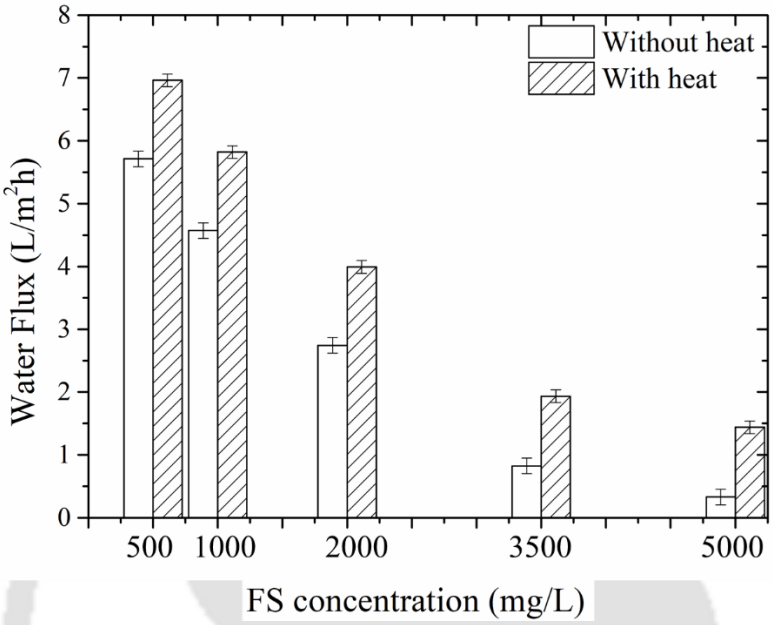

Figure 5.21 Average water flux (in, L m^{-2} h^{-1}) in first 60 min against different FS concentration

Further, to determine the practical applicability of the synthesised hydrogel as a draw solute. Using the integrated FO setup (refer, to Figure 4.7 (b)), 202 mL of freshly brewed tea extract (10 g L^{-1}, TDS: 354 mg L^{-1}) against synthesised hydrogel 'C5'. The dewatering efficiency of the given process was estimated in terms of change in weight and TDS of the FS over time. The change in concentration of essential tea components is estimated using HPLC, and the RSF was estimated in terms of sodium and potassium ion concentration in the final FS.

Figure 5.22 represents the permeate flux declined from 5.714 L m^{-2} h^{-1} to 1.714 L m^{-2} h^{-1} in the first 6 h of the experiment, and after 6 h, the change in flux to time became almost negligible. The declining flux trend can potentially occur in the FO process due to the reduced concentration gradient between the feed and draw solution. The reduced concentration gradient may be due to feed solute (FS) deposition in the porous membrane support layer (SL). Although the chances of concentration polarisation in ALDS mode are less severe, the effect cannot be entirely ignored. The effect of deposition of the FS component on the membrane can be minimised by increasing turbulence near the membrane surface. As the FO process progressed, a decrease in water flux was observed with time. The decreasing trend in the water flux was

evidently due to the decreased concentration gradient between the FS to the draw solute due to the swelling of the hydrogel.

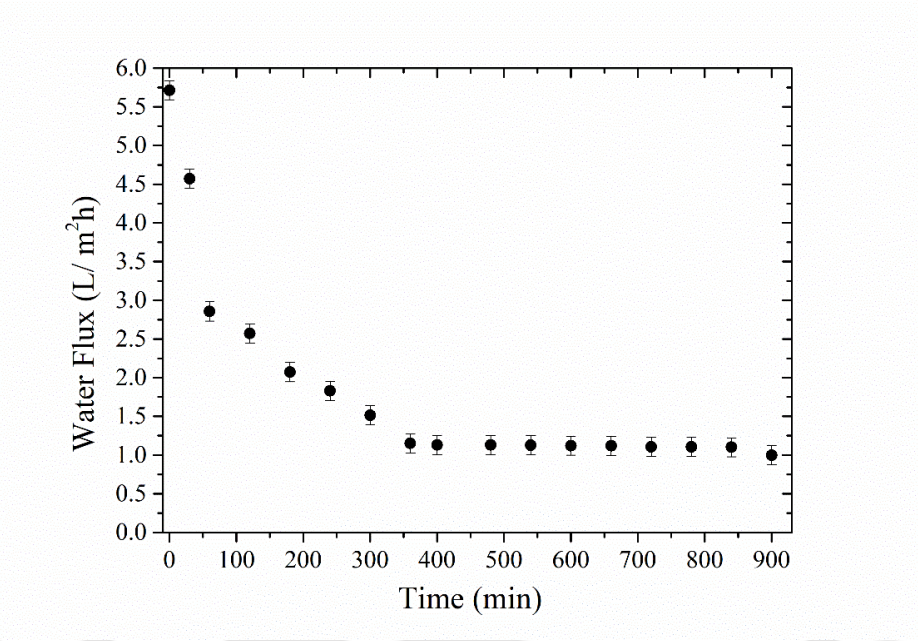

Figure 5.22 FO performance (in terms of permeate flux) using C5 (as DS) against 10 g L^{-1} tea extract

In our study, the swelling and deswelling of the hydrogel are happening simultaneously. It can be believed that due to low contact time, the dewatering of hydrogel is happening only on the dense outer layer of hydrogel. However, the inner volume of hydrogel still consists of water (solvent). Therefore, it can be concluded that for complete deswelling of hydrogel, only thermal influence is insufficient for generating higher apparent flux.

The potassium (K^+) ion concentration in the initial and final FS was estimated using Ion chromatography (IC). The estimated K^+-ion concentration of the final concentrated sample was 0.643 ± 0.02 mg L^{-1} after 6 h of operation, and RSF was 6.641 mg m^{-2} h^{-1}. In 6 h of operation, the estimated SRSF was 0.006 g L^{-1}, significantly lower than conventional DS (inorganic/ organic salts) used to prepare concentrated liquid food using the FO process.

5.3.3.2. Batch FO process using dual draw solute

Due to the simultaneous movement of solvent molecules from tea extract (liquid food) to hydrogel to RO brine (50000 mg L^{-1}) (Figure 4.8). The performance of this integrated membrane module was measured in terms of the rate of solvent permeation (water flux).

Compared to an inorganic salt solution as DS (50000 mg L^{-1}), the initial flux for DI (FS) was found to be superior. Theoretically, for inorganic salt such as DS (NaCl), the concentration gradient is the only driving force, whereas, for hydrogel, the driving force comprises both swelling pressure and osmotic pressure gradient. Evidently, after a specific interval of time (~240 min), the flux for DI and NaCl solution became almost similar. Thereby indicating that the driving force between all three components (DI, hydrogel, and NaCl) reached equilibrium (Figure 5.23 (a)). A similar trend was observed when freshly brewed tea extract was used as FS (Figure 5.23 (b)).

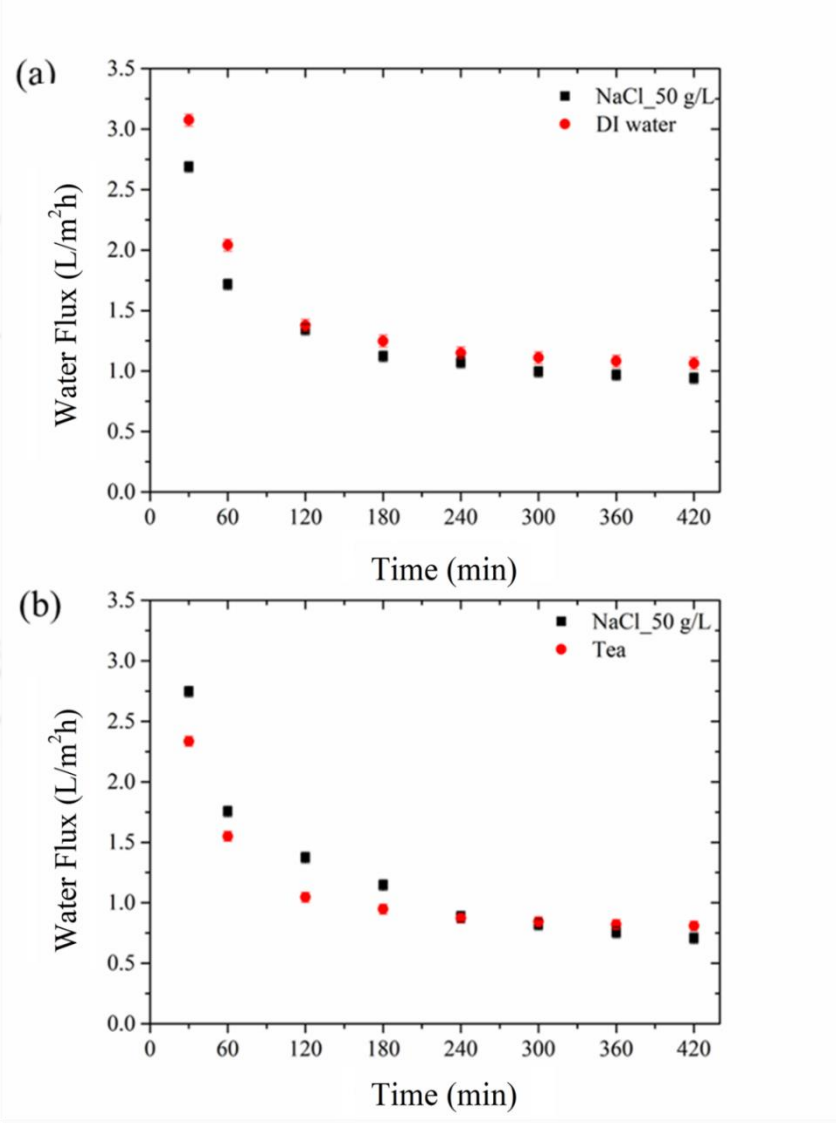

Figure 5.23 FO performance (in terms of permeate flux) using batch dual draw solute against (a) DI and (b) 10 g L^{-1} freshly brewed tea extract

5.3.3.3. Continuous FO process using dual draw solute

Figure A2.4 represents the change in osmotic pressure with respect to the change in concentrate volume (for 100 g L^{-1}) tea extract. Compared to using direct application RO brine as DS for liquid food concentration, hydrogel ensured lower RSF while allowing continuous movement of solvent from liquid food to hydrogel layer to RO brine. Due to the swelling pressure and osmotic pressure gradient, the solvent from liquid food permeated the hydrogel. A high concentration RO brine stream (π = 50.05 bar) ensured the continuous permeation of solvent from the hydrogel network. Here, since the gel was dewatered using an osmotic pressure gradient instead of thermal treatment, the chances of degradation of the overall hydrogel structure were expected to be less.

The FO performance was measured in terms of permeate flux, RSF, and SRSF estimated using equations (4.1 to 4.3). In the first hour of the given process, a permeate flux and RSF of 27.81 ± 0.09 L m^{-2} h^{-1} and 0.081 ± 0.025 g m^{-2} h^{-1}, respectively. Over 6 h of the FO process, the permeate flux and RSF reduce 8.550 ± 1.220 L m^{-2} h^{-1} and 0.057 ± 0.026 g m^{-2} h^{-1}. The given trial study suggests the feasibility of the given 3-tier design of the membrane module. However, further investigation needs to be performed to enhance the FO performance. The effect of the flow rate of the FS/ high concentration NaCl, the thickness of the middle tier, and other factors need further investigation to enhance FO performance.

The concentrated brine discharged by the desalination plants are denser than ambient seawater and therefore sinks and flows along the sea bottom, causing. Therefore, the highly concentrated brine must be diluted and treated before being released into the environment. This design suggests that the highly concentrated RO-reject brine can be diluted and passed to the aquatic body without causing a significant environmental impact.

Summary on performance analysis of hydrogel as draw solute for forward osmosis process

This section investigated the performance analysis of hydrogel as draw solute for the FO process. This study confirmed the synthesis of an ideal DS, fulfilling all three primary criteria for an appropriate food-grade DS with high osmotic pressure, low RSF, and easy/cost-effective recovery. Furthermore, the flux of the synthesised hydrogel needs to be further improved to make the synthesised hydrogel more feasible for commercial applications.

Chapter 06

Conclusions

The primary objective of the present study was to address the limitations associated with commercialising FO processes in liquid food and beverage processing industries. As a maiden step, the feasibility of the FO process for the concentration of tea extract was performed using sodium chloride as draw solute and commercially available Aquaporin inside HFFO membrane (area, 2.3 m^2). The increasing concentration of essential tea components indicates no significant alteration in the final tea concentrate.

The effect of membrane orientation on FO performance for the concentration of black tea extract was systematically investigated using a bench-scale membrane system. The impact of membrane orientation on FO performance was evaluated in terms of water flux and RSF. In both ALDS and ALFS membrane orientation, the trend of SRSF was almost the same. Based on the severity of fouling and frequency of required chemical cleaning, the ALDS membrane orientation was used in this study for the concentration of black tea extract using the FO process.

6.1. Performance Analysis of HFFO Membrane Module for Tea Concentration using Inorganic Draw Solution

Once the feasibility of the FO process for the concentration of tea extract was established, then the study focused on selecting suitable draw solutes for the given process. For the preparation of liquid food concentrate, the RSF can result in an altered taste in the final product. Therefore, the study focuses on understanding the effect of draw solute composition on the overall FO process.

(i) Single-component inorganic salt solution

- The performance of mono-, di-, and multivalent inorganic salt as draw solution was evaluated for the concentration of freshly brewed tea extract was evaluated in this section.
- Irrespective of the DS composition, the increasing trend of the essential tea components suggests that the FO can be potentially used for preserving the phenolic compounds of *Camellia sinensis var. assamica* extract.
- Compared to monovalent inorganic salt, the RSF effect of di- and multi-valent inorganic salts was observed to be less, but the permeate flux was also significantly less. Thus, providing scope for developing an appropriate DS composition with enhanced permeate flux and reduced RSF for liquid food concentration.

(ii) Multi-component inorganic salt solution

- To enhance the water flux and reduce the RSF, a multi-component DS composition was optimised by mixing inorganic salts such as NaCl, KCl, $MgCl_2$, and Na_2SO_4 at different compositions.
- The performance of multi-component DS was evaluated for the concentration of tea extract using the FO process. The role of DS composition and FO membrane was evaluated in this section.
- Compared to the single-component draw solution, due to the addition of $MgCl_2$ to multi-component DS, the RSF and SRSF got significantly reduced by 42 – 45%.

In the FO process, apart from the appropriate selection of DS, selecting an appropriate FO membrane also plays a significant role in determining the overall membrane performance. In such case, the FO performance of two commercially available HFFO membranes was evaluated:

- The FO membrane with a lower structural parameter (S) is usually preferred to reduce the severity of ICP-effect. Compared to Toyobo HFFO membranes (S =1024 µm), the aquaporin-inside HFFO membranes (S = 210.5 ± 55.5 µm) exhibited lower SRSF (0.11 g L^{-1}) with about 7.7 to 9.8 times higher water flux.
- The effect of draw solution composition on the quality of the final product was determined in terms of change in essential tea component concentration.
- The process was also able to retain colour (5583 ± 118 Hazen unit), theaflavin (1.84 ± 0.29%), and TPC (131.52 ± 7.75 mg GAE per g of sample) as compared to freshly brewed tea extract with colour (6000 Hazen unit), TF (1.913 ± 0.050%), and TPC (165.79 ± 0.02 mg GAE per g of sample).

These results show that an integrated FO-crystallisation technique can potentially be used to prepare tea crystals. The final product can be either directly used as an RTD beverage or further purified to isolate essential tea components for other related industries.

6.2. Simulation and Design Analysis of HFFO Module

- A one-dimensional mathematical model was developed by integrating the membrane transport (solution-diffusion) model for active layer transport and the concentration polarisation (film theory) model for internal/ external concentration polarisation.
- The developed dynamic Hollow Fibre Forward Osmosis (HFFO) model was validated using experimental data to predict the change in volume and concentration of feed and draw solution tank within an error limit of 10%.

- Further, the same model was validated for divalent and multivalent inorganic salts as DS (such as $MgCl_2$ and Na_2SO_4) for the concentration of tea extract using the FO process.

To estimate the optimal process design for essential tea concentrate and FO performance. A series of simulation studies were reported in this section with different flow rates and DS concentrations.

- To determine the improved values of model parameters (FS and DS flowrates) by multi-criteria optimisation based on simulation runs were performed: (i) to minimise SRSF and (ii) maximise the net flux (J_w). The identified optimal flow rate for FS and DS was found to be 45.14 ± 0.08 g L^{-1} and 45.21 ± 0.29 g L^{-1} with a 66.87% reduction in SRSF.

Further, the best-performing process flowsheet was investigated to determine the feasibility of seawater, and high-concentration RO rejects brine as a draw solute was also investigated in this study.

- Due to high concentration, the reject brine (from the seawater desalination plant) can result in rapid dewatering of FS (tea extract) by 93.103% in just 2.183 min, with minimal SRSF (0.185 g L^{-1}).
- The study suggests that the developed model can be further used to design and optimise large-scale FO processes in the food and beverage industries.

6.3. Performance Analysis of Hydrogel as Draw Solute for Forward Osmosis Process

This section investigates the feasibility of hydrogels as a draw solute for the FO process. The natural osmotic pressure gradient between the hydrogel and feed solution acts as a driving force resulting in the permeation of pure water from feed to draw agent (hydrogel) through a semi-permeable membrane while rejecting the hydrated salts. The swelling of hydrogel is driven by the osmotic pressure originating from the dissociation of ionic groups and solvation force generated by the hydrogen bond in the hydrogel network and water molecule. Due to high regenerative capability and minimal RSF, the recent research trend has shifted toward developing hydrogel with a high swelling rate, high deswelling rate, low cost, and high mechanical strength.

This study demonstrated a foam-like hydrogel with a spongy and porous structure as a potential draw agent for the forward osmosis process.

- The synthesised gel (PVA-*polyDADMAC*) can provide 1.81 L m^{-2} h^{-1} against 2500 mg L^{-1} NaCl solution as feed solution.
- At 50 ^{o}C, the hydrogel releases nearly >70% of the water absorbed during the FO process at room temperatures, and water flux can be recovered to 86.6% of the initial flux after 12-times of hydrogel (draw solute) regeneration.
- The study confirmed the synthesis of an ideal DS, fulfilling all three primary criteria for an appropriate food-grade DS with high osmotic pressure, low RSF, and easy/cost-effective recovery. Furthermore, the flux of the synthesised hydrogel needs to be further improved to make the synthesised hydrogel more feasible for commercial application.

This study demonstrates a series of experiments using a thermoresponsive fast-swelling hydrogel as a draw solution in the FO system.

- NIPAM is a thermosensitive monomer; thereby, incorporating NIPAM into the hydrogel improves the water-releasing capacity, and as a result, the flux after the 6^{th} hour of improved from 1.804 L m^{-2} h^{-1} to 2.454 L m^{-2} h^{-1}.
- Using the synthesised hydrogel as draw solute for the FO process, 10 g L^{-1} of tea extract (liquid food) was dewatered while maintaining the essential tea component concentration. The results inferred from the study provide further insight into the future direction required for ideal food-grade hydrogel as a draw agent. The work encourages further study and development focused on applying hydrogel to a liquid food concentration. The prospect of regeneration of swollen hydrogel using high-concentration brine solution was explored in this study, along with the thermal effect (hot air).
- A three-tier membrane module design was also proposed in this study. Compared to thermal regeneration, average FO flux was observed to be improved from 4.37 L m^{-2} h^{-1} to 27.81 L m^{-2} h^{-1} when high concentration RO reject brine was used as regenerating fluid against DI water as feed solution. Thus, suggesting the practical feasibility of this process in the food and beverage processing industries and effective management of brine discharge.

Future scope

The current research tried to address the challenges associated with the large-scale application of the FO process in the food and beverage processing industries. Based on the observation and outcomes outlined in this thesis, the following are the identified scope for future work:

- The validated mathematical model presented in this study can be further modified to determine the process's techno-economic feasibility.
- Further, the effect of the mass transfer coefficient and related membrane properties should be investigated for other liquid foods and beverages.
- A dynamic mathematical model using mixed DS for liquid food concentration using the FO process needs to be developed.
- The lab-scale hybrid FO-crystallisation process in this process provides a novel approach to the development of instant tea powder in batch scale. Consequently, similar studies need to be conducted in the future on a pilot- and large scale.
- The present study provides a test-scale module design for liquid food concentration (black tea extract). However, a large-scale membrane module for hydrogel as DS for the concentration of tea extract needs to be developed for commercial feasibility.
- Further, a hollow fibre and spiral wound membrane module for hydrogel as DS for liquid food concentration need to be developed.

References

[1] A. Bardhan, S. Subbiah, K. Mohanty, Application of Membrane in Food-Processing Industries, in: Food Processing Advances in Non-Thermal Technologies, 1st ed., CRC Press, 2021: p. 42. https://doi.org/https://doi.org/10.1201/9781003163213.

[2] C.C. Yang, Y.S. Chen, J. Chen, The Impact of the COVID-19 Pandemic on Food Consumption Behavior: Based on the Perspective of Accounting Data of Chinese Food Enterprises and Economic Theory, Nutrients. 14 (2022). https://doi.org/10.3390/nu14061206.

[3] L.A. Handojo, K. Khoiruddin, A.K. Wardani, A.N. Hakim, I.G. Wenten, Advancement in Forward Osmosis (FO) Membrane for Concentration of Liquid Foods, IOP Conf Ser Mater Sci Eng. 547 (2019). https://doi.org/10.1088/1757-899X/547/1/012053.

[4] N. Pap, S. Kert, E. Pongr, Concentration of blackcurrant juice by reverse osmosis, 241 (2009) 2–6. https://doi.org/10.1016/j.desal.2008.01.069.

[5] A. Alkhudhiri, N. Darwish, N. Hilal, Membrane distillation: A comprehensive review, Desalination. 287 (2012) 2–18. https://doi.org/10.1016/j.desal.2011.08.027.

[6] P. Onsekizoglu, Membrane Distillation: Principle, Advances, Limitations and Future Prospects in Food Industry, Distillation - Advances from Modeling to Applications. (2012). https://doi.org/10.5772/37625.

[7] V.D. Alves, I.M. Coelhoso, Orange juice concentration by osmotic evaporation and membrane distillation: A comparative study, (2006) 125–133. https://doi.org/10.1016/j.jfoodeng.2005.02.019.

[8] S. Nene, G. Patil, K. Raghavarao, Membrane Distillation in Food Processing, Handbook of Membrane Separations. (2010) 513–551. https://doi.org/10.1201/9781420009484.ch19.

[9] M. Purwasasmita, D. Kurnia, F.C. Mandias, I.G. Wenten, Beer dealcoholization using non-porous membrane distillation, Food and Bioproducts Processing. 94 (2015) 180–186. https://doi.org/10.1016/j.fbp.2015.03.001.

[10] V.D. Alves, I.M. Coelhoso, Orange juice concentration by osmotic evaporation and membrane distillation : A comparative study, 74 (2006) 125–133. https://doi.org/10.1016/j.jfoodeng.2005.02.019.

[11] D. Pepper, A.C.J. Orchard, A.J. Merry, Concentration of tomato juice and other fruit juices by reverse osmosis, Desalination. 53 (1985) 157–166. https://doi.org/10.1016/0011-9164(85)85058-X.

[12] K.B. Petrotos, H.N. Lazarides, Osmotic concentration of liquid foods, J Food Eng. 49 (2001) 201–206. https://doi.org/10.1016/S0260-8774(00)00222-3.

[13] K.B. Petrotos, P. Quantick, H. Petropakis, A study of the direct osmotic concentration of tomato juice in tubular membrane - Module configuration. I. The effect of certain basic process parameters on the process performance, J Memb Sci. 150 (1998) 99–110. https://doi.org/10.1016/S0376-7388(98)00216-6.

[14] M.I. Dova, K.B. Petrotos, H.N. Lazarides, On the direct osmotic concentration of liquid foods: Part II. Development of a generalized model, J Food Eng. 78 (2007) 431–437. https://doi.org/10.1016/j.jfoodeng.2005.10.011.

[15] B. Jiao, A. Cassano, E. Drioli, Recent advances on membrane processes for the concentration of fruit juices: A review, J Food Eng. 63 (2004) 303–324. https://doi.org/10.1016/j.jfoodeng.2003.08.003.

[16] W.A. Suwaileh, D.J. Johnson, S. Sarp, N. Hilal, Advances in forward osmosis membranes: Altering the sub-layer structure via recent fabrication and chemical

modification approaches, Desalination. 436 (2018) 176–201. https://doi.org/10.1016/j.desal.2018.01.035.

[17] D.L. Shaffer, J.R. Werber, H. Jaramillo, S. Lin, M. Elimelech, Forward osmosis: Where are we now?, Desalination. 356 (2015) 271–284. https://doi.org/10.1016/j.desal.2014.10.031.

[18] D.J. Johnson, W.A. Suwaileh, A.W. Mohammed, N. Hilal, Osmotic's potential: An overview of draw solutes for forward osmosis, Desalination. 434 (2018) 100–120. https://doi.org/10.1016/j.desal.2017.09.017.

[19] R. Nakka, A.A. Mungray, Biodegradable and biocompatible temperature sensitive triblock copolymer hydrogels as draw agents for forward osmosis, Sep Purif Technol. 168 (2016) 83–92. https://doi.org/10.1016/j.seppur.2016.05.021.

[20] J. Wang, S. Gao, J. Tian, F. Cui, W. Shi, Recent developments and future challenges of hydrogels as draw solutes in forward osmosis process, Water (Switzerland). 12 (2020) 1–20. https://doi.org/10.3390/w12030692.

[21] D. Li, X. Zhang, J. Yao, G.P. Simon, H. Wang, Stimuli-responsive polymer hydrogels as a new class of draw agent for forward osmosis desalination, Chemical Communications. 47 (2011) 1710. https://doi.org/10.1039/c0cc04701e.

[22] W. Suwaileh, N. Pathak, H. Shon, N. Hilal, Forward osmosis membranes and processes: A comprehensive review of research trends and future outlook, Desalination. 485 (2020) 114455. https://doi.org/10.1016/J.DESAL.2020.114455.

[23] J. Wang, X. Liu, Forward osmosis technology for water treatment: Recent advances and future perspectives, J Clean Prod. 280 (2021) 124354. https://doi.org/10.1016/j.jclepro.2020.124354.

[24] S. Yadav, H. Saleem, I. Ibrar, O. Naji, A.A. Hawari, A.A. Alanezi, S.J. Zaidi, A. Altaee, J. Zhou, Recent developments in forward osmosis membranes using carbon-based nanomaterials, Desalination. 482 (2020) 114375. https://doi.org/10.1016/j.desal.2020.114375.

[25] K. Lutchmiah, L. Lauber, K. Roest, D.J.H. Harmsen, J.W. Post, L.C. Rietveld, J.B. van Lier, E.R. Cornelissen, Zwitterions as alternative draw solutions in forward osmosis for application in wastewater reclamation, J Memb Sci. 460 (2014) 82–90. https://doi.org/10.1016/j.memsci.2014.02.032.

[26] H. Teklu, D.K. Gautam, S. Subbiah, Axial flow hollow fiber forward osmosis module analysis for optimum design and operating conditions in desalination applications, Chem Eng Sci. 216 (2020) 115494. https://doi.org/10.1016/j.ces.2020.115494.

[27] D. Xiao, W. Li, S. Chou, R. Wang, C.Y. Tang, A modeling investigation on optimizing the design of forward osmosis hollow fiber modules, J Memb Sci. 392–393 (2012) 76–87. https://doi.org/10.1016/j.memsci.2011.12.006.

[28] J. Jeon, J. Jung, S. Lee, J.Y. Choi, S. Kim, A simple modeling approach for a forward osmosis system with a spiral wound module, Desalination. 433 (2018) 120–131. https://doi.org/10.1016/j.desal.2018.01.004.

[29] Y. Xu, X. Peng, C.Y. Tang, Q.S. Fu, S. Nie, Effect of draw solution concentration and operating conditions on forward osmosis and pressure retarded osmosis performance in a spiral wound module, J Memb Sci. 348 (2010) 298–309. https://doi.org/10.1016/j.memsci.2009.11.013.

[30] L.A. Handojo, K. Khoiruddin, A.K. Wardani, A.N. Hakim, I.G. Wenten, Advancement in Forward Osmosis (FO) Membrane for Concentration of Liquid Foods, in: IOP Conf

Ser Mater Sci Eng, Institute of Physics Publishing, 2019. https://doi.org/10.1088/1757-899X/547/1/012053.

[31] I.G. Wenten, K. Khoiruddin, R. Reynard, G. Lugito, H. Julian, Advancement of forward osmosis (FO) membrane for fruit juice concentration, J Food Eng. 290 (2021) 110216. https://doi.org/10.1016/J.JFOODENG.2020.110216.

[32] C.F. Wan, T. Yang, G.G. Lipscomb, D.J. Stookey, T.-S. Chung, Design and fabrication of hollow fiber membrane modules, J Memb Sci. 538 (2017) 96–107. https://doi.org/10.1016/j.memsci.2017.05.047.

[33] A. Haupt, A. Lerch, Forward osmosis application in manufacturing industries: A short review, Membranes (Basel). 8 (2018). https://doi.org/10.3390/membranes8030047.

[34] D. Chen, J.R. Werber, X. Zhao, M. Elimelech, A facile method to quantify the carboxyl group areal density in the active layer of polyamide thin-film composite membranes, J Memb Sci. 534 (2017) 100–108. https://doi.org/10.1016/J.MEMSCI.2017.04.001.

[35] C.Y. Tang, Q. She, W.C.L. Lay, R. Wang, A.G. Fane, Coupled effects of internal concentration polarization and fouling on flux behavior of forward osmosis membranes during humic acid filtration, J Memb Sci. 354 (2010) 123–133. https://doi.org/10.1016/J.MEMSCI.2010.02.059.

[36] T.Y. Cath, A.E. Childress, M. Elimelech, Forward osmosis: Principles, applications, and recent developments, J Memb Sci. 281 (2006) 70–87. https://doi.org/10.1016/j.memsci.2006.05.048.

[37] E. Arkhangelsky, F. Wicaksana, S. Chou, A.A. Al-Rabiah, S.M. Al-Zahrani, R. Wang, Effects of scaling and cleaning on the performance of forward osmosis hollow fiber membranes, J Memb Sci. 415–416 (2012) 101–108. https://doi.org/10.1016/j.memsci.2012.04.041.

[38] H. Yoon, Y. Baek, J. Yu, J. Yoon, Biofouling occurrence process and its control in the forward osmosis, Desalination. 325 (2013) 30–36. https://doi.org/10.1016/j.desal.2013.06.018.

[39] Q. She, R. Wang, A.G. Fane, C.Y. Tang, Membrane fouling in osmotically driven membrane processes: A review, J Memb Sci. 499 (2016) 201–233. https://doi.org/10.1016/j.memsci.2015.10.040.

[40] N. Duc Viet, S.-J. Im, A. Jang, Characterization and control of membrane fouling during dewatering of activated sludge using a thin film composite forward osmosis membrane, J Hazard Mater. 396 (2020) 122736. https://doi.org/10.1016/j.jhazmat.2020.122736.

[41] F. Zaviska, L. Zou, Using modelling approach to validate a bench scale forward osmosis pre-treatment process for desalination, Desalination. 350 (2014) 1–13. https://doi.org/10.1016/j.desal.2014.07.005.

[42] Aquaporin Asia receives first prototypes of spiral-wound FO elements, (2017) 2118. https://doi.org/10.1016/S0958-2118(17)30001-0.

[43] J. Jeon, J. Jung, S. Lee, J.Y. Choi, S. Kim, A simple modeling approach for a forward osmosis system with a spiral wound module, Desalination. 433 (2018) 120–131. https://doi.org/10.1016/j.desal.2018.01.004.

[44] D. Attarde, M. Jain, K. Chaudhary, S.K. Gupta, Osmotically driven membrane processes by using a spiral wound module - Modeling, experimentation and numerical parameter estimation, Desalination. 361 (2015) 81–94. https://doi.org/10.1016/j.desal.2015.01.025.

[45] J. Minier-Matar, A. Santos, A. Hussain, A. Janson, R. Wang, A.G. Fane, S. Adham, Application of Hollow Fiber Forward Osmosis Membranes for Produced and Process

Water Volume Reduction: An Osmotic Concentration Process, Environmental Science and Technol. 50 (2016) 6044–6052. https://doi.org/10.1021/acs.est.5b04801.

[46] Y. Lv, X. Yu, S.-T. Tu, J. Yan, E. Dahlquist, Experimental studies on simultaneous removal of CO2 and SO2 in a polypropylene hollow fiber membrane contactor, Appl Energy. 97 (2012) 283–288. https://doi.org/10.1016/j.apenergy.2012.01.034.

[47] A. Akhtar, M. Singh, S. Subbiah, K. Mohanty, Modelling, experimental validation and process design of forward osmosis process for sugarcane juice concentration, LWT. 141 (2021) 110852. https://doi.org/10.1016/j.lwt.2021.110852.

[48] A. Bardhan, S. Subbiah, K. Mohanty, Modelling and experimental validation of osmotic driven energy efficient process for tea solution concentration, Environ Technol Innov. 20 (2020) 101065. https://doi.org/10.1016/j.eti.2020.101065.

[49] D.L. Meneses, Y. Ruiz, E. Hernandez, F.L. Moreno, Multi-stage block freeze-concentration of green tea (Camellia sinensis) extract, J Food Eng. 293 (2021) 110381. https://doi.org/10.1016/j.jfoodeng.2020.110381.

[50] International tea market: market situation, prospects and emerging issues, 2022.

[51] J.D. Petty, J.N. Huckins, A. David, Instant tea powder, 2006. https://doi.org/10.1093/iwc/iwv022.

[52] K.K. Dubey, M. Janve, A. Ray, R.S. Singhal, Ready-to-drink tea, Elsevier Inc., 2019. https://doi.org/10.1016/B978-0-12-816938-4.00004-5.

[53] S. Saklar, E. Ertas, I.S. Ozdemir, B. Karadeniz, Effects of different brewing conditions on catechin content and sensory acceptance in Turkish green tea infusions, J Food Sci Technol. 52 (2015) 6639–6646. https://doi.org/10.1007/s13197-015-1746-y.

[54] E. Sharpe, F. Hua, S. Schuckers, S. Andreescu, R. Bradley, Effects of brewing conditions on the antioxidant capacity of twenty-four commercial green tea varieties, Food Chem. 192 (2016) 380–387. https://doi.org/10.1016/j.foodchem.2015.07.005.

[55] Y.-Q. Xu, C. Zou, Y. Gao, J.-X. Chen, F. Wang, G.-S. Chen, J.-F. Yin, Effect of the type of brewing water on the chemical composition, sensory quality and antioxidant capacity of Chinese teas, Food Chem. 236 (2017) 142–151. https://doi.org/10.1016/j.foodchem.2016.11.110.

[56] S.A. Ramalho, N. Nigam, G.B. Oliveira, P.A. de Oliveira, T.O.M. Silva, A.G.P. dos Santos, N. Narain, Effect of infusion time on phenolic compounds and caffeine content in black tea, Food Research International. 51 (2013) 155–161. https://doi.org/10.1016/j.foodres.2012.11.031.

[57] S. Saklar, E. Ertas, I.S. Ozdemir, B. Karadeniz, Effects of different brewing conditions on catechin content and sensory acceptance in Turkish green tea infusions, J Food Sci Technol. 52 (2015) 6639–6646. https://doi.org/10.1007/s13197-015-1746-y.

[58] D. Li, X. Zhang, J. Yao, Y. Zeng, G.P. Simon, H. Wang, Composite polymer hydrogels as draw agents in forward osmosis and solar dewatering, Soft Matter. 7 (2011) 10048–10056. https://doi.org/10.1039/c1sm06043k.

[59] M. Rizwan, R. Yahya, A. Hassan, M. Yar, A.D. Azzahari, V. Selvanathan, F. Sonsudin, C.N. Abouloula, pH sensitive hydrogels in drug delivery: Brief history, properties, swelling, and release mechanism, material selection and applications, Polymers (Basel). 9 (2017). https://doi.org/10.3390/polym9040137.

[60] D. Li, X. Zhang, J. Yao, Y. Zeng, G.P. Simon, H. Wang, Composite polymer hydrogels as draw agents in forward osmosis and solar dewatering, Soft Matter. 7 (2011) 10048–10056. https://doi.org/10.1039/c1sm06043k.

[61] A. Razmjou, M.R. Barati, G.P. Simon, K. Suzuki, Supporting Information : Fast deswelling of nanocomposite polymer hydrogels via magnetic field-induced heating for emerging FO desalination, (n.d.) 1–9.

[62] Y. Hartanto, M. Zargar, X. Cui, Y. Shen, B. Jin, S. Dai, Thermoresponsive cationic copolymer microgels as high performance draw agents in forward osmosis desalination, J Memb Sci. 518 (2016) 273–281. https://doi.org/10.1016/J.MEMSCI.2016.07.018.

[63] M. Cao, Y. Wang, X. Hu, H. Gong, R. Li, H. Cox, J. Zhang, T.A. Waigh, H. Xu, J.R. Lu, Reversible Thermoresponsive Peptide-PNIPAM Hydrogels for Controlled Drug Delivery, Biomacromolecules. 20 (2019) 3601–3610. https://doi.org/10.1021/acs.biomac.9b01009.

[64] X. Xu, Y. Liu, W. Fu, M. Yao, Z. Ding, J. Xuan, D. Li, S. Wang, Y. Xia, M. Cao, Poly(N-isopropylacrylamide)-based thermoresponsive composite hydrogels for biomedical applications, Polymers (Basel). 12 (2020) 1–22. https://doi.org/10.3390/polym12030580.

[65] M. Ahmed, R. Kumar, B. Garudachari, J.P. Thomas, Performance evaluation of a thermoresponsive polyelectrolyte draw solution in a pilot scale forward osmosis seawater desalination system, Desalination. 452 (2019) 132–140. https://doi.org/10.1016/j.desal.2018.11.013.

[66] J.R. McCutcheon, R.L. McGinnis, M. Elimelech, A novel ammonia—carbon dioxide forward (direct) osmosis desalination process, Desalination. 174 (2005) 1–11. https://doi.org/10.1016/J.DESAL.2004.11.002.

[67] S. Zhao, L. Zou, D. Mulcahy, Effects of membrane orientation on process performance in forward osmosis applications, J Memb Sci. 382 (2011) 308–315. https://doi.org/10.1016/J.MEMSCI.2011.08.020.

[68] A.H. Hawari, N. Kamal, A. Altaee, Combined influence of temperature and flow rate of feeds on the performance of forward osmosis, Desalination. 398 (2016) 98–105. https://doi.org/10.1016/j.desal.2016.07.023.

[69] M. Arjmandi, M. Peyravi, A. Altaee, A. Arjmandi, M. Pourafshari Chenar, M. Jahanshahi, E. Binaeian, A state-of-the-art protocol to minimize the internal concentration polarization in forward osmosis membranes, Desalination. 480 (2020) 114355. https://doi.org/10.1016/j.desal.2020.114355.

[70] X. Zhang, L. Shen, C.-Y. Guan, C.-X. Liu, W.-Z. Lang, Y. Wang, Construction of SiO2@MWNTs incorporated PVDF substrate for reducing internal concentration polarization in forward osmosis, J Memb Sci. 564 (2018) 328–341. https://doi.org/10.1016/j.memsci.2018.07.043.

[71] G.T. Gray, J.R. McCutcheon, M. Elimelech, Internal concentration polarization in forward osmosis: role of membrane orientation, Desalination. 197 (2006) 1–8. https://doi.org/10.1016/j.desal.2006.02.003.

[72] A. Abdelrasoul, H. Doan, A. Lohi, C.-H. Cheng, Fouling in Forward Osmosis Membranes: Mechanisms, Control, and Challenges, in: Osmotically Driven Membrane Processes - Approach, Development and Current Status, InTech, 2018. https://doi.org/10.5772/intechopen.72644.

[73] M.F. Gruber, C.J. Johnson, C.Y. Tang, M.H. Jensen, L. Yde, C. Hélix-Nielsen, Computational fluid dynamics simulations of flow and concentration polarization in forward osmosis membrane systems, J Memb Sci. 379 (2011) 488–495. https://doi.org/10.1016/j.memsci.2011.06.022.

[74] J. Su, S. Zhang, M.M. Ling, T.-S. Chung, Forward osmosis: an emerging technology for sustainable supply of clean water, Clean Technol Environ Policy. 14 (2012) 507–511. https://doi.org/10.1007/s10098-012-0486-1.

[75] S.S. Manickam, J.R. McCutcheon, Understanding mass transfer through asymmetric membranes during forward osmosis: A historical perspective and critical review on measuring structural parameter with semi-empirical models and characterization approaches, Desalination. 421 (2017) 110–126. https://doi.org/10.1016/j.desal.2016.12.016.

[76] J. Ren, J.R. McCutcheon, A new commercial biomimetic hollow fiber membrane for forward osmosis, Desalination. 442 (2018) 44–50. https://doi.org/10.1016/j.desal.2018.04.015.

[77] V. Sanahuja-Embuena, G. Khensir, M. Yusuf, M.F. Andersen, X.T. Nguyen, K. Trzaskus, M. Pinelo, C. Helix-Nielsen, Role of Operating Conditions in a Pilot Scale Investigation of Hollow Fiber Forward Osmosis Membrane Modules, Membranes (Basel). 9 (2019) 66. https://doi.org/10.3390/membranes9060066.

[78] L. Xia, M.F. Andersen, C. Hélix-Nielsen, J.R. McCutcheon, Novel Commercial Aquaporin Flat-Sheet Membrane for Forward Osmosis, Ind Eng Chem Res. 56 (2017) 11919–11925. https://doi.org/10.1021/acs.iecr.7b02368.

[79] S. Chou, L. Shi, R. Wang, C.Y. Tang, C. Qiu, A.G. Fane, Characteristics and potential applications of a novel forward osmosis hollow fiber membrane, Desalination. 261 (2010) 365–372. https://doi.org/10.1016/j.desal.2010.06.027.

[80] D. Khanafer, S. Yadav, N. Ganbat, A. Altaee, J. Zhou, A.H. Hawari, Performance of the Pressure Assisted Forward Osmosis-MSF Hybrid Desalination Plant, Water (Basel). 13 (2021) 1245. https://doi.org/10.3390/w13091245.

[81] G. Blandin, H. Vervoort, A. D'Haese, K. Schoutteten, J. vanden Bussche, L. Vanhaecke, D.T. Myat, P. Le-Clech, A.R.D. Verliefde, Impact of hydraulic pressure on membrane deformation and trace organic contaminants rejection in pressure assisted osmosis (PAO), Process Safety and Environmental Protection. 102 (2016) 316–327. https://doi.org/10.1016/j.psep.2016.04.004.

[82] B. Corzo, T. de la Torre, C. Sans, E. Ferrero, J.J. Malfeito, Evaluation of draw solutions and commercially available forward osmosis membrane modules for wastewater reclamation at pilot scale, Chemical Engineering Journal. 326 (2017) 1–8. https://doi.org/10.1016/j.cej.2017.05.108.

[83] Q. Ge, M. Ling, T.-S. Chung, Draw solutions for forward osmosis processes: Developments, challenges, and prospects for the future, J Memb Sci. 442 (2013) 225–237. https://doi.org/10.1016/j.memsci.2013.03.046.

[84] Q. Ge, M. Ling, T.-S. Chung, Draw solutions for forward osmosis processes: Developments, challenges, and prospects for the future, J Memb Sci. 442 (2013) 225–237. https://doi.org/10.1016/j.memsci.2013.03.046.

[85] T.Y. Cath, A.E. Childress, M. Elimelech, Forward osmosis: Principles, applications, and recent developments, J Memb Sci. 281 (2006) 70–87. https://doi.org/10.1016/j.memsci.2006.05.048.

[86] W.C.L. Lay, J. Zhang, C. Tang, R. Wang, Y. Liu, A.G. Fane, Factors affecting flux performance of forward osmosis systems, J Memb Sci. 394–395 (2012) 151–168. https://doi.org/10.1016/j.memsci.2011.12.035.

[87] Q. She, Y.K.W. Wong, S. Zhao, C.Y. Tang, Organic fouling in pressure retarded osmosis: Experiments, mechanisms and implications, J Memb Sci. 428 (2013) 181–189. https://doi.org/10.1016/j.memsci.2012.10.045.

[88] D.L. Shaffer, J.R.; Werber, J. Humberto, L. Shihong, M. Elimelech, Forward osmosis : Where are we now Related papers, Desalination. 356 (2015) 271–284. https://doi.org/http://dx.doi.org/10.1016/j.desal.2014.10.031.

[89] A. Achilli, T.Y. Cath, A.E. Childress, Selection of inorganic-based draw solutions for forward osmosis applications, J Memb Sci. 364 (2010) 233–241. https://doi.org/10.1016/j.memsci.2010.08.010.

[90] R. Alnaizy, A. Aidan, M. Qasim, Copper sulfate as draw solute in forward osmosis desalination, J Environ Chem Eng. 1 (2013) 424–430. https://doi.org/10.1016/j.jece.2013.06.005.

[91] A.J. Ansari, F.I. Hai, W.E. Price, L.D. Nghiem, Phosphorus recovery from digested sludge centrate using seawater-driven forward osmosis, Sep Purif Technol. 163 (2016) 1–7. https://doi.org/10.1016/j.seppur.2016.02.031.

[92] S. Phuntsho, H.K. Shon, S. Hong, S. Lee, S. Vigneswaran, A novel low energy fertilizer driven forward osmosis desalination for direct fertigation: Evaluating the performance of fertilizer draw solutions, J Memb Sci. 375 (2011) 172–181. https://doi.org/10.1016/j.memsci.2011.03.038.

[93] R.E. Kravath, J.A. Davis, Desalination of sea water by direct osmosis, Desalination. 16 (1975) 151–155. https://doi.org/10.1016/S0011-9164(00)82089-5.

[94] Y. Cai, W. Shen, J. Wei, T.H. Chong, R. Wang, W.B. Krantz, A.G. Fane, X. Hu, Energy-efficient desalination by forward osmosis using responsive ionic liquid draw solutes, Environ Sci (Camb). 1 (2015) 341–347. https://doi.org/10.1039/C4EW00073K.

[95] Y. Zhong, X. Feng, W. Chen, X. Wang, K.-W. Huang, Y. Gnanou, Z. Lai, Using UCST Ionic Liquid as a Draw Solute in Forward Osmosis to Treat High-Salinity Water, Environ Sci Technol. 50 (2016) 1039–1045. https://doi.org/10.1021/acs.est.5b03747.

[96] N.C. Nguyen, S.-S. Chen, S.-T. Ho, H.T. Nguyen, S.S. Ray, N.T. Nguyen, H.-T. Hsu, N.C. Le, T.T. Tran, Optimising the recovery of EDTA-2Na draw solution in forward osmosis through direct contact membrane distillation, Sep Purif Technol. 198 (2018) 108–112. https://doi.org/10.1016/j.seppur.2017.02.001.

[97] S. Wu, Y. An, J. Lu, Q. Yu, Z. He, EDTA-Na2 as a recoverable draw solute for water extraction in forward osmosis, Environ Res. 205 (2022) 112521. https://doi.org/10.1016/j.envres.2021.112521.

[98] K. Lutchmiah, L. Lauber, K. Roest, D.J.H. Harmsen, J.W. Post, L.C. Rietveld, J.B. van Lier, E.R. Cornelissen, Zwitterions as alternative draw solutions in forward osmosis for application in wastewater reclamation, J Memb Sci. 460 (2014) 82–90. https://doi.org/10.1016/j.memsci.2014.02.032.

[99] C. Ju, H. Kang, Zwitterionic polymers showing upper critical solution temperature behavior as draw solutes for forward osmosis, RSC Adv. 7 (2017) 56426–56432. https://doi.org/10.1039/c7ra10831a.

[100] M. Pejman, M. Dadashi Firouzjaei, S. Aghapour Aktij, P. Das, E. Zolghadr, H. Jafarian, A. Arabi Shamsabadi, M. Elliott, M. Sadrzadeh, M. Sangermano, A. Rahimpour, A. Tiraferri, In Situ Ag-MOF Growth on Pre-Grafted Zwitterions Imparts Outstanding Antifouling Properties to Forward Osmosis Membranes, ACS Appl Mater Interfaces. 12 (2020) 36287–36300. https://doi.org/10.1021/acsami.0c12141.

[101] Y. Na, S. Yang, S. Lee, Evaluation of citrate-coated magnetic nanoparticles as draw solute for forward osmosis, Desalination. 347 (2014) 34–42. https://doi.org/10.1016/j.desal.2014.04.032.

[102] I. Tavakol, S. Hadadpour, Z. Shabani, M. Ahmadzadeh Tofighy, T. Mohammadi, S. Sahebi, Synthesis of novel thin film composite (TFC) forward osmosis (FO) membranes

incorporated with carboxylated carbon nanofibers (CNFs), J Environ Chem Eng. 8 (2020) 104614. https://doi.org/10.1016/j.jece.2020.104614.

[103] Z. Dabaghian, A. Rahimpour, Carboxylated carbon nanofibers as hydrophilic porous material to modification of cellulosic membranes for forward osmosis desalination, Chemical Engineering Research and Design. 104 (2015) 647–657. https://doi.org/10.1016/j.cherd.2015.10.008.

[104] C.-H. Hsu, C. Ma, N. Bui, Z. Song, A.D. Wilson, R. Kostecki, K.M. Diederichsen, B.D. McCloskey, J.J. Urban, Enhanced Forward Osmosis Desalination with a Hybrid Ionic Liquid/Hydrogel Thermoresponsive Draw Agent System, ACS Omega. 4 (2019) 4296–4303. https://doi.org/10.1021/acsomega.8b02827.

[105] M. Bahram, N. Mohseni, M. Moghtader, An Introduction to Hydrogels and Some Recent Applications, in: Emerging Concepts in Analysis and Applications of Hydrogels, InTech, 2016. https://doi.org/10.5772/64301.

[106] W.A. Laftah, S. Hashim, A.N. Ibrahim, Polymer Hydrogels: A Review, Polym Plast Technol Eng. 50 (2011) 1475–1486. https://doi.org/10.1080/03602559.2011.593082.

[107] F. Osmosis, O. Pressure, S. Pressure, Osmotic Pressure versus Swelling Pressure: Comment on " Bifunctional Polymer Hydrogel Layers As Forward Osmosis Draw Agents for Continuous Production of Fresh Water Using Solar Energy ," (2014) 4212–4213. https://doi.org/dx.doi.org/10.1021/es5006994 | Environ. Sci. Technol. 2014, 48, 4212−4213.

[108] A. Razmjou, Q. Liu, G.P. Simon, H. Wang, Bifunctional polymer hydrogel layers as forward osmosis draw agents for continuous production of fresh water using solar energy, Environ Sci Technol. (2013) 1–9. https://doi.org/dx.doi.org/10.1021/es403266y | Environ. Sci. Technol. 2013, 47, 13160−13166.

[109] P. Höhne, K. Tauer, How much weighs the swelling pressure, Colloid Polym Sci. 292 (2014) 2983–2992. https://doi.org/10.1007/s00396-014-3347-0.

[110] H. Wang, J. Wei, G.P. Simon, Response to Osmotic Pressure versus Swelling Pressure: Comment on "Bifunctional Polymer Hydrogel Layers As Forward Osmosis Draw Agents for Continuous Production of Fresh Water Using Solar Energy," Environ Sci Technol. 48 (2014) 4214–4215. https://doi.org/10.1021/es5011016.

[111] J. Wang, S. Gao, J. Tian, F. Cui, W. Shi, Recent developments and future challenges of hydrogels as draw solutes in forward osmosis process, Water (Switzerland). 12 (2020) 1–20. https://doi.org/10.3390/w12030692.

[112] D. Li, X. Zhang, J. Yao, G.P. Simon, H. Wang, Stimuli-responsive polymer hydrogels as a new class of draw agent for forward osmosis desalination, Chemical Communications. 47 (2011) 1710–1712. https://doi.org/10.1039/c0cc04701e.

[113] Y. Cai, W. Shen, S.L. Loo, W.B. Krantz, R. Wang, A.G. Fane, X. Hu, Towards temperature driven forward osmosis desalination using Semi-IPN hydrogels as reversible draw agents, Water Res. 47 (2013) 3773–3781. https://doi.org/10.1016/j.watres.2013.04.034.

[114] H. Wang, J. Yao, Y. Zeng, D. Li, X. Zhang, G.P. Simon, Composite polymer hydrogels as draw agents in forward osmosis and solar dewatering, Soft Matter. 7 (2011) 10048. https://doi.org/10.1039/c1sm06043k.

[115] K.L. Tu, G.P. Simon, H. Wang, Fast-responsive monolithic hydrogels as draw agent for forward osmosis membrane process, Separation Science and Technology (Philadelphia). 52 (2017) 2583–2590. https://doi.org/10.1080/01496395.2017.1310237.

[116] H. Luo, K. Wu, Q. Wang, T.C. Zhang, H. Lu, H. Rong, Q. Fang, Forward osmosis with electro-responsive P(AMPS-co-AM) hydrogels as draw agents for desalination, J Memb Sci. 593 (2020) 117406. https://doi.org/10.1016/J.MEMSCI.2019.117406.

[117] H. Cui, H. Zhang, M. Yu, F. Yang, Performance evaluation of electric-responsive hydrogels as draw agent in forward osmosis desalination, Desalination. 426 (2018) 118–126. https://doi.org/10.1016/J.DESAL.2017.10.045.

[118] H. Zhang, J. Li, H. Cui, H. Li, F. Yang, Forward osmosis using electric-responsive polymer hydrogels as draw agents: Influence of freezing–thawing cycles, voltage, feed solutions on process performance, Chemical Engineering Journal. 259 (2015) 814–819. https://doi.org/10.1016/J.CEJ.2014.08.065.

[119] H. Wang, X. Yang, D. Liu, W. Pan, Y. Li, Q. Li, S. Yu, A novel hydrogel with dual temperature and pH responsiveness based on a nanostructured lipid carrier as an ophthalmic delivery system: enhanced trans-corneal permeability and bioavailability of nepafenac, New Journal of Chemistry. 41 (2017) 3920–3929. https://doi.org/10.1039/c7nj00112f.

[120] H. Rabiee, B. Jin, S. Yun, S. Dai, Gas-responsive cationic microgels for forward osmosis desalination, Chemical Engineering Journal. 347 (2018) 424–431. https://doi.org/10.1016/j.cej.2018.04.148.

[121] N.K. Rastogi, Opportunities and Challenges in Application of Forward Osmosis in Food Processing, Crit Rev Food Sci Nutr. 56 (2016) 266–291. https://doi.org/10.1080/10408398.2012.724734.

[122] K. Raghavarao, N. Nagaraj, G. Patil, B. Ravindra Babu, K. Niranjan, Athermal Membrane Processes for the Concentration of Liquid Foods and Natural Colours, 2005. https://doi.org/10.1016/B978-012676757-5/50012-8.

[123] V. Sant'Anna, L.D.F. Marczak, I.C. Tessaro, Membrane concentration of liquid foods by forward osmosis: Process and quality view, J Food Eng. 111 (2012) 483–489. https://doi.org/10.1016/j.jfoodeng.2012.01.032.

[124] N.K. Rastogi, Opportunities and Challenges in Application of Forward Osmosis in Food Processing, Crit Rev Food Sci Nutr. 56 (2016) 266–291. https://doi.org/10.1080/10408398.2012.724734.

[125] G. Blandin, F. Ferrari, G. Lesage, P. Le-Clech, M. Héran, X. Martinez-Lladó, Forward osmosis as concentration process: Review of opportunities and challenges, Membranes (Basel). 10 (2020) 1–40. https://doi.org/10.3390/membranes10100284.

[126] W.L. Popper, K., Camirand, W.M., Nury, F., Stanley, Dialyzer concentrates beverages, J Food Eng. 38 (1966) 102–104.

[127] D. Trishitman, P.S. Negi, N.K. Rastogi, Concentration of pomegranate juice by forward osmosis or thermal evaporation and its shelf-life kinetic studies, Food Chem. 399 (2023) 133972. https://doi.org/10.1016/J.FOODCHEM.2022.133972.

[128] D. Trishitman, P.S. Negi, N.K. Rastogi, Concentration of beetroot juice colorant (betalains) by forward osmosis and its comparison with thermal processing, Lwt. 145 (2021) 111522. https://doi.org/10.1016/j.lwt.2021.111522.

[129] H.M. Tavares, I.C. Tessaro, N.S.M. Cardozo, Concentration of grape juice: Combined forward osmosis/evaporation versus conventional evaporation, Innovative Food Science & Emerging Technologies. 75 (2022) 102905. https://doi.org/10.1016/J.IFSET.2021.102905.

[130] J. Pei, S. Pei, W. Wang, S. Li, W. Youravong, Z. Li, Athermal forward osmosis process for the concentration of liquid egg white: Process performance and improved

physicochemical property of protein, Food Chem. 312 (2020) 126032. https://doi.org/https://doi.org/10.1016/j.foodchem.2019.126032.

[131] E.M. Garcia-Castello, J.R. McCutcheon, M. Elimelech, Performance evaluation of sucrose concentration using forward osmosis, J Memb Sci. 338 (2009) 61–66. https://doi.org/10.1016/j.memsci.2009.04.011.

[132] H. Wang, Y. Zhang, S. Ren, J. Pei, Z. Li, Athermal concentration of apple juice by forward osmosis: Process performance and membrane fouling propensity, Chemical Engineering Research and Design. 177 (2022) 569–577. https://doi.org/10.1016/J.CHERD.2021.11.023.

[133] D.I. Kim, G. Gwak, M. Zhan, S. Hong, Sustainable dewatering of grapefruit juice through forward osmosis: Improving membrane performance, fouling control, and product quality, J Memb Sci. 578 (2019) 53–60. https://doi.org/10.1016/J.MEMSCI.2019.02.031.

[134] A. Artemi, G.Q. Chen, S.E. Kentish, J. Lee, Pilot scale concentration of cheese whey by forward osmosis: A short-cut method for evaluating the effective pressure driving force, Sep Purif Technol. 250 (2020) 117263. https://doi.org/10.1016/J.SEPPUR.2020.117263.

[135] Z. Li, S. Xiao, Q. Xiong, C. Wu, J. Huang, R. Zhou, Y. Jin, Assessment of highly concentrated pear juice production through single-run forward osmosis using sodium lactate as the draw solute, J Food Eng. 333 (2022) 111122. https://doi.org/10.1016/J.JFOODENG.2022.111122.

[136] K. Zhang, X. An, Y. Bai, C. Shen, Y. Jiang, Y. Hu, Exploration of food preservatives as draw solutes in the forward osmosis process for juice concentration, J Memb Sci. 635 (2021) 119495. https://doi.org/10.1016/J.MEMSCI.2021.119495.

[137] X. An;, Y. Hu, N. Wang;, Z. Zhou;, Z. Liu;, Continuous juice concentration by integrating forward osmosis with membrane distillation using potassium sorbate preservative as a draw solute, J Memb Sci. 573 (2019) 192–199. https://doi.org/10.1016/j.memsci.2018.12.010.

[138] Y.C. Kim, S.-J. Park, Experimental Study of a 4040 Spiral-Wound Forward-Osmosis Membrane Module, Environ Sci Technol. 45 (2011) 7737–7745. https://doi.org/10.1021/es202175m.

[139] A. Altaee, A. Braytee, G.J. Millar, O. Naji, Energy efficiency of hollow fibre membrane module in the forward osmosis seawater desalination process, J Memb Sci. 587 (2019) 117165. https://doi.org/10.1016/j.memsci.2019.06.005.

[140] Y. Tanaka, M. Yasukawa, S. Goda, H. Sakurai, M. Shibuya, T. Takahashi, M. Kishimoto, M. Higa, H. Matsuyama, Experimental and simulation studies of two types of 5-inch scale hollow fiber membrane modules for pressure-retarded osmosis, Desalination. 447 (2018) 133–146. https://doi.org/10.1016/j.desal.2018.09.015.

[141] K.K. Munubarthi, D.K. Gautam, K.A. Reddy, S. Subbiah, Distributed parameter system modeling approach for the characterization of a high flux hollow fiber forward osmosis (HFFO) membrane, Desalination. 496 (2020) 114706. https://doi.org/10.1016/j.desal.2020.114706.

[142] M. Shibuya, M. Yasukawa, S. Goda, H. Sakurai, T. Takahashi, M. Higa, H. Matsuyama, Experimental and theoretical study of a forward osmosis hollow fiber membrane module with a cross-wound configuration, J Memb Sci. 504 (2016) 10–19. https://doi.org/10.1016/j.memsci.2015.12.040.

[143] S. Lin, Mass transfer in forward osmosis with hollow fiber membranes, J Memb Sci. 514 (2016) 176–185. https://doi.org/10.1016/j.memsci.2016.04.053.

[144] M. Shibuya, M. Yasukawa, S. Goda, H. Sakurai, T. Takahashi, M. Higa, H. Matsuyama, Experimental and theoretical study of a forward osmosis hollow fiber membrane module with a cross-wound configuration, J Memb Sci. 504 (2016) 10–19. https://doi.org/10.1016/j.memsci.2015.12.040.

[145] S. Phuntsho, S. Hong, M. Elimelech, H.K. Shon, Osmotic equilibrium in the forward osmosis process: Modelling, experiments and implications for process performance, J Memb Sci. 453 (2014) 240–252. https://doi.org/10.1016/j.memsci.2013.11.009.

[146] G. Blandin, A. Galizia, H. Monclús, G. Lesage, M. Héran, X. Martinez-Lladó, Submerged osmotic processes: Design and operation of hollow fiber forward osmosis modules, Desalination. 518 (2021) 115281. https://doi.org/10.1016/j.desal.2021.115281.

[147] J.J. Hermans, Physical aspects governing the design of hollow fiber modules, Desalination. 26 (1978) 45–62. https://doi.org/10.1016/S0011-9164(00)84127-2.

[148] Y. Tanaka, M. Yasukawa, S. Goda, H. Sakurai, M. Shibuya, T. Takahashi, M. Kishimoto, M. Higa, H. Matsuyama, Experimental and simulation studies of two types of 5-inch scale hollow fiber membrane modules for pressure-retarded osmosis, Desalination. 447 (2018) 133–146. https://doi.org/https://doi.org/10.1016/j.desal.2018.09.015.

[149] S. Guo, M. Kumar Awasthi, Y. Wang, P. Xu, Current understanding in conversion and application of tea waste biomass: A review, Bioresour Technol. 338 (2021) 125530. https://doi.org/10.1016/j.biortech.2021.125530.

[150] R.P. Soni, M. Katoch, A. Kumar, R. Ladohiya, P. Verma, Tea: Production, Composition, Consumption and its Potential as an Antioxidant and Antimicrobial Agent, International

Journal of Food and Fermentation Technology. 5 (2015) 95. https://doi.org/10.5958/2277-9396.2016.00002.7.

[151] W. Łuczaj, E. Skrzydlewska, Antioxidative properties of black tea, Prev Med (Baltim). 40 (2005) 910–918. https://doi.org/10.1016/J.YPMED.2004.10.014.

[152] S.C. Larsson, J. Virtamo, A. Wolk, Black tea consumption and risk of stroke in women and men, Ann Epidemiol. 23 (2013) 157–160. https://doi.org/10.1016/J.ANNEPIDEM.2012.12.006.

[153] S. Devi, Catechins, in: A Centum of Valuable Plant Bioactives, Academic Press, 2021: pp. 525–544. https://doi.org/10.1016/B978-0-12-822923-1.00009-1.

[154] P.V. Gadkari, M. Balaraman, Catechins: Sources, extraction and encapsulation: A review, Food and Bioproducts Processing. 93 (2015) 122–138. https://doi.org/10.1016/J.FBP.2013.12.004.

[155] M.S. Butt, A. Imran, M.K. Sharif, R.S. Ahmad, H. Xiao, M. Imran, H.A. Rsool, Black Tea Polyphenols: A Mechanistic Treatise, Crit Rev Food Sci Nutr. 54 (2014) 1002–1011. https://doi.org/10.1080/10408398.2011.623198.

[156] T. Tanaka, Y. Matsuo, I. Kouno, Chemistry of secondary polyphenols produced during processing of tea and selected foods, Int J Mol Sci. 11 (2010) 14–40. https://doi.org/10.3390/ijms11010014.

[157] J. Shi, H. Nawaz, J. Pohorly, G. Mittal, Y. Kakuda, Y. Jiang, Extraction of polyphenolics from plant material for functional foods - Engineering and technology, Food Reviews International. 21 (2005) 139–166. https://doi.org/10.1081/FRI-200040606.

[158] N. Khan, H. Mukhtar, Tea and Health: Studies in Humans, Curr Pharm Des. 19 (2013) 6141–6147. https://doi.org/10.2174/1381612811319340008.

[159] S. Shahrzad, K. Aoyagi, A. Winter, A. Koyama, I. Bitsch, Pharmacokinetics of Gallic Acid and Its Relative Bioavailability from Tea in Healthy Humans, Human Nutrition and Metabolism–Research Communication Pharmacokinetics. (2001) 1207–1210. https://academic.oup.com/jn/article/131/4/1207/4686988.

[160] H. Mukhtar, N. Ahmad, Tea polyphenols: prevention of cancer and optimizing health, Am J Clin Nutr. 71 (2000) 1698S-1702S. https://doi.org/10.1093/ajcn/71.6.1698S.

[161] Zainab Khudhur Ahmad Al-Mahdi; Ruqaya M.J. Ewadh; Nada Khazal Kadhim Hindi, Health Benefits of Aqueous Extract of Black and Green Tea Leaves, in: K.K.S. and C.D. Kavita Sharma, Kanchan Mishra (Ed.), Bioactive Compounds in Nutraceutical and Functional Food for Good Human Health, 2012: p. 13. https://doi.org/10.5772/intechopen.91636.

[162] J. Bae, N. Kim, Y. Shin, S.-Y. Kim, Y.-J. Kim, Activity of catechins and their applications, Biomedical Dermatology. 4 (2020) 1–10. https://doi.org/10.1186/s41702-020-0057-8.

[163] Y. Yilmaz, Novel uses of catechins in foods, Trends Food Sci Technol. 17 (2006) 64–71. https://doi.org/10.1016/J.TIFS.2005.10.005.

[164] I.C.W. Arts, P.C.H. Hollman, E.J.M. Feskens, H.B. Bueno de Mesquita, D. Kromhout, Catechin intake and associated dietary and lifestyle factors in a representative sample of Dutch men and women, Eur J Clin Nutr. 55 (2001) 76–81. https://doi.org/10.1038/sj.ejcn.1601115.

[165] Z. Danrong, C. Yuqiong, N. Dejiang, Effect of water quality on the nutritional components and antioxidant activity of green tea extracts, Food Chem. 113 (2009) 110–114. https://doi.org/10.1016/j.foodchem.2008.07.033.

[166] M.P. Marques, V.D. Alves, I.M. Coelhoso, Concentration of tea extracts by osmotic evaporation: Optimisation of process parameters and effect on antioxidant activity, Membranes (Basel). 7 (2017) 1–14. https://doi.org/10.3390/membranes7010001.

[167] Y. Yoda, Z.-Q. Hu, T. Shimamura, W.-H. Zhao, Different susceptibilities of Staphylococcus and Gram-negative rods to epigallocatechin gallate, Journal of Infection and Chemotherapy. 10 (2004) 55–58. https://doi.org/https://doi.org/10.1007/s10156-003-0284-0.

[168] H. Wang, G.J. Provan, K. Helliwell, Tea flavonoids: their functions, utilisation and analysis, Trends Food Sci Technol. 11 (2000) 152–160. https://doi.org/10.1016/S0924-2244(00)00061-3.

[169] V. Kraujalyte, E. Pelvan, C. Alasalvar, Volatile compounds and sensory characteristics of various instant teas produced from black tea, Food Chem. 194 (2016) 864–872. https://doi.org/10.1016/j.foodchem.2015.08.051.

[170] C. Someswararao, P.P. Srivastav, A novel technology for production of instant tea powder from the existing black tea manufacturing process, Innovative Food Science and Emerging Technologies. 16 (2012) 143–147. https://doi.org/10.1016/j.ifset.2012.05.005.

[171] S. Liang, Y. Gao, Y.-Q. Fu, J.-X. Chen, J.-F. Yin, Y.-Q. Xu, Innovative technologies in tea-beverage processing for quality improvement, Curr Opin Food Sci. 47 (2022) 100870. https://doi.org/10.1016/j.cofs.2022.100870.

[172] S. Liang, D. Granato, C. Zou, Y. Gao, Y. Zhu, L. Zhang, J.-F. Yin, W. Zhou, Y.-Q. Xu, Processing technologies for manufacturing tea beverages: From traditional to advanced hybrid processes, Trends Food Sci Technol. 118 (2021) 431–446. https://doi.org/10.1016/j.tifs.2021.10.016.

[173] V.R. Sinija, H.N. Mishra, S. Bal, Process technology for production of soluble tea powder, J Food Eng. 82 (2007) 276–283. https://doi.org/10.1016/J.JFOODENG.2007.01.024.

[174] K.A.P. Dalpathadu, H.U.K.D.Z. Rajapakse, S.P. Nissanka, C.V.L. Jayasinghe, Improving the quality of instant tea with low-grade tea aroma, Arabian Journal of Chemistry. 15 (2022) 104147. https://doi.org/10.1016/j.arabjc.2022.104147.

[175] S. Senthilmurugan, S.K. Gupta, Separation of inorganic and organic compounds by using a radial flow hollow-fiber reverse osmosis module, Desalination. 196 (2006) 221–236. https://doi.org/10.1016/j.desal.2006.02.001.

[176] J.G. Wijmans, R.W. Baker, The solution-diffusion model : a review, 107 (1995) 1–21. https://doi.org/10.1016/0376-7388(95)00102-I.

[177] J. Duan, E. Litwiller, I. Pinnau, Solution-diffusion with defects model for pressure-assisted forward osmosis, J Memb Sci. 470 (2014) 323–333. https://doi.org/10.1016/j.memsci.2014.07.018.

[178] M. Khraisheh, N. Dawas, M.S. Nasser, M.J. Al-Marri, M.A. Hussien, S. Adham, G. McKay, Osmotic pressure estimation using the Pitzer equation for forward osmosis modelling, Environmental Technology (United Kingdom). 41 (2020) 2533–2545. https://doi.org/10.1080/09593330.2019.1575476.

[179] T. Wolfe, W. Bourcier, P. Metcalfe, Osmotic Pressure Calculation Using Pitzer Equation Modeling, in: IDA World Congress, 2011: pp. PER11-210.

[180] C. Suh, S. Lee, Modeling reverse draw solute flux in forward osmosis with external concentration polarization in both sides of the draw and feed solution, J Memb Sci. 427 (2013) 365–374. https://doi.org/https://doi.org/10.1016/j.memsci.2012.08.033.

[181] E. Matthiasson, B. Sivik, Concentration polarization and fouling, Desalination. 35 (1980) 59–103. https://doi.org/10.1016/S0011-9164(00)88604-X.

[182] J.R. McCutcheon, M. Elimelech, Influence of concentrative and dilutive internal concentration polarization on flux behavior in forward osmosis, J Memb Sci. 284 (2006) 237–247. https://doi.org/10.1016/j.memsci.2006.07.049.

[183] A. Haupt, C. Marx, A. Lerch, Modelling forward osmosis treatment of automobile wastewaters, Membranes (Basel). 9 (2019). https://doi.org/10.3390/membranes9090106.

[184] S. Kingori, P. Ongoma, S. Ochanda, Development of an Improved Isocratic HPLC Method for the Determination of Gallic Acid, Caffeine and Catechins in Tea, J Nutrit Health Food Sci. 6 (2018) 1–9. https://doi.org/10.15226/jnhfs.2018.001135.

[185] H. Wang, K. Helliwell, X. You, Isocratic elution system for the determination of catechins, caffeine and gallic acid in green tea using HPLC, Food Chem. 68 (2000) 115–121. https://doi.org/10.1016/S0308-8146(99)00179-X.

[186] H. Deka, P.P. Sarmah, A. Devi, P. Tamuly, T. Karak, Changes in major catechins, caffeine, and antioxidant activity during CTC processing of black tea from North East India, RSC Adv. 11 (2021) 11457–11467. https://doi.org/10.1039/d0ra09529j.

[187] S. Shin, A.S. Kim, Temperature Effect on Forward Osmosis, in: Osmotically Driven Membrane Processes - Approach, Development and Current Status, InTech, 2018. https://doi.org/10.5772/intechopen.72044.

[188] W. Michaeli, M. Koschmieder, Processing Principles for Thermoplastic Polymers, Comprehensive Composite Materials. (2000) 853–872. https://doi.org/10.1016/B0-08-042993-9/00202-3.

[189] S. Kiatkamjornwong, P. Phunchareon, Influence of reaction parameters on water absorption of neutralized poly(acrylic acid-co-acrylamide) synthesized by inverse suspension polymerization, J Appl Polym Sci. 72 (1999) 1349–1366. https://doi.org/https://doi.org/10.1002/(SICI)1097-4628(19990606)72:10<1349::AID-APP16>3.0.CO;2-K.

[190] Z. Li, R. Valladares Linares, S. Bucs, L. Fortunato, C. Hélix-Nielsen, J.S. Vrouwenvelder, N. Ghaffour, T.O. Leiknes, G. Amy, Aquaporin based biomimetic membrane in forward osmosis: Chemical cleaning resistance and practical operation, Desalination. 420 (2017) 208–215. https://doi.org/10.1016/J.DESAL.2017.07.015.

[191] H.N. Shalini, C.A. Nayak, Forward Osmosis Membrane Concentration of Raw Sugarcane Juice, in: I. Regupathi, V. Shetty K, M. Thanabalan (Eds.), Recent Advances in Chemical Engineering, Springer Singapore, Singapore, 2016: pp. 81–88.

[192] W.C.L. Lay, J. Zhang, C. Tang, R. Wang, Y. Liu, A.G. Fane, Factors affecting flux performance of forward osmosis systems, J Memb Sci. 394–395 (2012) 151–168. https://doi.org/10.1016/J.MEMSCI.2011.12.035.

[193] C. Conidi, R. Castro-Muñoz, A. Cassano, Membrane-Based Operations in the Fruit Juice Processing Industry: A Review, Beverages. 6 (2020) 18. https://doi.org/10.3390/beverages6010018.

[194] M. Eyvaz, S. Arslan, D. İmer, E. Yüksel, İ. Koyuncu, Forward Osmosis Membranes – A Review: Part II, in: H. Du, A. Thompson, X. Wang (Eds.), Osmotically Driven Membrane Processes - Approach, Development and Current Status, INTECH, 2018: pp. 41–68. https://doi.org/http://dx.doi.org/ 10.5772/intechopen.74659.

[195] M. Eyvaz, S. Arslan, D. Koseoglu-Imer, E. Yuksel, I. Koyuncu, Forward Osmosis Membranes – A Review: Part I, in: 2018. https://doi.org/10.5772/intechopen.72287.

[196] W. Xue, K.K.K. Sint, C. Ratanatamskul, P. Praserthdam, K. Yamamoto, Binding TiO2 nanoparticles to forward osmosis membranes: Via MEMO-PMMA-Br monomer chains for enhanced filtration and antifouling performance, RSC Adv. 8 (2018) 19024–19033. https://doi.org/10.1039/c8ra03613f.

[197] I. Ibrar, S. Yadav, A. Altaee, A. Hawari, V. Nguyen, J. Zhou, A novel empirical method for predicting concentration polarization in forward osmosis for single and multicomponent draw solutions, Desalination. 494 (2020) 114668. https://doi.org/10.1016/j.desal.2020.114668.

[198] Z. Li, R. Valladares Linares, S. Bucs, L. Fortunato, C. Hélix-Nielsen, J.S. Vrouwenvelder, N. Ghaffour, T.O. Leiknes, G. Amy, Aquaporin based biomimetic membrane in forward osmosis: Chemical cleaning resistance and practical operation, Desalination. 420 (2017) 208–215. https://doi.org/10.1016/j.desal.2017.07.015.

[199] I. Petrinic, H. Bukšek, I. Galambos, R. Gerencsér-Berta, M.S. Sheldon, C. Helix-Nielsen, Removal of naproxen and diclofenac using an aquaporin hollow fiber forward osmosis module, Desalination Water Treat. 192 (2020) 415–423. https://doi.org/10.5004/dwt.2020.26082.

[200] M.S. Manna, P. Saha, A.K. Ghoshal, Iron complexation of pharmaceutical catechins through selective separation, RSC Adv. 4 (2014) 26247–26250. https://doi.org/10.1039/C4RA03683B.

[201] M.A. Brza, S.B. Aziz, H. Anuar, F. Ali, E.M.A. Dannoun, S.J. Mohammed, R.T. Abdulwahid, S. Al-Zangana, Tea from the drinking to the synthesis of metal complexes and fabrication of PVA based polymer composites with controlled optical band gap, Sci Rep. 10 (2020) 18108. https://doi.org/10.1038/s41598-020-75138-x.

[202] S.J. Saghanezhad, M.H. Sayahi, I. Imanifar, M. Mombeni, S. Deris Hamood, Caffeine-H3PO4: a novel acidic catalyst for various one-pot multicomponent reactions, Research on Chemical Intermediates. 43 (2017) 6521–6536. https://doi.org/10.1007/s11164-017-3002-8.

[203] K. Rajam, S. Rajendran, N.N. Banu, Effect of caffeine-Zn2+ system in preventing corrosion of carbon steel in well water, J Chem. (2013). https://doi.org/10.1155/2013/521951.

[204] A.K. Biswas, A.R. Sarkar, A.K. Biswas, Biological and chemical factors affecting the valuation of North East Indian plains teas. III. Statistical Evaluation of the Biochemical Constituents and their Effects on Colour, Brightness and Strength of Black Teas, J Sci Food Agric. 24 (1973) 1457–1477. https://doi.org/https://doi.org/10.1002/jsfa.2740241202.

[205] B. Zhang, S. Yu, Y. Zhu, Y. Shen, X. Gao, W. Shi, J.H. Tay, Efficiencies and mechanisms of the chemical cleaning of fouled polytetrafluoroethylene (PTFE) membranes during the microfiltration of alkali/ surfactant/polymer flooding oilfield wastewater †, (2019). https://doi.org/10.1039/c9ra06745k.

[206] P.T.N. Nguyen, C.K. Van, N.A.T. Do, T.C.T. Tran, T.K.T. Dang, T.M.T. Pham, B.L. Tran, N.T.A. Ton, Applicability of convection drying process for production of instant tea powder from Condonopsis javanica root extract, Mater Today Proc. 56 (2022) 1461–1467. https://doi.org/10.1016/J.MATPR.2021.12.316.

[207] S. Qi, R. Wang, G.K.M. Chaitra, J. Torres, X. Hu, A.G. Fane, Aquaporin-based biomimetic reverse osmosis membranes: Stability and long term performance, J Memb Sci. 508 (2016) 94–103. https://doi.org/10.1016/J.MEMSCI.2016.02.013.

[208] S. Khruengsai, T. Sripahco, P. Pripdeevech, Volatile profiles and antioxidant activity of different cultivars of Camellia sinensis var. assamica grown in Thailand, Food Res. 5 (2021) 354–362. https://doi.org/10.26656/fr.2017.5(2).581.

[209] A. Rashidinejad, S. Boostani, A. Babazadeh, A. Rehman, A. Rezaei, S. Akbari-Alavijeh, R. Shaddel, S.M. Jafari, Opportunities and challenges for the nanodelivery of green tea catechins in functional foods, Food Research International. 142 (2021) 110186. https://doi.org/10.1016/J.FOODRES.2021.110186.

[210] T. Majeed, S. Phuntsho, S. Sahebi, J.E. Kim, J.K. Yoon, K. Kim, H.K. Shon, Influence of the process parameters on hollow fiber-forward osmosis membrane performances, Desalination Water Treat. 54 (2015) 817–828. https://doi.org/10.1080/19443994.2014.916232.

[211] I.W. Mwangi, J.C. Ngila, P. Ndungu, T.A.M. Msagati, Method development for the determination of diallyldimethylammonium chloride at trace levels by epoxidation process, Water Air Soil Pollut. 224 (2013). https://doi.org/10.1007/s11270-013-1638-6.

[212] A. Kharazmi, N. Faraji, R.M. Hussin, E. Saion, W.M.M. Yunus, K. Behzad, Structural, optical, opto-thermal and thermal properties of ZnS-PVA nanofluids synthesized through a radiolytic approach, Beilstein Journal of Nanotechnology. 6 (2015) 529–536. https://doi.org/10.3762/bjnano.6.55.

[213] I.W. Mwangi, J. Catherine Ngila, P. Ndungu, A new spectrophotometric method for determination of residual polydiallyldimethylammonium chloride focculant in treated water based on a diazotization-coupledion pair, Water SA. 38 (2012) 707–714. https://doi.org/10.4314/wsa.v38i5.8.

[214] H. Chavda, C. Patel, Effect of crosslinker concentration on characteristics of superporous hydrogel, Int J Pharm Investig. 1 (2011) 17. https://doi.org/10.4103/2230-973x.76724.

[215] T. Sharma, G. Madras, Effect of crosslinker on the swelling and adsorption properties of cationic superabsorbent, Bulletin of Materials Science. 39 (2016) 613–626. https://doi.org/10.1007/s12034-016-1220-0.

[216] R. Ou, H. Zhang, S. Kim, G.P. Simon, H. Hou, H. Wang, Improvement of the Swelling Properties of Ionic Hydrogels by the Incorporation of Hydrophobic, Elastic Microfibers for Forward Osmosis Applications, Ind Eng Chem Res. 56 (2017) 505–512. https://doi.org/10.1021/acs.iecr.6b03689.

[217] K. Lejcuś, M. Śpitalniak, J. Dabrowska, Swelling behaviour of superabsorbent polymers for soil amendment under different loads, Polymers (Basel). 10 (2018). https://doi.org/10.3390/polym10030271.

[218] D.R. Barleany, R.S.D. Lestari, M. Yulvianti, T.R. Susanto, Shalina, Erizal, Acrylic acid neutralization for enhancing the production of grafted chitosan superabsorbent hydrogel, Int J Adv Sci Eng Inf Technol. 7 (2017) 702–708. https://doi.org/10.18517/ijaseit.7.2.2340.

[219] D.J. Hourston, G.D. Williams, R. Satguru, J.C. Padget, D. Pears, The influence of the degree of neutralization, the ionic moiety, and the counterion on water-dispersible polyurethanes, J Appl Polym Sci. 74 (1999) 556–566. https://doi.org/https://doi.org/10.1002/(SICI)1097-4628(19991017)74:3<556::AID-APP10>3.0.CO;2-D.

[220] D.R. Barleany, R. Sulistyo, D. Lestari, M. Yulvianti, T.R. Susanto, Acrylic Acid Neutralization for Enhancing the Production of Grafted Chitosan Superabsorbent

Hydrogel, Internation Journal on Advanced Science Engineering Information Technology. 7 (2017) 702–708. https://doi.org/DOI:10.18517/IJASEIT.7.2.2340.

[221] J. Zeng, S. Cui, Q. Wang, R. Chen, Multi-layer temperature-responsive hydrogel for forward-osmosis desalination with high permeable flux and fast water release Multi-layer temperature-responsive hydrogel for forward-osmosis desalination with high permeable flux and fast water release, Desalination. 459 (2019) 105–113. https://doi.org/10.1016/j.desal.2019.02.002.

[222] D. Dutta, B. Podder, A. Biswas, Solar Energy Potential of Silchar, Assam, India—A Resource Assessment BT - Advances in Optical Science and Engineering, in: V. Lakshminarayanan, I. Bhattacharya (Eds.), Springer India, New Delhi, 2015: pp. 119–127.

[223] S. Loeb, L. Titelman, E. Korngold, J. Freiman, Effect of porous support fabric on osmosis through a Loeb-Sourirajan type asymmetric membrane, J Memb Sci. 129 (1997) 243–249. https://doi.org/10.1016/S0376-7388(96)00354-7.

Appendix-1: Performance analysis of HFFO membrane module for tea concentration using inorganic draw solute

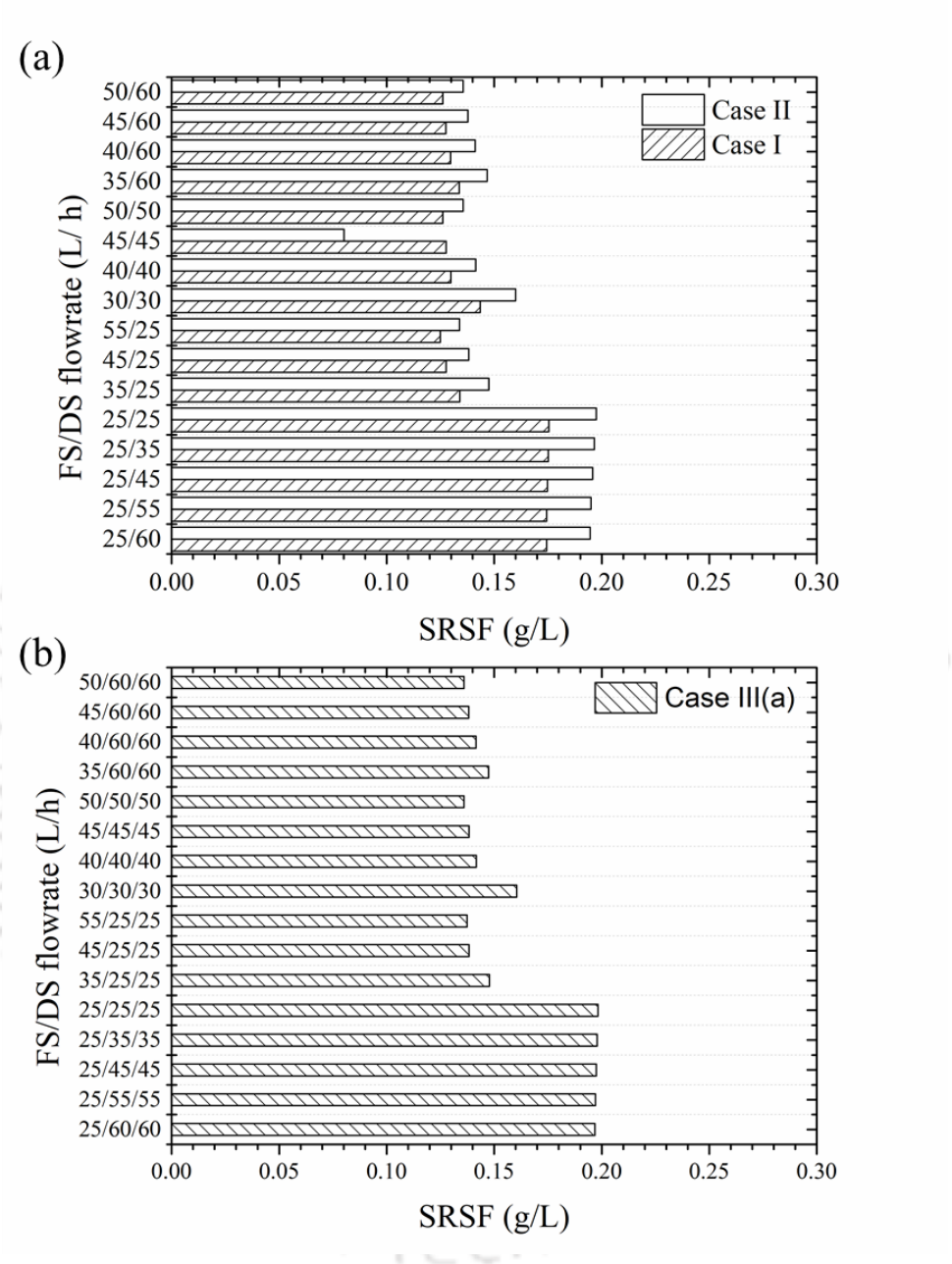

Figure A1.1 Effect of different feed and draw solution flowrate on SRSF (g L^{-1}) for a) Case I-II, and b) Case III (a)

Table A1.1 Comparison of different inorganic salt compositions as mixed-salt draw solute for preparation of concentrated tea extract using forward osmosis process

Sample Identity	NaCl	Na_2SO_4	$MgCl_2$	KCl	Osmolality (mosmos per kg H_2O)	Osmotic pressure (bar)
	(mol L^{-1})					
S1	0.5	0.5	0.5	0.5	2267	50.315
S2	1	0	1	0	2456	54.509
S3	1	0.5	0.5	0	2378	52.779
S4	0.5	1	0.5	0	2303	51.114
S5	0.5	0.5	1	0	2714	60.236
S6	0.5	0	0.5	1	2235	49.605
S7	0.5	0.5	0	1	1862	41.326
S8	0.25	0.25	1	0.5	2677	59.415
S9	0.25	1	0.25	0.5	2072	45.987
S10	0.25	0.5	1	0.25	2811	62.389
S11	0.5	1	0.25	0.25	2098	46.564
S12	1	0.25	0.5	0.25	2335	51.824
S13	1	0.25	0.25	0.5	2052	45.543
S14	0.5	0.25	1	0.25	2641	58.616
S15	0.25	1	0.5	0.25	2297	50.981
S16	1.25	0.25	0.25	0.25	1580	35.067
S17	0.25	1.25	0.25	0.25	2151	47.740
S18	0.25	0.25	1.25	0.25	1780	39.506
S19	0.25	0.25	0.25	1.25	1989	44.145
S20	1	1	0	0	1899	42.147
S21	1	0	0	1	1884	41.814

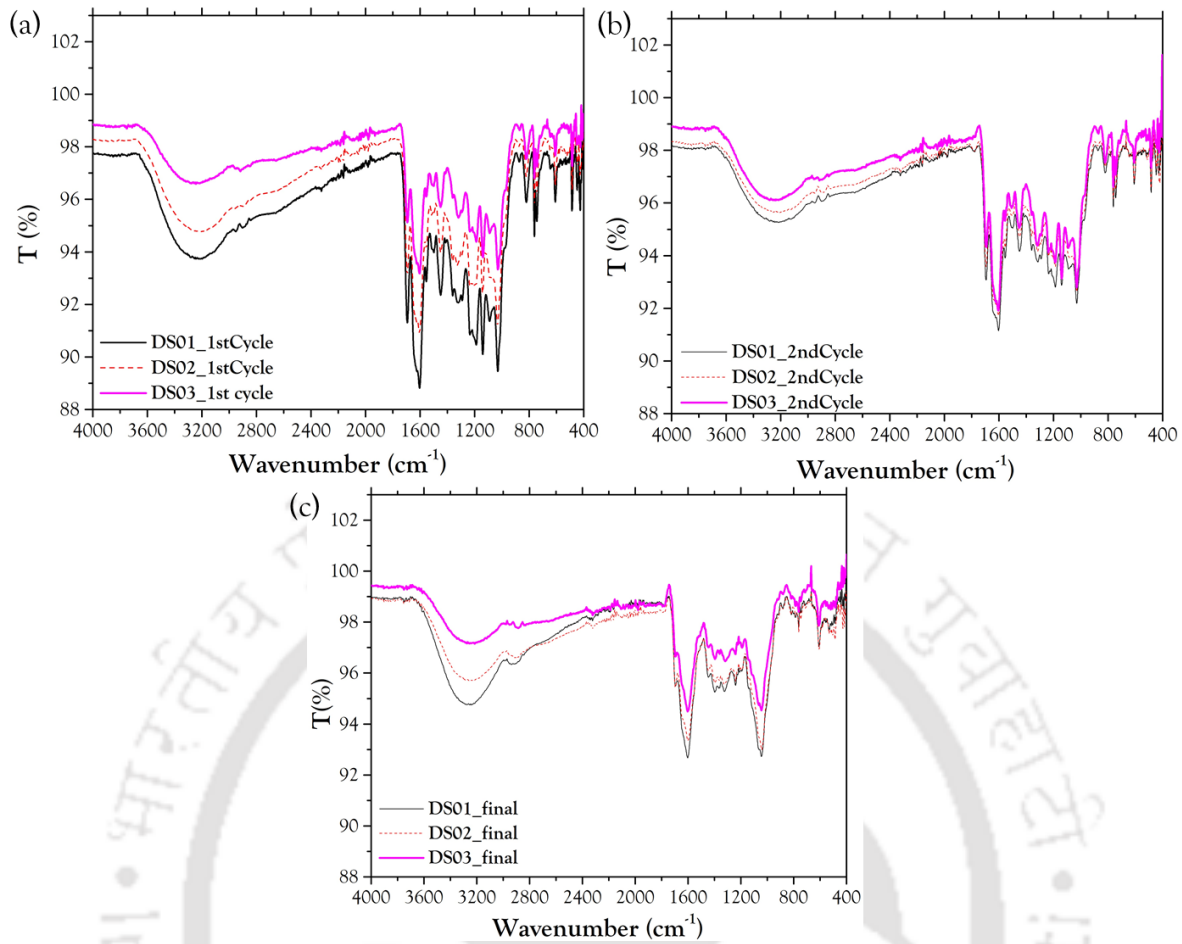

Figure A1.2 FTIR spectra of the instant tea powder were obtained after a) the first FO-cycle, b) the second FO-cycle, and c) the final cycle against DS-composition (DS01) using an integrated FO-crystallisation process

Table A1.2 Standard calibration peak for essential tea component

Components	Retention time (min.)	Equation	R^2
Caffeine	18.770 ± 0.026	*y = 132792x*	0.999
Gallic acid	4.630 ± 0.035	*y = 95720x*	0.977
Catechin	16.760 ± 0.140	*y = 328774x*	0.984
Epicatechin	32.244 ± 0.011	*y = 155267x*	0.999
Epigallocatechin	11.729 ± 0.014	*y = 23788x*	0.999
Epigallocatechin gallate	22.822 ± 0.310	*y = 188080x*	0.998
Epicatechin gallate	2.823 ± 0.091	*y = 202011x*	0.998
L-Theanine	2.612 ± 0.049	*y = 5366.8x*	0.995

Stationary phase (Column): C18 column (5µm; 25 cm ×4.6 mm) Mobile phase: 100 mL of Methanol, 399.5 mL of de-ionised distilled water, and 0.5 mL of orthophosphoric acid; Wavelength: 210 nm; Flow rate: 1 mL/min

Appendix 2: Performance analysis of hydrogel as draw solute for forward osmosis process

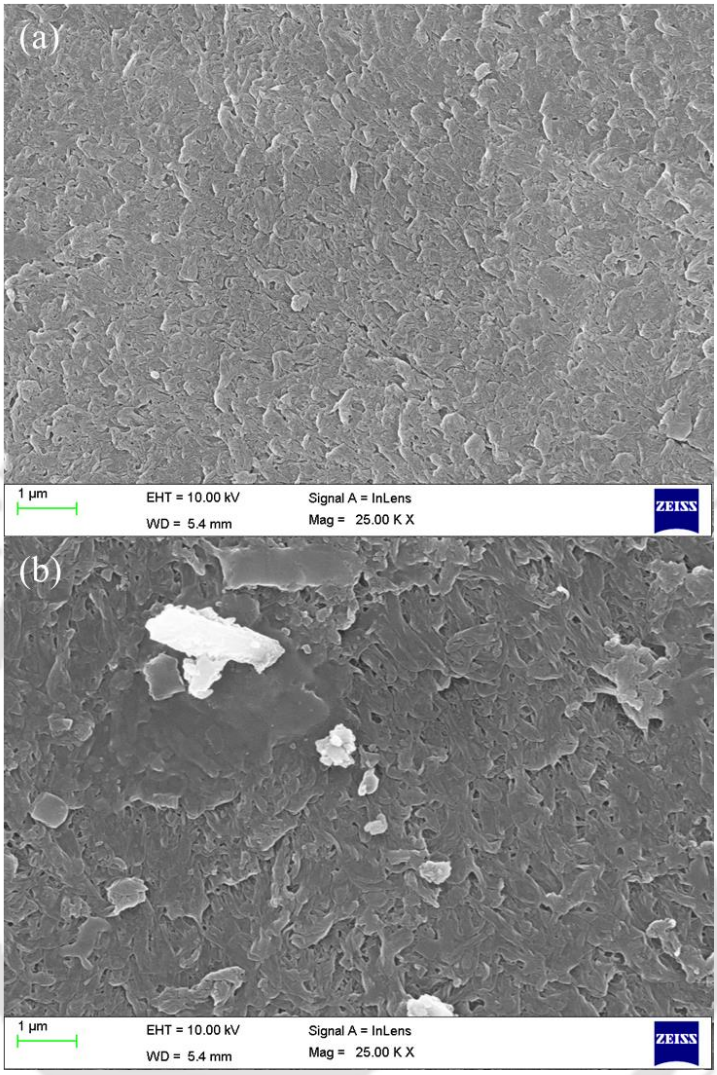

Figure A2.1 FESEM image of membrane (a) before, and (b) after 12 cycle of FO process

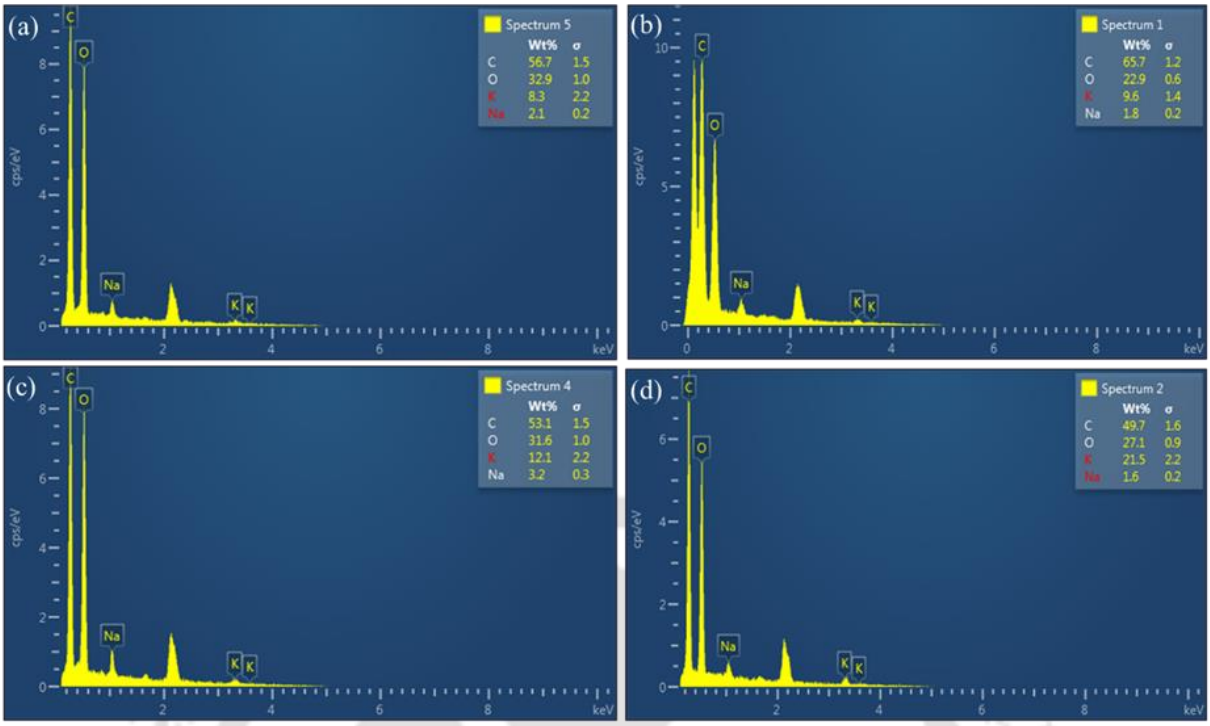

Figure A2.2 EDX spectra for synthesised hydrogel using 0.05 g of MBA 'cross-linker' with a) 45%, b) 60%, c) 75%, and d) 90% degree of neutralisation

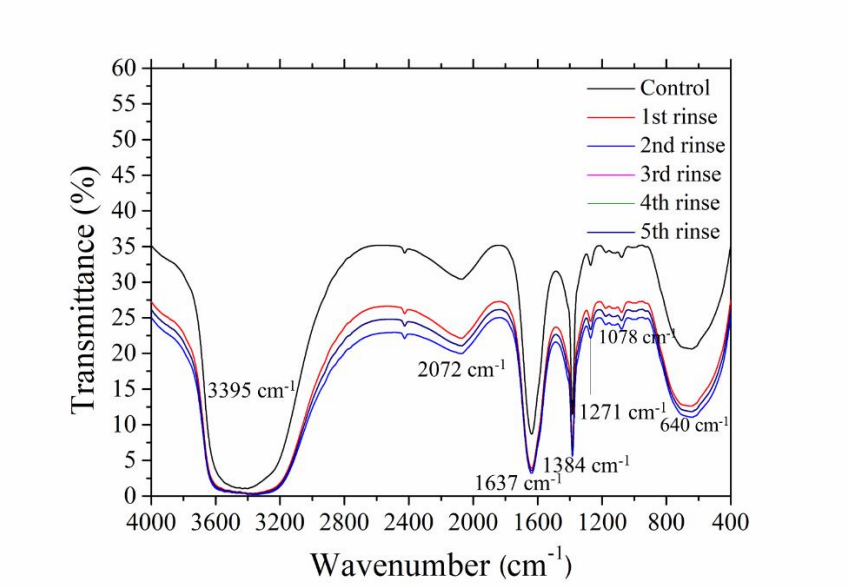

Figure A2.3 FTIR spectrum for water collected after each cycle of solar dewatering

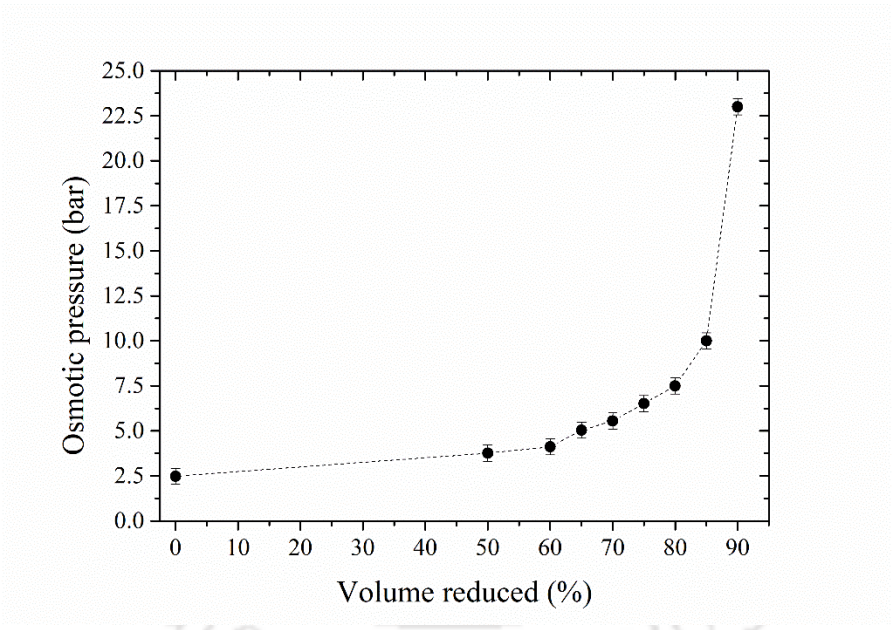

Figure A2.4 Data for correlating change in osmotic pressure with % volume reduced (for tea extract)

Appendix 3: Characterisation of flat-sheet membrane

The pure water and solute permeability coefficients were evaluated in a laboratory-scale cross-flow RO test unit as described in previous literature [78]. The pure-water permeance was measured at room temperature (25± 0.5 °C) and averaged over four pressures ranging from 0.7 to 4.1 bar. The pure-water flux (J_w) was obtained from dividing the volumetric permeate rate by the membrane area.

Salt rejection (R) tests were conducted with a 1000 mg L^{-1} NaCl solution (as feed solution) at pressures of 0.7 to 1.8 bar. The pure-water permeability coefficient (L_p) and salt rejection (R) were estimated using equations (A1.1) and (A1.2):

$$J_w = \frac{V}{A_m \times t} = (L_p \times \Delta P) \quad \text{(A1.1)}$$

where, the term V, and A_m represents the collected permeate volume (L) at time 't', and membrane area.

$$R = 1 - \frac{C_p}{C_f} \quad \text{(A1.2)}$$

where, C_p and C_f represents the concentration (in g L^{-1}) of the permeate and feed solution

The salt permeability (B) was calculated using equation (S1.3):

$$B = J_w \left(\frac{1-R}{R}\right) \exp\left(\frac{-J_w}{k}\right) \quad \text{(A1.3)}$$

where k is the mass-transfer coefficient in the cross-flow RO membrane cell.

The support-layer properties can be described by structural parameter, S, which is defined as an intrinsic membrane property specified as the product of the thickness (t) and tortuosity (τ) of the support layer, divided by its porosity (ε). Experimentally, the S-value can be calculated with the empirical equation [223]:

$$S = \left(\frac{D}{J_w}\right) \ln\left[\frac{B + L_p \pi_{DS,b}}{B + J_w}\right] \quad \text{(A1.4)}$$

Where, the term D represents diffusion coefficient of draw solution,

Table A3.3. Properties of the membrane

Manufacturer	DOW Filmtec membrane	
Material	Polyamide TFC	
pH	2-11	
Pure water permeability coefficient, L_p (L m^{-2} h^{-1} bar^{-1})	5.99	R^2 = 0.99
Solute permeability coefficient, B (L m^{-2} h^{-1})	3.44	R^2 = 0.91
A/B (bar)	0.57	
Structural parameter, S (µm)	424-786	

Research output

❖ ***Journal publications***

i) **A. Bardhan**, S. Subbiah, K. Mohanty, Modelling and experimental validation of osmotic driven energy efficient process for tea solution concentration, Environ Technol Innov. 20 (2020) 101065. https://doi.org/10.1016/j.eti.2020.101065.

ii) **A. Bardhan**, S. Subbiah, K. Mohanty, Ibrar Ibrar, Ali Altaee (2022) Feasibility of Poly (Vinyl Alcohol)/Poly (Diallyldimethylammonium Chloride) Polymeric Network Hydrogel as Draw Solute for Forward Osmosis Process. Membranes 2022 12:1097. https://doi.org/10.3390/membranes12111097.

iii) P. Deka, V.K. Verma, A. Chandrasekaran, A.B. Neog, **A. Bardhan**, K. Raidongia, S. Subbiah, Performance of novel sericin doped reduced graphene oxide membrane for FO based membrane crystallisation application, J Memb Sci. 660 (2022) 120884. https://doi.org/10.1016/J.MEMSCI.2022.120884.

iv) **A. Bardhan**, S. Subbiah, K. Mohanty, Optimisation of multi-component inorganic salt composition as draw solute for preparation of concentrated tea extract using forward osmosis process, Food and Bioproducts Processing, 138 (2023). https://doi.org/10.1016/j.fbp.2023.01.007.

v) **A. Bardhan**, S. Subbiah, K. Mohanty, Modelling and experimental validation for the preparation of concentrated tea extract using a forward osmosis process using a food-grade inorganic draw solute, Industrial & Engineering Chemistry Research (2023). https://doi.org/10.1021/acs.iecr.2c04219.

❖ ***Conferences***

i) **A. Bardhan**, S. Subbiah, K. Mohanty, Modelling and validation of the concentration of tea solution using aquaporin hollow fibre forward osmosis module, Bioprocessing India 2018 Conference held at IIT- Delhi from December 16th to 18th, 2018.

ii) **A. Bardhan**, S. Subbiah, K. Mohanty, Optimisation of multi-component draw solute for preparation of concentrated tea extract using forward osmosis process, Research conclave-2022, IIT-Guwahati from January 21st -23rd, 2022.

❖ ***Patents filed***

i) **Ananya Bardhan**, S. Senthilmurugan, K. Mohanty, Synthesis of a robust hydrogel as draw solute for preparation of concentrated liquid extract using forward osmosis, TEMP/E-1/10552/2022-KOL.

ii) **Ananya Bardhan**, S. Senthilmurugan, K. Mohanty, A multi-layered membrane module for preparing liquid food concentrate, TEMP/E-1/10536/2022-KOL.

❖ ***Book chapter***

i) **A. Bardhan**, S. Subbiah, K. Mohanty, Application of Membrane in Food-Processing Industries, in: Food Process. Adv. Non-Thermal Technol., 1st ed., CRC Press, 2021: p. 42. https://doi.org/https://doi.org/10.1201/9781003163213.

ii) **A. Bardhan**, A. Akhtar, S. Subbiah, Microfiltration and ultrafiltration membrane technologies, Advancement in Polymer-based Membranes for Water Remediation, Elsevier, 2022: pp. 3–42. https://doi.org/https://doi.org/10.1016/B978-0-323-88514-0.00001-2.

iii) **A. Bardhan**, S. Subbiah, Polymer-based microfiltration/ultrafiltration membranes, Advancement in Polymer-based Membranes for Water Remediation, Elsevier, 2022: pp. 43–80. https://doi.org/https://doi.org/10.1016/B978-0-323-88514-0.00005-X.